GENERAL ATOMIC

DIVISION OF GENERAL DYNAMICS

GA-4071

THERMIONIC SPACE POWER REACTOR SYSTEM RESEARCH AND DEVELOPMENT

by

N. B. Elsner, J. W. Holland, R. W. Pidd, J. T. Ream, Jr., W. B. Wright, and L. Yang

---

ANNUAL SUMMARY REPORT

May 1, 1962 through April 30, 1963

Contract AT(04-3)-167
Project Agreement No. 14
U. S. Atomic Energy Commission

December 17, 1963

DISCLAIMER

GENERAL ATOMIC

DIVISION OF

GENERAL DYNAMICS

JOHN JAY HOPKINS LABORATORY FOR PURE AND APPLIED SCIENCE

P.O. BOX 608, SAN DIEGO 12, CALIFORNIA

GA-4071

Copy No.

THERMIONIC SPACE POWER REACTOR SYSTEM RESEARCH AND DEVELOPMENT

ANNUAL SUMMARY REPORT

May 1, 1962 through April 30, 1963

Work done by:

Thermionic Staff

Report written by:

N. B. Elsner
J. W. Holland
R. W. Pidd
J. T. Ream, Jr.
W. B. Wright
L. Yang

Contract AT(04-3)-167
Project Agreement No. 14
U. S. Atomic Energy Commission
General Atomic Project No. 278

December 17, 1963

FOREWORD

This annual summary report was prepared by General Dynamics/ General Atomic Division, San Diego, California, on USAEC contract AT(04-3)-167, Project Agreement No. 14, titled Thermionic Space Power Reactor System Research and Development. Dr. R. W. Pidd is the General Atomic principal investigator on this project, the purpose of which is to "Investigate the feasibility of developing fission-heated thermionic cells with an operating life of 10,000 hours or more for use in thermionic space power reactor systems."

This first annual summary report for this contract covers research conducted during the period of May 1, 1962 through April 30, 1963. The General Atomic project number is 278.

CONTENTS

BLANK

FIGURES

FIGURES (cont.)

FIGURES (cont.)

BLANK

TABLES

I. INTRODUCTION AND SUMMARY

This report summarizes the research and development work conducted by General Atomic under AEC contract AT(04-3)-167, Project Agreement 14, during the period of May 1, 1962 through April 30, 1963. The objective of this program has been to develop and test a fission-heated thermionic cell of a design which closely corresponds to a fuel element unit cell component of a thermionic power reactor for space applications. During this reporting period, three thermionic cells, two with tungsten-clad fuel-emitters and one of the unclad type, were tested in the TRIGA Mark F reactor. Concurrently with the program of cell development, a program of tests on the emitter-fuel combination was conducted to determine its life-performance characteristics. Fuel-emitter proof tests on the tungsten-clad systems demonstrated operability for 1000 hours.

Studies of the thermionic space power application singled out two parameters which have a dominant effect on the weight-performance characteristics of the system. One parameter is the output power density; that is, the electrical power produced per unit emitter surface area. The other is the temperature of heat rejection. Design objectives selected for the power density and the heat rejection temperature determined the choice of materials and the configuration of the in-pile test cell. A power density objective of 5 to 10 electrical watts per cm^2 of emitter surface area places the emitter surface temperature at approximately 1750°C. This temperature condition restricts the selection of fuel materials to uranium dioxide or uranium carbide. Tungsten is the only known cladding material compatible with these fuels and capable of long operation at temperatures above 1750°C. The chemical and physical properties of the W-UO_2 and W-UC fuel-emitter are consistent with operational lifetimes considerably in excess of one year at surface temperatures above 1750°C, although proven operation of the fuel-emitter is limited to 1000 hours. The properties of the basic materials provide little guidance in choosing between the UO_2 and UC fuels. It now appears that the selection depends primarily on the behavior of the fuel materials during fuel burn-up and fission-product build-up. On the basis of the limited available information, the need for venting fission products out of the fuel, to avoid excessive fuel swelling, appears obvious. Venting of the fission products implies the loss of fuel in some proportionate measure, even for the clad fuel configuration. For this reason the UC fuel, which has a much lower vaporization rate than the UO_2 fuel, is presently preferred and is used in the in-pile test cell. The use of an oxide fuel will depend on the stability of the W-UO_2 cermets which will be determined from material irradiation tests now under way. The research and development program to date has seen an almost complete transition of emphasis from the measurement of physical and chemical

properties of the fuels, which are now established, to the initial investigation of the effects of radiation. These latter effects will dominate the further selection of fuels for the thermionic reactor application during the second program year.

One marked advance in high-temperature fuel technology during this program year has been in the area of tungsten fabrication. The selection of tungsten as a physically- and chemically-compatible cladding for thermionic fuel elements left unsolved the difficulty of fabricating all but the most simple tungsten forms. In a parallel program the process of vapor-plating, or vapor deposition, of tungsten was extensively investigated, particularly in regard to the direct vapor plating of tungsten on uranium-bearing fuels. Basic information and fabrication techniques did not become available in time to apply the new process to the production of the test cell fuel-emitters. The tungsten cladding utilized in the two clad test cells was machined from a tungsten-molybdenum alloy. However, the techniques of vapor deposition had advanced sufficiently before the end of the period to permit the introduction of this means of fabrication in the construction of new in-pile and out-of-pile cells. This advance in fabrication technology should have a considerable effect on the utilization of tungsten in high-temperature reactor systems.

A principal research emphasis has been placed on the uranium-bearing fuel-emitter, since the performance of the materials in this component will determine the ultimate life-performance characteristics of the thermionic reactor system. The selection of a high heat rejection temperature (up to 1000°C) for thermionic space power systems is undoubtedly the second major factor affecting test cell life. Three important factors lead to the selection of a temperature range for heat rejection of 700°C to 1000°C. First, the collector can be operated in this range without a substantial reduction of generator output. Second, the rejection of heat by radiation in space power systems permits a very low system weight in this temperature range. Third, the development of liquid-metal coolant-loop technology by the AEC has lifted the operating temperature limit, for the lithium-niobium system, to 1000°C. At the same time, the selection of this temperature range places thermionic generator technology well above the limits of current power-tube technology. Power-tube envelopes and insulators must be operated at much lower temperatures ($< 200^{\circ}C$) for long-life operation. For this reason, much of the development program in the first year centered on advanced technology. The basic components selected for the envelope-insulator system are niobium and alumina. The development of the envelope-insulator requires continuing emphasis, since currently the termination of a thermionic in-pile test is attributable most often to a problem associated with the envelope rather than with the fuel-emitter.

A considerable effort was applied to the testing of out-of-pile cells of a design identical to that of the in-pile cell, except for the mode of heating. The principal objective of the out-of-pile testing program was to confirm mechanical and thermal design principles. The unpredictable element was the integrity of the mechanical design of a completely new cell. Of particular significance was the means of maintaining an inter-electrode spacing of 10 mils under conditions of extreme temperature gradients (20°C to 2000°C) and cycling. The design principle adopted was that of providing a high precision alignment between a cantilevered fuel-emitter and the surrounding collector. Machined surfaces were prepared, tested, and lapped to yield the required alignment. Components were precycled sufficiently to expose all possible internal stresses that could lead to dimensional changes during operation. The record of operation of the out-of-pile and subsequent in-pile cells with 10-mil spacing and without inter-electrode shorting, under conditions of extensive cycling, provides an excellent experimental test of the design concept. This test series indicates that the requirement of close spacing of electrodes in thermionic reactors can be adequately satisfied.

The selection and development of the fuel-emitter, the design and development of the cell components and assembly, and the testing of out-of-pile and in-pile cells, are described in detail in this report. Design and component development occupied approximately 10 months of the 12-month program, while the initial integral tests of the cells were performed in the remaining 2 months. Operation of the clad-type test cells at design power density and at design temperature was achieved for short operating periods. Operation of the unclad in-pile cell yielded unsatisfactory performance.

On the basis of these trials, it is concluded that the clad type fuel-emitter design and the materials selected will be retained for the planned long-duration (1000 hours) in-pile tests.

The immediate goals for the second year of the program follow directly from the progress made during the first year; namely the testing of a series of in-pile thermionic cells for 100 to 1000 hour periods to obtain statistical operational data. While problems of cell technology remain, they will be treated in a program of systematic upgrading. Consequently the program direction can be shifted away from a primary emphasis on cell development to a primary emphasis on cell testing.

BLANK

II. TEST CELL DESIGN

2.1 DESIGN PRINCIPLES FOR IN-PILE TEST CELL

The following design principles were adopted at the beginning of this program to provide guidance in the development of a satisfactory cell for in-pile testing:

1. The test cell should represent a unit of a thermionic reactor fuel element from the standpoint of materials employed and component geometry.
2. Instrumentation should provide for accurate measurement of cesium temperature (±5°C), collector temperature (±25°C), the temperature of the emitter surface (±50°C), and the temperature distribution over the emitter surface. It should also provide for independent control of each of these temperatures over a broad range.
3. Test cell packaging should provide containment for short term (< 100 hrs) in-pile experiments.
4. Design checks of the in-pile test cell should be provided through the out-of-pile operation of fully instrumental cells similar in geometry and materials to the in-pile cell.

2.2 SELECTION OF MATERIALS

Two types of fuel-emitters were employed in the tests carried out during this reporting period; that is, (1) unclad uranium carbide fuel-emitters and, (2) fuel-emitters consisting of fuel clad with tungsten.

2.2.1 Unclad Fuel-Emitters

The vaporization characteristics of the UC-ZrC system in vacuum have been studied, by means of the Langmuir technique, at both the low-UC and the high-UC content using samples of better than 93 percent of theoretical density. The observed results are summarized in Fig. 1. New samples always exhibit high rates of vaporization, presumably because of the presence of large amounts of gaseous impurities. Consistent results are obtained only after long periods of outgassing at vaporization temperatures. Results obtained by alpha counting indicate that, for the temperature ranges

shown in Fig. 1, the uranium depletion near the surface regions is negligible for samples with low-UC content and amounts to less than 10 percent for the high-UC samples; however, the depletion at the top surface layer is undoubtedly higher than this. Electron microprobe analysis after vaporization shows that the uranium concentration at a distance of one micron from the surface of a 19 UC-81 ZrC (mol %) sample is only 60 percent of the value in the bulk. The latest information on rates of vaporization of Uc-ZrC samples of various combinations and pore structure is shown in Fig. A-3 of the Appendix.

It has now been established that UC-ZrC is a dispenser-type emitter and that the emission is associated with the presence of a layer of uranium adsorbed on the surface. If the sample is thoroughly outgassed and care taken to prevent the contamination of its surface, both the 10 UC-90 ZrC and the 30 UC-70 ZrC samples emit as well as the 90 UC-10 ZrC samples, and emission of 5 amp/cm^2 can be obtained from all of these samples at about 1950°K to 2000°K. However, the low-UC samples, especially the 10 UC-90 Zrc samples, are very easily poisoned by exposure to a poor vacuum (e.g. 10^{-4} mm Hg), probably because of the poor ability of the low-UC samples to maintain an adsorbed uranium layer on the surface in the presence of factors which tend to remove such a layer.

On the basis of information from vacuum vaporization and vacuum emission, it has been shown that the UC-ZrC system, at both the high-UC and the low-UC ends, is capable of providing 5 amp/cm^2 at temperatures where the loss of materials by vaporization amounts to a few mils or less per year. On the basis of this type of information, unclad fuel-emitters of UC-ZrC were selected as one of the test candidates.

2.2.2 Clad Fuel-Emitters

In the selection of cladding and fuel of a clad fuel-emitter, primary consideration was given to the following two requirements:

1. There should be no interaction between the fuel and the cladding (emitter) which would affect the mechanical integrity and the electron-emission properties of the emitter.
2. The emitter should retain its dimensional stability despite the fission products formed in the fuel.

If an emitter is to achieve useful long life and reproducible performance, these requirements must be fulfilled by the materials chosen.

The materials proposed as the emitter are the refractory metals - W, Mo, Ta, Nb, and, recently, Re and Ir. The selection of suitable emitter-fuel combinations from these materials for the cell-testing

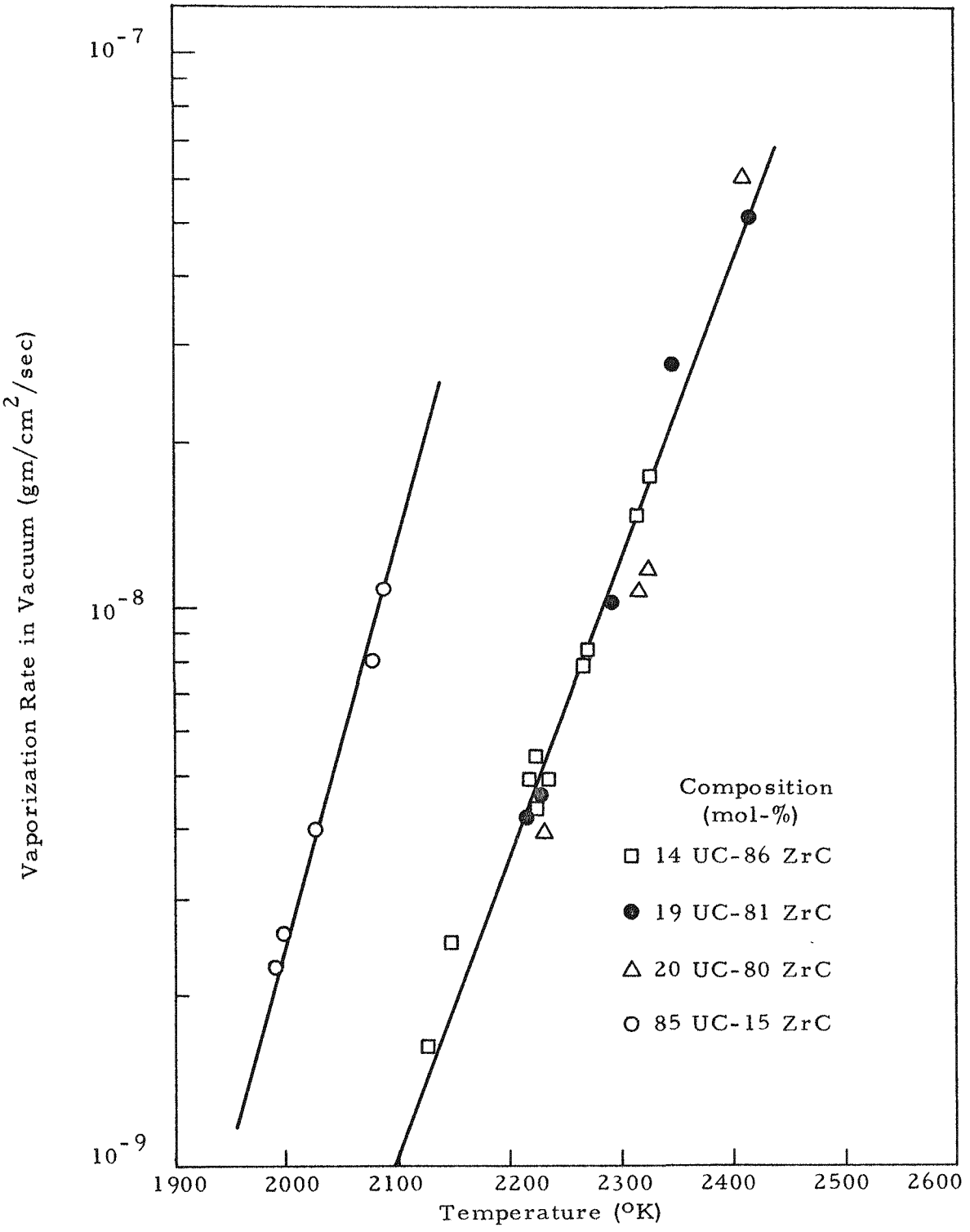

Fig. 1--Rate of vaporization of UC-ZrC system in vacuum

program is analyzed below, in the light of existing experimental data.

Interaction Between Fuel and Emitter Materials - Diffusion studies, employing various fuel-emitter combinations and using the standard diffusion-couple method, have been carried out in the temperature range of 1800°C to 2000°C.[1][2] The nature of phases formed at the interfaces and concentration distribution of the components of the couples after the diffusion runs were examined both metallographically and by electron microprobe analysis. The results obtained are summarized in Table A-1 of the Appendix. For an operating temperature of 1800°C, the suitable candidates are (1) W-clad UC and UC-ZrC, (2) W-clad UO_2, and (3) Mo-clad 10 UC-10 ZrC. The first candidate was chosen for the in-pile test series on the basis of this information. Subsequent information has supported this choice. Recently, diffusion runs of 933 hours at 2023°K have been made for W versus UC and W versus 90 UC-10 ZrC. No significant interaction was observed in either case.

Dimensional Stability of the Emitter in Neutron Environment - On the basis of the consideration of the diffusion-interaction between emitter and fuel, the clad systems operable at a temperature of 2073°K are narrowed down to (1) W-clad UC and UC-ZrC, (2) W-clad UO_2, and (3) Mo-clad 10 UC-90 ZrC. There is no long-term diffusion data for the Mo-(10 UC-90 ZrC) system; the satisfactory operation of this system therefore cannot be ensured at this moment. For the other two systems, the choice should be based upon the capability of the system to retain its dimension in a neutron environment. It is generally recognized that both the fuel and the emitter materials are mechanically soft at these high temperatures. The fission gases formed, if trapped inside the fuel as bubbles, tend to build up pressure. This leads to fuel swelling and subsequent deformation of the emitter, resulting in electrical shorting of the cell. The proposed solution to this difficulty is the use of relatively low density fuel containing open pores so that the release of the fission gases from the fuel is facilitated and the swelling of the fuel minimized. The released fission gases, however, would have to be bled from the emitter-can (cladding) to prevent pressure buildup and thus the rupture of the can. In the process of bleeding the fission gases from the emitter-can, the vapor transport of the fuel also occurs. Since UO_2 has a vaporization rate about 100 times higher than UC and 10^4 times higher than 20 UC-80 ZrC, it would obviously suffer a much heavier vaporization loss than UC and UC-ZrC (see Fig. 2). In addition, because of the poor thermal conductivity of UO_2, the fuel centerline would be much higher than that in UC or UC-ZrC fuels for the same emitter-can temperature. This would further enhance the vaporization loss.

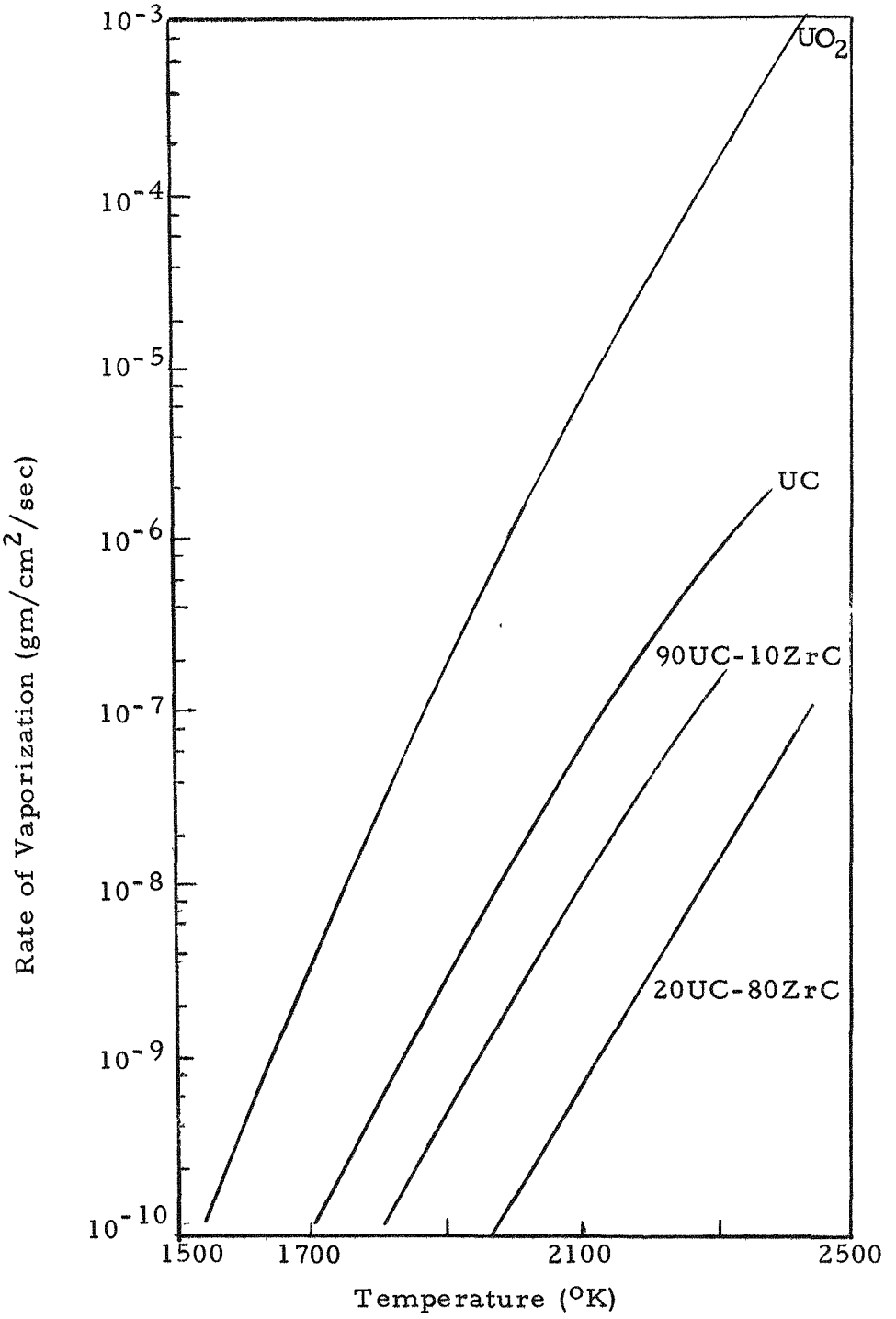

Fig. 2--Rate of vaporization of UO_2, UC, and UC-ZrC in vacuum

It has often been suggested that the vaporization loss of the fuel can be reduced if the fuel is dispersed in a continuous W or Mo matrix as a cermet. The additional advantages are the higher thermal and electrical conductivities of the cermet, which helps to reduce the fuel centerline temperature and also the Joule loss of the electrical output. It must be pointed out, however, that the use of a cermet fuel is more for fission gas retention rather than for fission gas release and thus defeats the original purpose of trying to maintain the emitter dimension by releasing the fission gases from the fuel body. The metal matrix is fairly weak at these temperatures. At 2073°K the yield strength of W is about 1000 psi, while the yield strength of Mo is less than 300 psi. The ability of these metal matrices to withstand the fission gas pressure generated in the fuel particle without excessively reducing the fuel fraction in the cermet remains to be proven.

In contrast to UO_2, UC stabilized with ZrC or other refractory metal carbides (such as Mo carbide) has low rates of vaporization and good electrical and thermal conductivities. It has been shown that UC-ZrC particles less than 40 micron in size, readily release fission gases at about 2100°K. Fabrication techniques for the production of UC-ZrC bodies of controlled pore structure and the release of fission gases from such bodies are currently under investigation at General Atomic.

A comparison of the problem areas for clad emitter systems using W and Mo and operating at 2073°K is shown in Table 1.

Not given in Table 1 is the high vapor pressure of Mo at high temperatures, since it has been shown that the presence of cesium vapor can reduce the vaporization loss of Mo. The difficulty in fabricating and joining W parts, experienced by previous workers, is no longer a serious problem. Recently the fabrication of fueled W emitters by cladding the fuel with thermochemically-deposited W from W halide vapors has proven to be an easy and versatile technique. Not only is the clad impermeable to helium but also the clad emitter is dimensionally stable after repeated thermal cycling. The thermal bond between the emitter and the fuel is excellent since the W is formed directly onto the surface of the fuel. Furthermore, no appreciable grain growth has been observed after being heated at 2073°K for over 1000 hours in vacuum. The shape of the fuel body (flat disc, cylindrical body, doughnut-shaped) which can be clad is almost unlimited and the emitter stem can be bonded to the emitter by the same technique during a one-step cladding operation.

Table 1

COMPARISON OF PROBLEM AREAS FOR CLAD EMITTER SYSTEMS USING W AND MO AT 2073°K

Emitter (cladding)	Fuel		
	UC-ZrC	UO_2	UO_2 Cermet
Mo	1. Only 10 UC-90 ZrC has been studied	1. Work function of Mo affected by fuel diffusion	1. Fission gas release impeded. Ability to retain fission gases without swelling to be proved
	2. Long-term compatibility test lacking	2. Excessive loss of fuel during fission gas bleeding	2. Fuel fraction is reduced
		3. Fuel has low thermal and electrical conductivities	3. Long-term compatibility test lacking
W	1. Satisfactory on basis of laboratory tests. Long-term irradiation properties to be studied.	1. Excessive loss of fuel during fission gas bleeding	1. Fission gas release impeded. Ability to retain fission gases without fuel swelling to be proved
		2. Fuel has low thermal and electrical conductivities	2. Fuel fraction is reduced

Figure 3 is a photo of the as-deposited appearance of UC cylindrical bodies supported on W stems and clad with W deposited from a mixture of $WF_6 + H_2$. Figure 4 shows the appearance of a UC disc clad with vapor-deposited W in the as-deposited state and after polishing. This technique eliminates the objection raised against the use of W for thermionic applications because of its poor fabricability. Moreover, the vapor-deposited W, formed under controlled conditions, may offer the opportunity of obtaining an emitting surface of reproducible performance.

Thus, the above materials considerations clearly indicate that at this time the preferred clad emitter system is the W-clad UC-ZrC system.

2.2.3 Emitter Stem

In the test cell, the emitter stem maintains the emitter-collector spacing. Since a cantilever design was chosen, there is a possibility of non-uniform expansion and resulting shortening of electrodes if care is not taken in choosing the stem materials. Tantalum was chosen for the stem material rather than niobium because its thermal expansion coefficient is closer to that of tungsten. Also, tantalum is easily diffusion-bonded to tungsten, forming tantalum alloy at the interface.

Although stems of cast or sintered tungsten or tungsten alloy were not chosen because of the brittle failure problem, vapor-deposited tungsten may be a possible candidate for the stem material since this form of tungsten is found to be relatively fine-grained and ductile.

The stem of the unclad UC-ZrC emitter was composed of a short transition of normal uranium UC-ZrC joined to a tantalum stem. Normal uranium carbide is used to decrease the temperature at the tantalum-carbide joint.

2.2.4 Collector

The maxiumum operating temperature of the collector in the Mark VI cell is 1000°C. The refractory metals are the only materials suitable for use at this temperature because of their strength and the matching thermal expansion of the ceramic electrical insulator. Niobium was selected for the collector material for the following reasons:

1. Niobium has a thermal expansion coefficient that matches the coefficients of Al_2O_3 and BeO more closely than that of any other pure refractory metal. This is shown in Fig. 5, where the linear expansion coefficients (as a function of temperature) of ceramics and various metals are compared. At a temperature

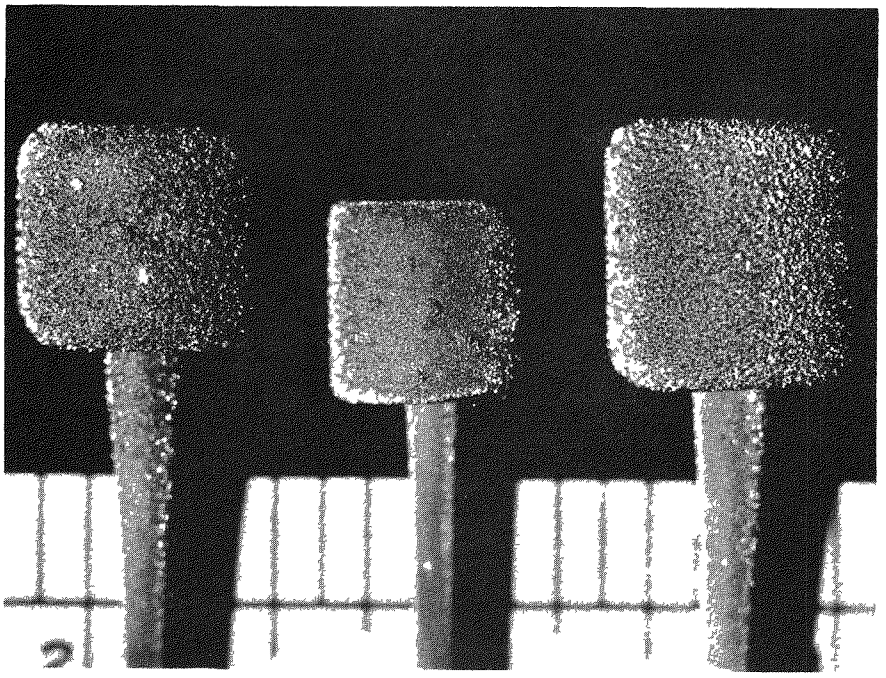

Fig. 3--Cylindrical UC bodies supported on tungsten rods and clad with thermochemically-deposited tungsten

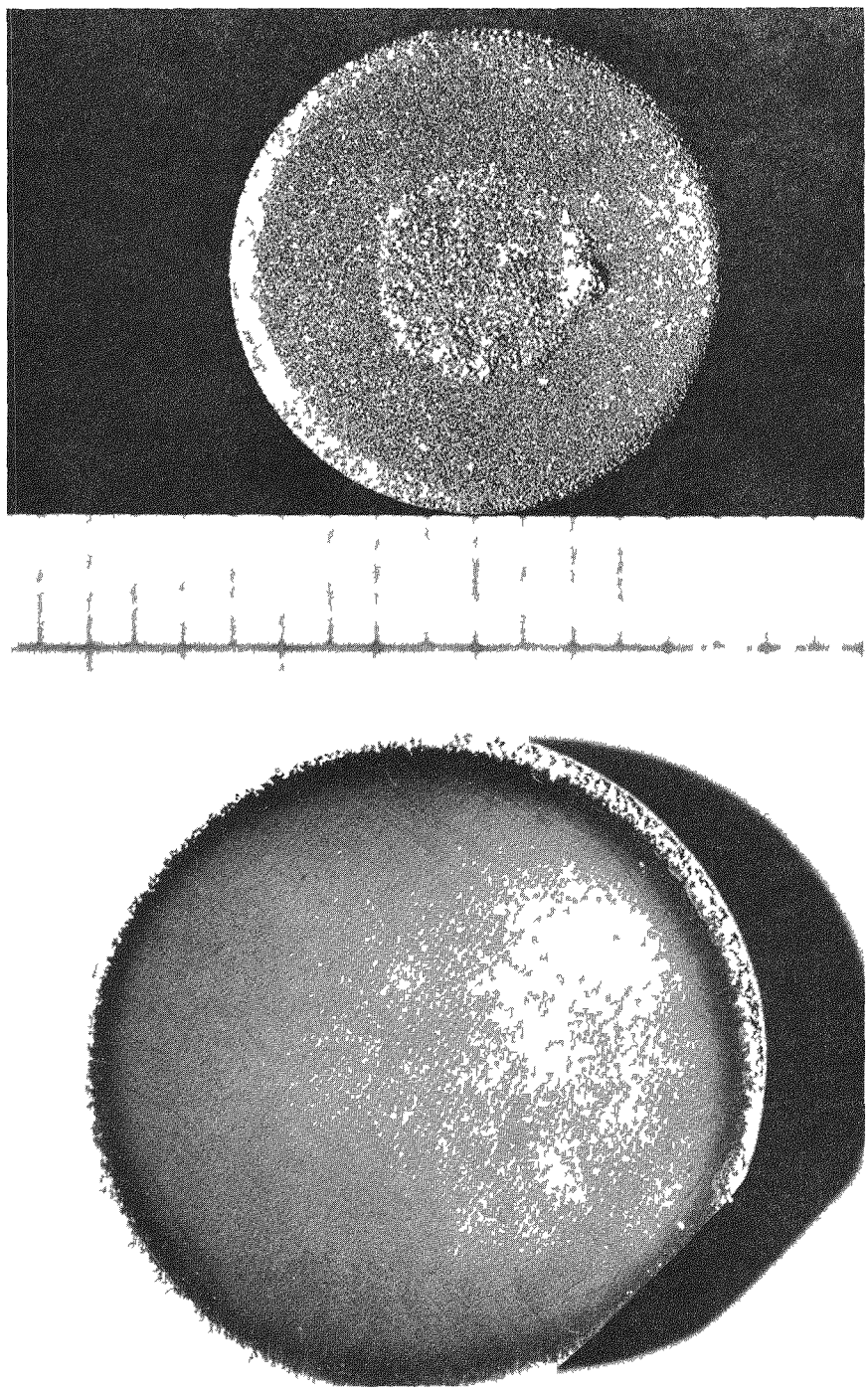

Fig. 4--UC disc clad with thermochemically deposited tungsten
(a) As-deposited
(b) Appearance of clad surface after polishing

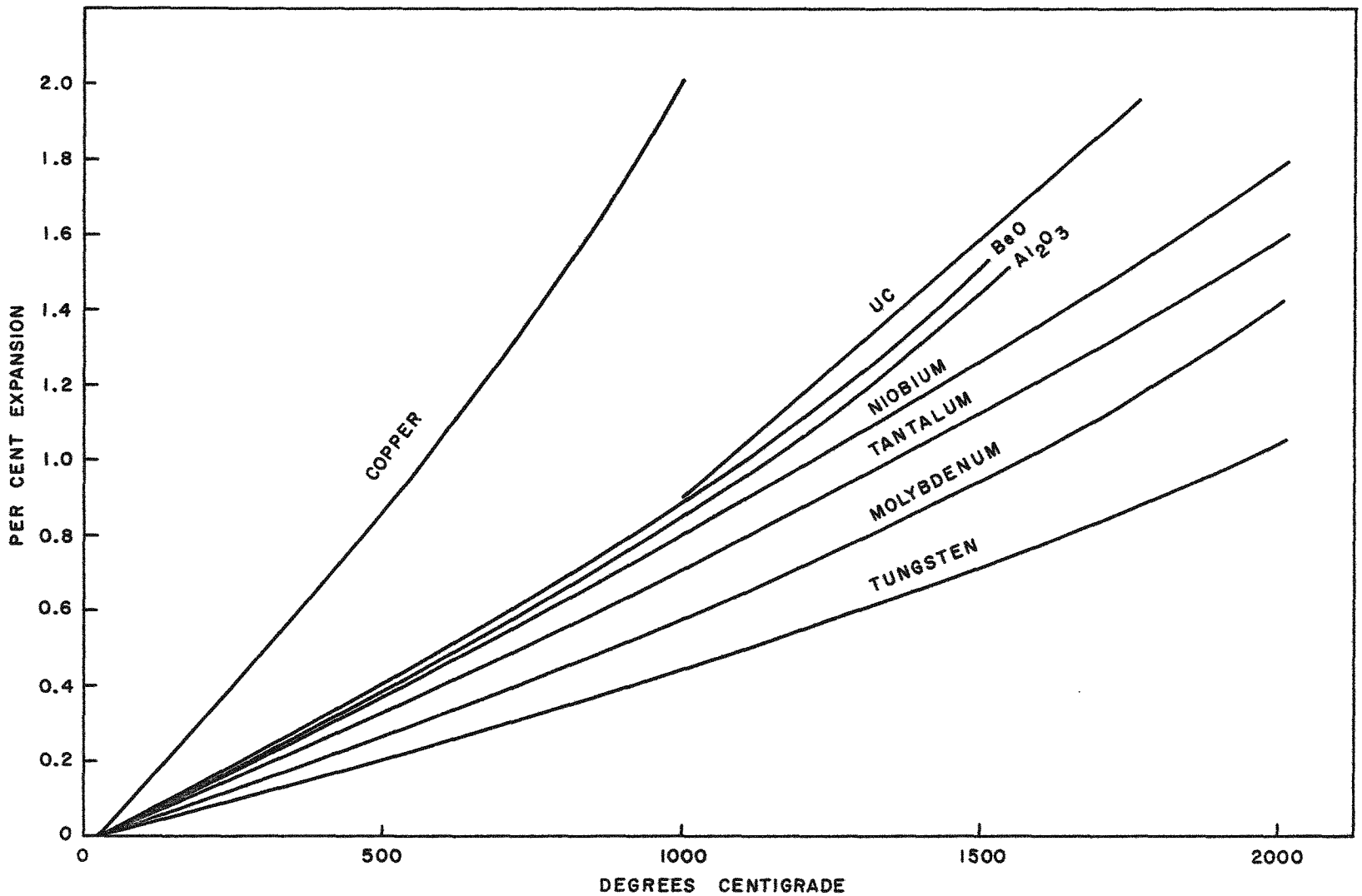

Fig. 5--Comparative thermal expansion of materials for thermionic cells

of 1000°C, the differential expansion is 0.0004 in. per in. Since the ceramic expands into the niobium, an Al_2O_3-niobium insulator interface is in compression. The resulting tensile stress in the niobium (1-in. diam. seal) is close to its yield strength of 10,000 psi.

2. Niobium is compatible with corrosive liquid-metal coolants such as lithium at high temperatures.
3. Niobium is relatively easy and economical to fabricate; i. e., it has good machineability, is easily welded, and is brazed with high temperature brazes.

2.2.5 Interelectrode Insulator

The insulator material used in the Mark VI test cell is high-purity, high-density Al_2O_3. The metal-to-ceramic seal is designed to be stress free as far as possible. The choice of niobium with alumina insulation was predicated on the fact that both materials have nearly the same thermal expansion coefficients; hence, the thermal stress in the seal is at a minimum.

2.3 TEST CELL COMPONENTS

The configurations of the Mark VI test cell evolved from experience with two previously developed cell designs. The first cell design was designated as the Mark IV series and was developed for in-pile testing. The final cell of that series is shown in Fig. 6. The second cell design was the Mark V* and is shown in Fig. 7. The Mark V was developed for laboratory testing of unclad uranium-zirconium carbide fuel-emitters with high temperature collectors. The technology from both the Mark IV and Mark V programs was utilized in the design of the Mark VI test vehicle which is shown in Fig. 8. The following sections describe the components of this vehicle.

---

*Developed under USAF sponsorship.

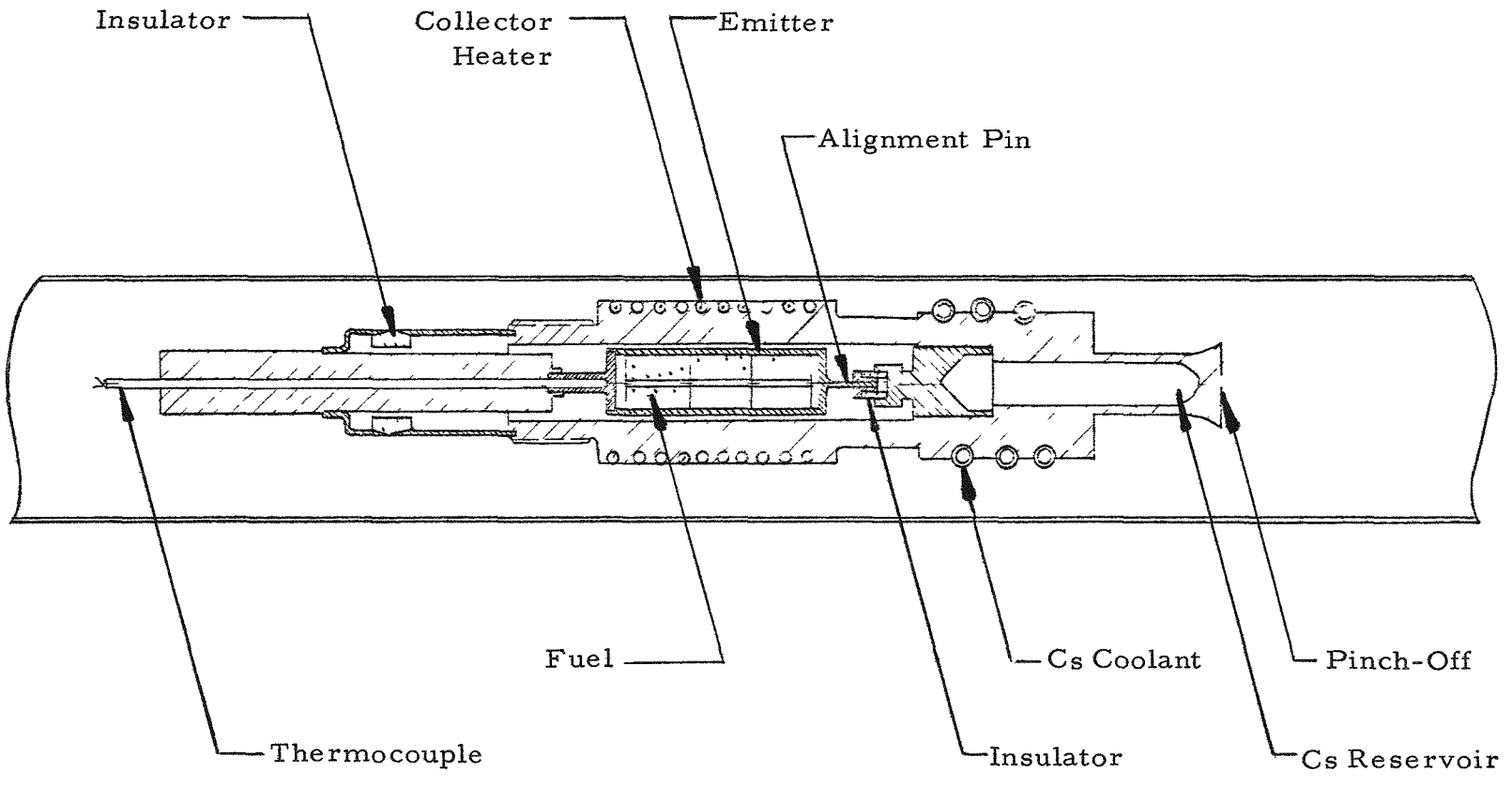

Fig. 6--Mark IV cell for in-pile testing

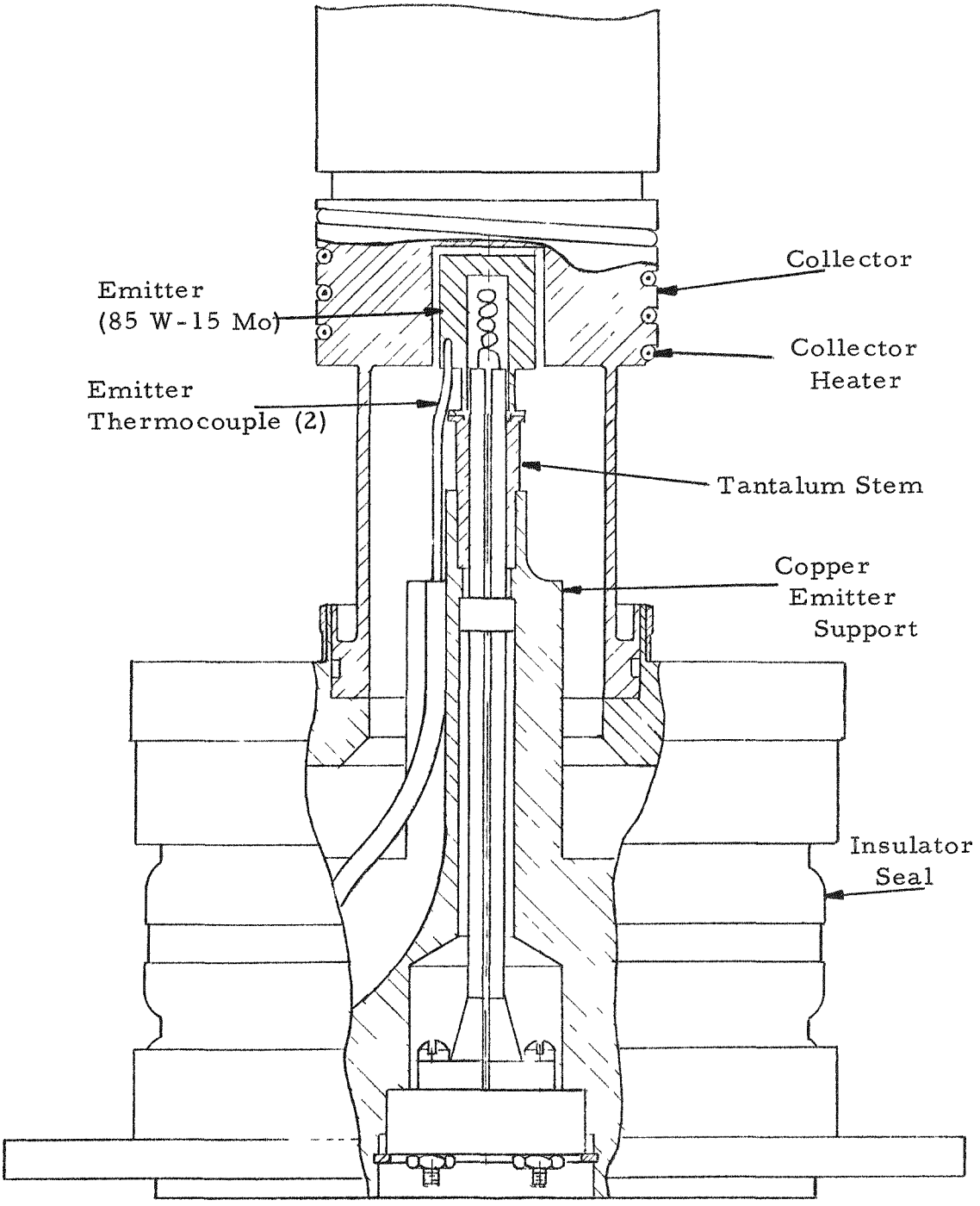

Fig. 7--Mark V cell design

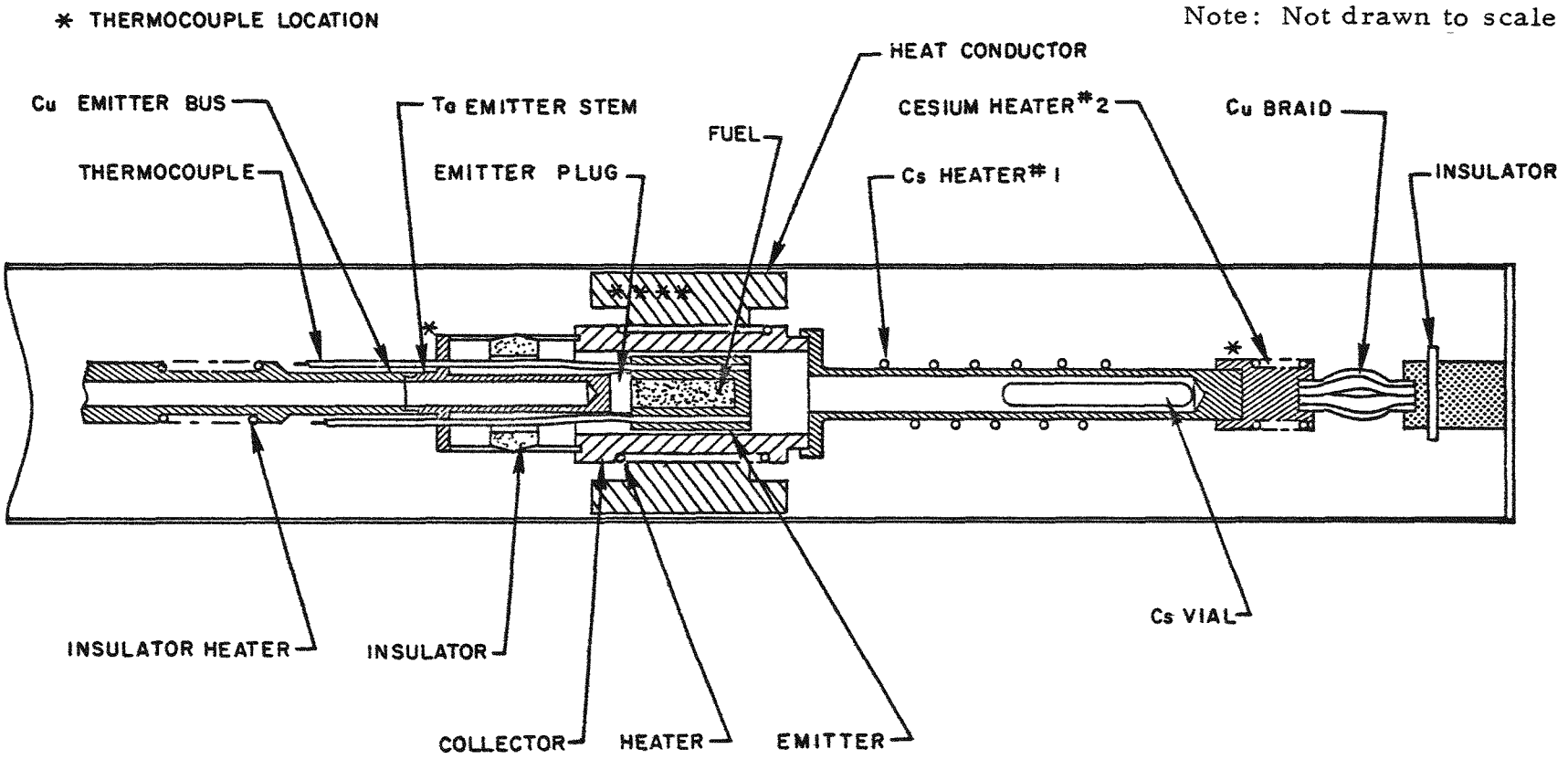

Fig. 8--Mark VI test cell for in-pile testing (IC-1)

2.3.1 Fuel-Emitter Assemblies

Two basic fuel-emitters were utilized in the in-pile test series - unclad UC-ZrC and tungsten-clad UC.

Tungsten-Clad Emitter Assembly - The tungsten emitter assembly design is shown in Fig. 9. The tungsten can (cladding) has 8 holes machined axially along the wall. Four of these holes are closed at one end and four are open at both ends. The open holes are for high-temperature emitter thermocouples and the closed-end holes are for fuel pins. The fuel pins are used to provide fuel near the emitter surface in order to simulate 20-mil cladding conditions in the relatively thick emitter can. The fuel pins are sealed into the holes by plugs pressed into the open ends. The tungsten emitter cap is diffusion bonded on top of the canned tungsten emitter to seal the fuel inside the can. An intermediate foil of 75 percent tungsten-25 percent rhenium is used to connect the bond between the cap and the emitter. The tantalum stem is then diffusion-bonded directly to the emitter cap.

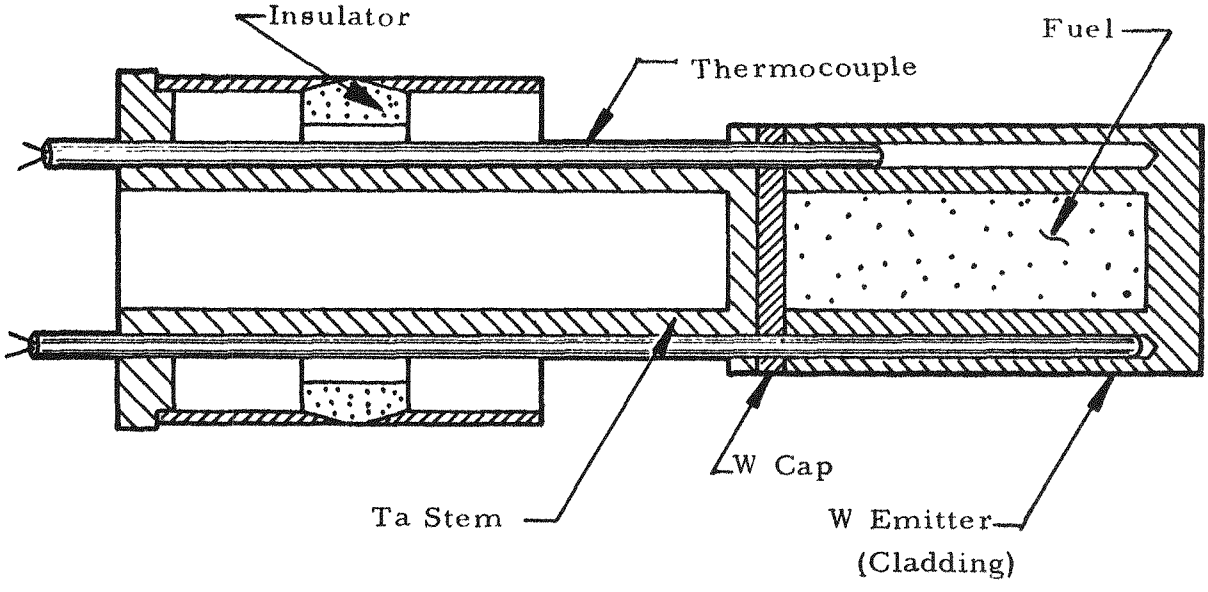

Fig. 9--Tungsten emitter assembly for Mark VI in-pile test cell (IC-1)

Unclad Emitter Assembly - The unclad emitter assembly design is shown in Fig. 10. The emitter is composed of UC-ZrC with a composition of 30 UC-70 ZrC. A tantalum stem is brazed to the emitter base with a Zr-Mo braze. A tantalum-sheathed tungsten-rhenium thermocouple is inserted inside of a tungsten thermocouple well in the center of the fuel-emitter. The thermocouple sheath is sealed into the tantalum stem by a copper braze in the top of the cell.

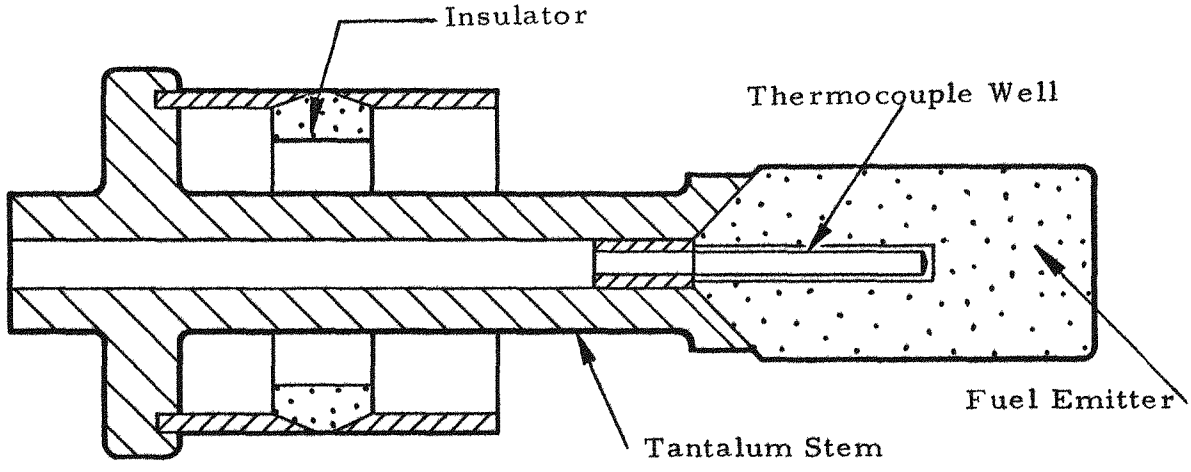

Fig. 10--Unclad UC-ZrC emitter for Mark VI in-pile test cell (IC-2)

2.3.2 Emitter Stem

Both the clad and unclad fuel-emitters are supported in a cantilever fashion by a rigid hollow tantalum stem. The cantilever support has maintained the emitter-to-collector spacing of 0.01 inch during 300 hours of high temperature operation. Post test analyses of cell components have indicated that no problems developed in the cantilever support during the test period. The length-to-area ratio was chosen for optimum operation at an efficiency of 10 percent and an ouput current of 10 amps/cm, using the following equation:

$$R_o = \frac{1}{JA_e}\left[\frac{2\eta}{(1-\eta)}\,\rho k(T_1-T_2)\right]^{\frac{1}{2}}$$

where:

J = current density, amp/cm^2
η = cell efficiency
ρ = stem electrical resistivity, ohm-cm
k = stem thermal conductivity, watt/cm$^\circ$C
T_1 = emitter temperature, $^\circ$C
T_2 = sink temperature, $^\circ$C
$R_o = \rho(\ell/A_e)$
ℓ/A_e = stem-length to cross-sectional-area ratio, cm^{-1}
A_e = emission area, cm^2

The emitter stem dimensions for both the clad and unclad fuel-emitters were: length, 1.7 inches; o.d., 0.44 inch; i.d., 0.28 inch.

Copper bus bars, welded to the tantalum stem, carried the cell current to the external load. The stem is kept above cesium reservoir temperature by the heat from the emitter which flows to a water sink and the copper bus bar. Electrical heat is provided for maintaining the stem temperature when the emitter is not heated.

2.3.3 Collector Assembly

The collector for the Mark VI test cell is made of niobium and is wrapped with a two-foot length of sheathed and insulated heater wire brazed to its outside surface. A niobium conductor sleeve is brazed to the collector outer surface over the heater wire. This sleeve conducts the heat radially to the outer container which is surrounded by water. Two thermocouples located at different radial locations in the conductor are used to measure the heat transfer to the collector to provide a means of calibrating the power input to the cell in the reactor through calorimetry. The outer surface of the collector heat sink assembly has a coating of Al_2O_3 to insulate it electrically from the metal outer container. The refractory metal collector extends about one inch below the emitter where it joins to a cesium reservoir assembly.

2.3.4 Interelectrode Spacing

An interelectrode spacing of 10 mil was selected for the Mark VI cell. The primary engineering limitation on the spacing is determined by the close tolerance required between the insulator and the collector. This is because the final assembly alignment between the emitter and the collector is obtained by self-jigging the collector and insulator on the emitter assembly. However, it has been demonstrated in the fabrication technique that this alignment method maintains a tolerance on the interelectrode

spacing to within one mil so that the spacing can be maintained to within ±10 percent.

2.3.5 Interelectrode Insulator Seal

The insulator seal of the Mark VI test cell is made of Al_2O_3 ceramic joined to niobium metal and is purchased from Litton Engineering Laboratories. Copper braze is used for joining the metalized ceramic to the niobium. The maximum operating temperature of the seal has been 850°C in a cesium vapor of 10 mm Hg vapor pressure.

2.3.6 Cesium Reservoir Assembly

The cesium reservoir tube is made of niobium and it is welded to the bottom of the collector. A copper tube welded to the cesium reservoir tube is used for final bake-out, evacuation, and sealing of the cell. Cesium is contained in a Kovar metal capsule in the niobium cesium reservoir tube. The cesium vial is opened after final bake-out pinch-off. A sheathed heater is provided to maintain the cesium reservoir at the desired temperature. Another heater on the niobium tube maintains it at temperatures above the cesium reservoir sink temperature.

2.4 INSTRUMENTATION AND CONTROL

The thermal design of the Mark VI test cell permits investigation of thermionic performance with many combinations of cell parameters. In addition to the emitter, there are three independent heating systems: the insulator, the collector, and the cesium well. These individual heating systems allow wide, independent variations of emitter, insulator, collector, and cesium temperatures, thus permitting investigation of all thermionic modes of operation. Descriptions of the various heat-transfer systems and the degree of control of each are found in the following subsections.

2.4.1 Emitter

The emitter temperatures and their distribution are measured by four tungsten-rhenium thermocouples. These thermocouples measure the axial distribution of the emitter surface temperature. Heat is supplied to the emitter by nuclear fission during in-pile operation. Heat transfer occurs by conduction along the emitter bus by thermal radiation and by evaporative cooling resulting from electron emission from the emitter surface.

2.4.2 Upper Insulator

An auxiliary heater on the copper emitter bus bar maintains the insulator temperature above the cesium condensation temperature. The heat sink for this heater is a water coolant line brazed to the bus bar above the heater. This system is capable of maintaining insulator temperatures between 350°C to 650°C, depending on the emitter temperature.

2.4.3 Collector

An auxiliary heat source for the collector is provided by an auxiliary heater brazed on the outside of the niobium collector. A niobium conductor sleeve is brazed to the collector. The heat is conducted across a gas space to the secondary containment can and to the reactor pool water. An additional temperature control is provided by varying the helium content of the helium-argon (or neon) gas mixture in the secondary containment. This heat transfer system is capable of maintaining the collector temperature within a range of 450°C to 1000°C. Two thermocouples measure the collector temperature. Two additional thermocouples measure the outside surface temperature of the niobium conductor. These radially-spaced thermocouples permit a calibration of the thermal power transferred to the collector.

2.4.4 Cesium Well

Two heaters are provided for cesium temperature control. The lower heater is used for maintaining the desired cesium temperature. It is automatically controlled and provides the bulk of the power for control. An auxiliary guard heater is wrapped around the length of the cesium well. A tantalum radiation shield is wrapped over the heater. The heat for cesium temperature control is conducted through a copper flexible lead to the stainless steel fuel element tip and thence to the reactor pool water. The cesium temperature is automatically maintained by control of the current to the lower heater. The auxiliary heater is maintained manually at collector temperature when the lower heater is controlling the cesium temperature.

2.5 TEST CELL

The in-pile Mark VI test cell is contained in a 1.5-in. diameter stainless steel TRIGA-type fuel-element cladding tube. All of the leads for thermocouples, coolant lines, and heater leads are brought through an epoxy seal at the top of the stainless steel tube and then through a 2-in.

aluminum tube to the reactor room floor. The containment tube is sealed by epoxy about 4 feet above the reactor core and by a gas-line valve at the top of the reactor. The sealed containment is baked out, evacuated, and then purged with helium. After purging, a backfill of helium is sealed inside the secondary containment, providing an inert gas environment around the niobium collector. During in-pile operation, this containment is continuously purged with a purified inert gas to sweep the gases evolved from the containment from the vicinity of the cell. The primary containment of the cell is the niobium collector, the cesium well, and the insulator assembly.

2.6 OUT-OF-PILE PROTOTYPE TEST CELL

In order to provide a design check for the in-pile operation of the Mark VI test cell, the design of the Mark VI was modified to accomodate electron bombardment heating of the emitter. The emitter assembly for the out-of-pile test-cell is shown in Fig. 11 and the cell is shown in Fig. 12. Although the central fuel plug of the in-pile Mark VI has been replaced by an electrical filament, the four fuel pins are still maintained in the emitter wall. Except for the change in the mode of heating between the in-pile and out-of-pile operation, the prototype was essentially identical to the test cell.

In order to mock-up the package configuration of the in-pile Mark VI, the out-of-pile prototype was also contained in a 1.5-in. diameter stainless steel tube. The tube is inserted in a tank of water for operation. This type of out-of-pile operation provided heat transfer data for the in-pile tests.

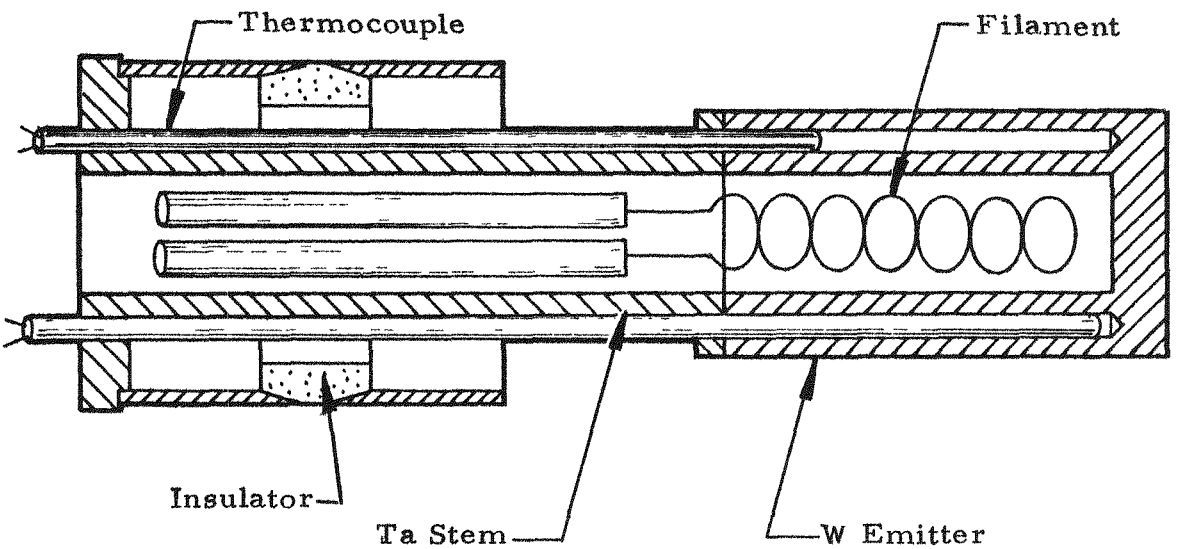

Fig. 11--Tungsten emitter assembly for out-of-pile testing

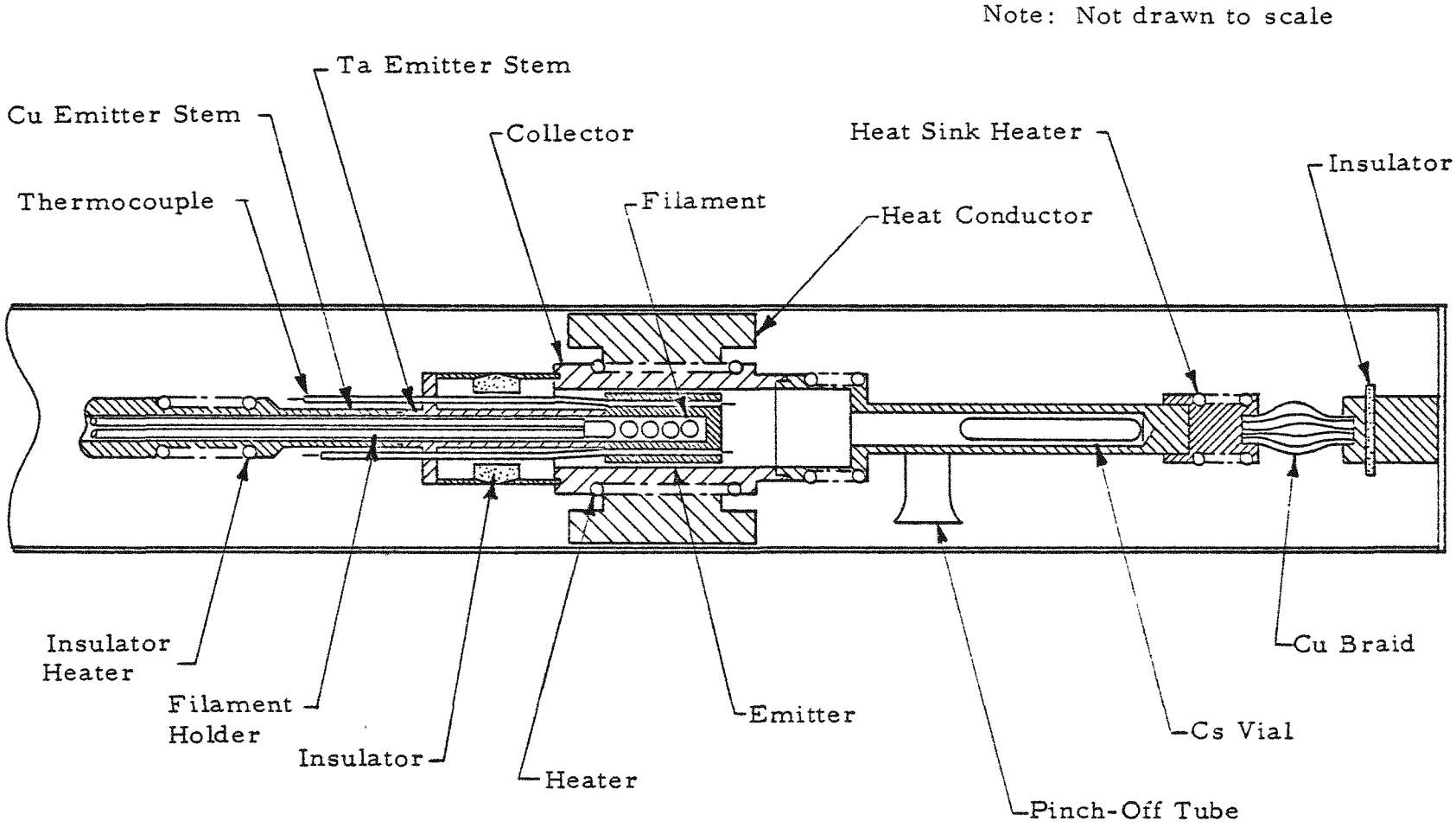

Fig. 12--Mark VI out-of-pile test cell with tungsten emitter

BLANK

III. FABRICATION DEVELOPMENT

The work carried on in the fabrication development area includes work on the development of manufacturing processes for thermionic converters and a complementary effort on process and component evaluation. Work on manufacturing processes includes metal-to-metal joining, metal-ceramic joining, assembly techniques, and emitter fabrication. The evaluation efforts include environmental and mechanical testing of metals being considered for use in the construction of thermionic converters, as well as supporting experiments to demonstrate that a given process satisfies the converter requirements.

The metals used in the fabrication of high-temperature thermionic converters for potential application to space reactor systems are largely materials for which little fabrication technology is available. They include tungsten, tantalum, niobium, beryllia and alumina ceramics, and various refractory uranium compounds. The requirements for long lifetime at high temperature in a nuclear environment and in the presence of high-temperature cesium vapor militate against many of the conventional methods of joining these materials. The noble metals are strongly attacked by cesium vapor, and copper is attacked at a slow rate. Ultimately, the ceramics employed in thermionic reactor fuel elements must operate at temperatures of the order of 1000°C and must simultaneously provide vacuum seals and electrical insulation. The single thermionic cell, and later, the thermionic reactor fuel elements, will require advancement of high-vacuum fabrication technology.

3.1 DEVELOPMENT OF MANUFACTURING PROCESSES

3.1.1 Metal Joining

Table 2 presents a summary of the requirements and the brazing methods used in making the necessary metal-to-metal joints for the Mark VI thermionic cell. Brazing is included as a manufacturing method for metal-joining where it is possible to maintain close dimensional tolerances through use of the self-jigging technique during assembly operations. This may be more critical when multiple converters are manufactured, where the accumulative tolerances will become important in assembly alignment.

Table 2

OPERATING REQUIREMENTS AND JOINING METHODS FOR METAL-TO-METAL JOINTS

Joint	Location of Joint	Max. Joint Operating Temp. (°C)	Braze Alloy	Brazing Temp. (°C)	Comments
W-W	Tungsten cap to seal fuel into tungsten emitter (in-pile cell)	2000	Zr-31.2 Mo. Diffusion bond with rhenium foil Diffusion bond with W-25 Re foil	1650 1700 1700	Remelt >2150°C Remelt ~3900°C Remelt ~3900°C
W-Ta	Seal between the filament chamber and the internal cesium chamber and supporting fueled emitter	2000	Zr-5.7 Be Diffusion bond	1200 1700	Remelt >2150°C Remelt >3000°C
Ta-Ta	Thermocouple seal to tantalum emitter stem	800	Zr-5.7 Be Cu Cu-28 Ti	1200 1150 900	Remelt >2000°C No increase in remelt Remelt temp. approaches Cu melting point
Ta-Nb	Tantalum emitter stem to insulator	1000	Cu Shielded Arc Weld	1150	No increase in remelt
Ta-Cu	Bus-bar joint to emitter stem	800	Cu-28 Ti	900	Remelt temp. approaches Cu melting point
Nb-Nb	Collector-to-insulator seal and collector-to-Nb cesium well	1000	Cu Cu-28 Ti Shielded Arc Weld	1150 900	No increase in remelt Remelt ~1050°C
Nb-Ni	Collector-to Ni-cesium well	700	Cu	1100	No increase in remelt
Cu-Cu	Bus-bar joints	300	Ag-28 Cu	800	
Cu-Inconel	Bus-bar heater to bus-bar	800	Au-20 Ni	950	
Nb-Tantalum	Collector heater sheath to collector	800	Cu	1100	

The fuel-emitter in the in-pile Mark VI test cell was fueled with UC and clad with tungsten. To prevent vaporization of the fuel and release of fission products into the cesium volume, it was necessary to provide a tungsten-to-tungsten joint capable of operation at 1800°C for long periods of time. Several methods were investigated to provide this seal. Electron-beam welding was ruled out very early because of a reaction between the uranium fuel and the tungsten at the welding temperature. The use of the Zr-Be alloys was also unsuccessful because of difficulty with the unstable beryllides. More recent efforts on developing the tungsten-to-tungsten joints have employed diffusion-bonding techniques involving high pressure in a vacuum environment and extremely clean materials. The resulting bonds are vacuum leak tight and have extremely high remelt temperatures, as indicated in Table 2. The joints were successfully made using thin foils of zirconium, rhenium, and an alloy of 75 percent tungsten - 25 percent rhenium as the interface material between the tungsten parts. The present technique uses the tungsten-rhenium interface foil. This introduces the least amount of extraneous material to the emitter surface. The diffusion bond technique is also used successfully to bond the tantalum stem to the tungsten emitter.

The Mark VI thermionic converter is equipped with four emitter thermocouples. These thermocouples are W-(W-25% Re) insulated with BeO and sheathed in tantalum. The thermocouple sheath penetrates the cesium envelope, and it must be sealed to the emitter stem to complete the envelope. From a mechanical point of view, copper brazes have been found to be satisfactory for forming this joint. For extremely long life (>1000 hr) in a cesium environment, a copper braze would not be satisfactory. For this reason, active metal brazes such as zirconium-beryllium and copper titanium have been investigated. These brazes have been successful in a number of cases; but in others the braze has not provided a leak-tight vacuum seal. It has been found that sequential brazing at times adversely affected the joint previously made with the active braze material. Further investigation of process variables is necessary.

The cesium well in the preliminary development of the Mark VI was made of nickel. The first design utilized a nickel pinch-off tube. The nickel-cesium well was joined to the niobium collector by a copper braze. It was known that an exothermic reaction between nickel and niobium occurs at about 1300°C. To avoid this reaction, the cesium well was changed to niobium; however, after the remote assembly technique described below was developed, separate cesium wells and collectors were not necessary. The copper braze joining was changed to preassembly inert-gas arc welding.

The joint between the niobium cylinder on the insulator and the tantalum stem was made with copper, copper titanium, and zirconium beryllium. This joint sometimes leaked after thermal cycling when the active metal brazes had been used. The copper brazing of this joint was difficult to perform because of the adjacent thermocouple seals which had to be changed to copper for reliability. Thus, after the inert gas-arc welder was developed, this tantalum-niobium joint was changed to an arc-weld.

The design of the Mark VI cell for out-of-pile testing has a requirement for a leak-tight joint between the tantalum emitter stem and the tungsten emitter. The first method investigated for this joint was electron-beam welding. This weld is brittle and usually failed after thermal cycling. It was then decided to investigate reactive metal brazing of the tungsten-to-tantalum joint. The alloy investigated was 94.5 Zr - 5.5 Be. However, the formation of tungsten-beryllides caused embrittlement and cracking after thermal cycling. The tungsten-beryllide WBe_{13} formed during brazing is unstable and volatilized during subsequent heating at about 1400°C. Also, during fabrication and operation the braze interface would sometimes oxidize resulting in leaks through the joint. The final method developed for this joint was diffusion bonding, accomplished by electrical-resistance heating the mating metal parts in a hot press. The bonding takes place at moderate pressure and temperature over a period of about 1 hr. This method has proven to be highly reliable for high-temperature leak-free operation.

Methods are presently under development to provide improved process control so that active metal brazes may be used; but until these processes are available, cell fabrication will proceed using copper-braze material, inert gas arc-welding, or diffusion bonding.

3.1.2 Metal-Ceramic Joining

Many of the critical mechanical features of the thermionic cell relate to the inter-electrode ceramic insulator-seal and the surrounding sandwich insulator required to isolate the cell from a liquid-metal coolant. It is necessary that the thermal expansion coefficients of the ceramic and metal envelope match almost exactly so that the assemblies will not fail under thermal cycling. The best available combination appears to be niobium joined to either an aluminum-oxide or beryllium-oxide ceramic. This combination has the additional advantage that there already exists a significant technology on the use of niobium as a structural metal with lithium as a coolant for possible future reactors.

The Mark VI cell design allows sufficient distance between the collector and the electrical insulator so that the ceramic-metal seal

does not operate at excessively high temperature. This permits the use of conventional techniques for joining Al_2O_3 and niobium. An Al_2O_3-niobium insulator sealed with copper and metallized with tungsten-iron was procured from the Litton Engineering Laboratories. This seal has proven very reliable in the operation of the Mark VI cesium cell at temperatures up to 850°C in a cesium-vapor pressure of 10 mm Hg. However, it is predicted that, for very long operation (>1000 hr), the probability of failure will increase due to diffusion between iron, tungsten, and niobium, which form a brittle compound. Also, a copper braze is limited to a 1000-hr test because it is subject to slow cesium attack.

Early in the program, a limited investigation was conducted concerning methods of brazing niobium and Al_2O_3 with reactive metal alloys which directly wet Al_2O_3. The composition 70 Ti-30 Ni (mp 955°C, composition in wt-%) was investigated. This alloy wetted Al_2O_3 well and formed excellent joints when bonding niobium to Al_2O_3. The 70 Ti-30 Ni alloy appears to flow better on Al_2O_3 than Zr-Be alloys, presumably because no intermediate phases are formed. However, after thermal cycling, cracks appeared in this joint, apparently due to titanium diffusion into the ceramic. The composition 56.6 Nb-48.4 Ni (mp 1175°C) was investigated and was found to be quite brittle. Also, in the early phases of the program, Zr-Be compositions were investigated. These were 98 Zr-2 Be (hypoeutectic) and 90.5 Zr-5.5 Be (eutectic mp 980°C). Both alloys exhibited good wetting to Al_2O_3. Metallographic examination of specimens showed an intermediate metallic phase formed at the braze Al_2O_3 alloy interface. It is quite probable that this phase is $BeO \cdot 3\ Al_2O_3$.

In later investigations, niobium and Al_2O_3 were satisfactorily brazed with the alloys 94.3 Zr-5.7 Be (mp 1000°C) and 71 Zr-23 Re-6 Be without metallizing the Al_2O_3. These seal joints were thermally cycled and remained leak tight, as described in Section 3.5.

3.2 ASSEMBLY TECHNIQUES

The construction of a thermionic cell presently involves the fabrication of three subassemblies: the emitter, the collector, and the cesium reservoir. Each of these subassemblies may involve several metal-to-metal joints and perhaps a metal-to-ceramic joint. During final assembly, it is imperative that the cell be maintained in a clean condition and that the performance of the final assembly brazes does not adversely affect joints previously made. One of the major difficulties is that each assembly step requires close dimensional control that can be obtained only by jigging

and fixturing each subassembly before brazing. In the past, this operation has been performed on the bench and assemblies were then vacuum-outgassed before brazing. During this program, methods were developed to perform assembly and jigging operations after outgassing had been completed without breaking the vacuum. In this way, it has been possible to reduce the gas content of the cell to a point where previously-made brazes are not affected by the heating of adjacent joints.

One method of accomplishing a clean braze was to preplace a jig and braze material and assemble the emitter-collector assemblies in a vacuum tube for outgassing. This setup is shown in Fig. 13. The collector assembly is held on a pedestal support, and the emitter assembly is held on a pushrod which penetrates the vacuum through an O-ring seal. After both of these subassemblies have been outgassed in vacuum, the emitter assembly is lowered into the collector and jig assembly, as shown in Fig. 14. The joint is then taken to brazing temperature by rf induction heating. This manufacturing technique required an additional operation in air to join the cesium reservoir to the cell prior to final evacuation and bakeout of the cell.

Modifications and additions to this assembly procedure were made to allow complete assembly, bake-out, and sealing to take place in a single vacuum system without exposure to air during the intermediate steps. This was done by the addition of a second vacuum system to the assembly unit and minor design changes in the cell to allow self-jigging of the inter-electrode spacing and evacuation of the cell through the cesium reservoir. This allows the cell to be evacuated, baked out, and pinched off without exposing the cell to air. This processing technique was used satisfactorily in the assembly of the out-of-pile cell, OC-3, and the in-pile cells, IC-1, IC-1', and IC-2.

A schematic drawing of this remote assembly unit is shown in Fig. 15. The diagram to the left shows the assembly in the bakeout position. Each cell component is outgassed at a temperature above operating temperature using the rf induction coil with both vacuum systems in operation. Following outgassing, the emitter assembly is lowered into the self-jigging collector assembly that has been preloaded with braze material. This configuration is shown in the diagram to the right in Fig. 15. The final braze is then made using the induction unit and, after final outgassing, the cell is pinched off at the lower end of the cesium reservoir.

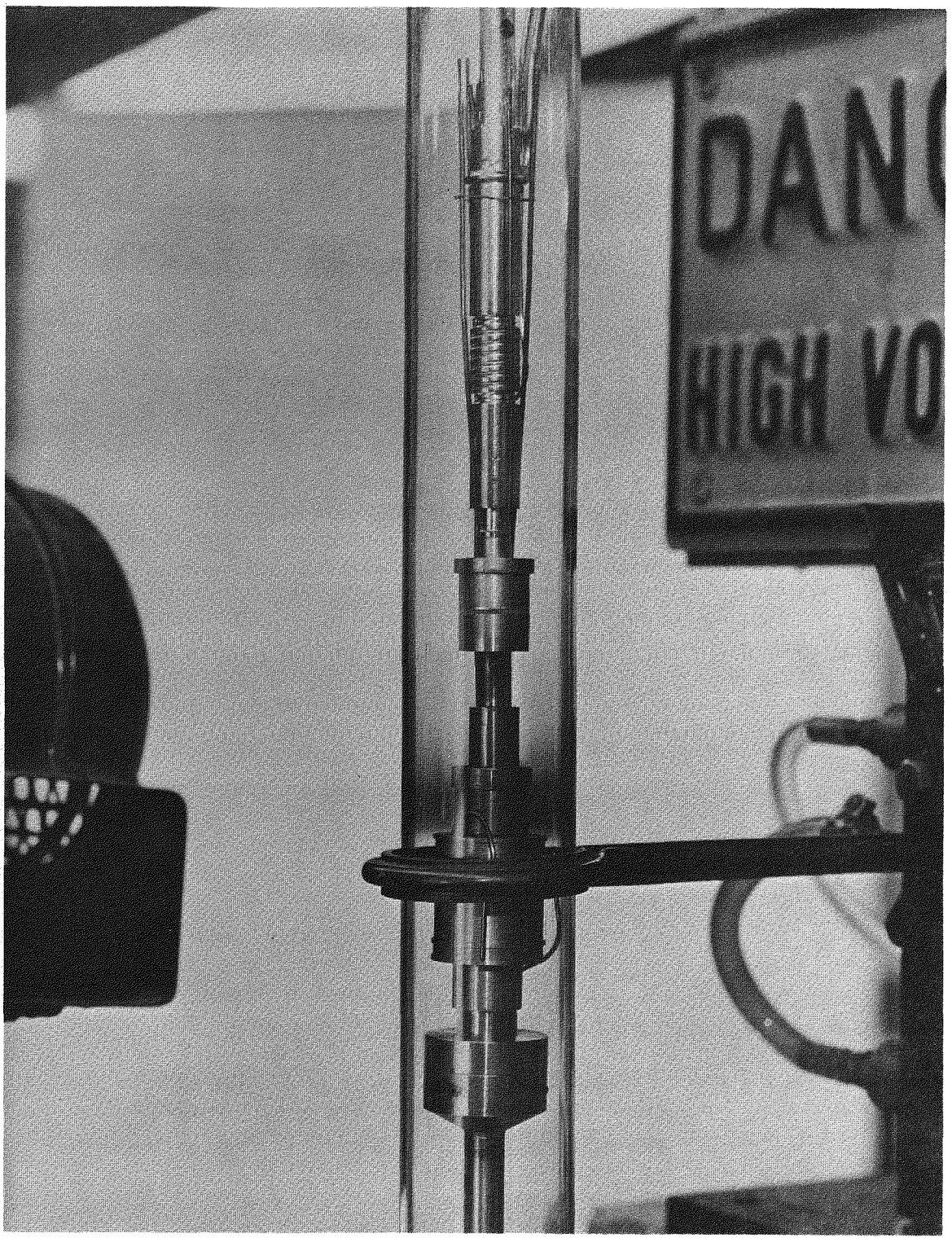

Fig. 13--Mark VI cesium cell being assembled remotely after high-temperature outgassing in vacuum with rf induction heating coil

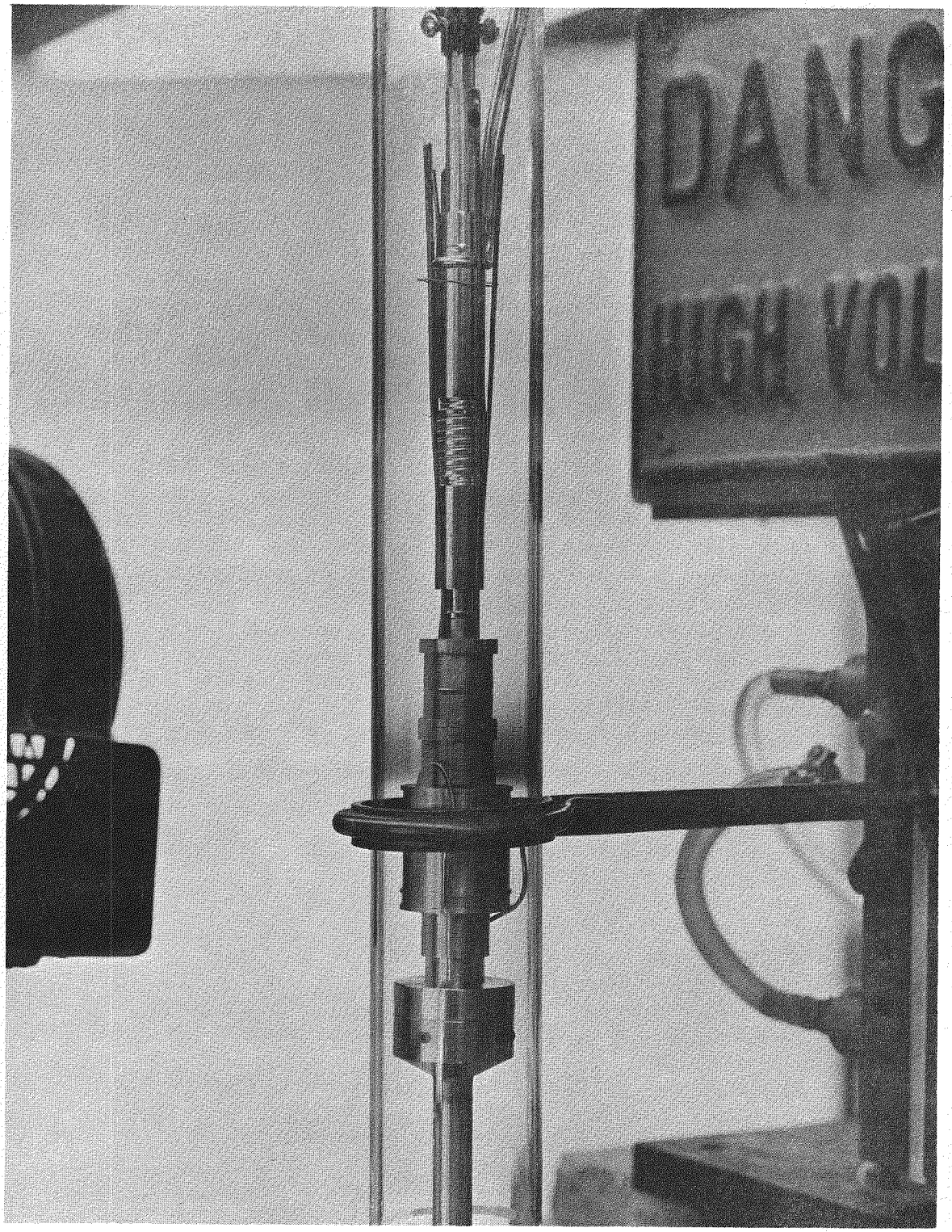

Fig. 14--Mark VI cesium cell assembled prior to vacuum brazing after high-temperature bakeout

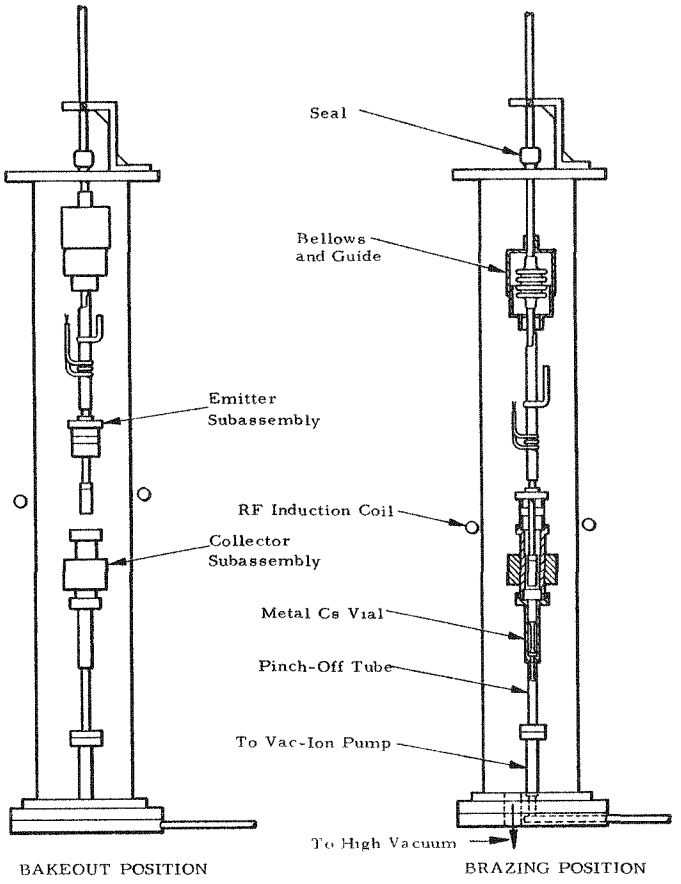

Fig. 15--High-vacuum remote assembly jig for Mark VI cell

3.3 CESIUM AMPOULE

Kovar metal was selected as the cesium ampoule material. The distillation into the Kovar tube is made presently through glass. Thus, the base part for this fabrication is a standard tubular glass-Kovar seal.

Methods were studied in detail for obtaining reliable pinch-off on one end and for filament-welding the other end of the Kovar tube. The Kovar is electropolished in hydrochloric acid and then pinched off on one end of the tube. Several of these tubes are then joined to a glass vacuum bakeout and distillation system and assembled in a bakeout oven as shown in Fig. 16. The glass cesium ampoules are then attached to the distillation system. The entire glass tubing and Kovar is then baked out at 450°C in the bakeout oven. After bakeout, the cesium is distilled into the Kovar tubes. The Kovar ampoule is then sealed by electro-bombardment filament-welding with the cesium portion held in a chill block. The ampoule is then ready to install in the cell for final outgassing.

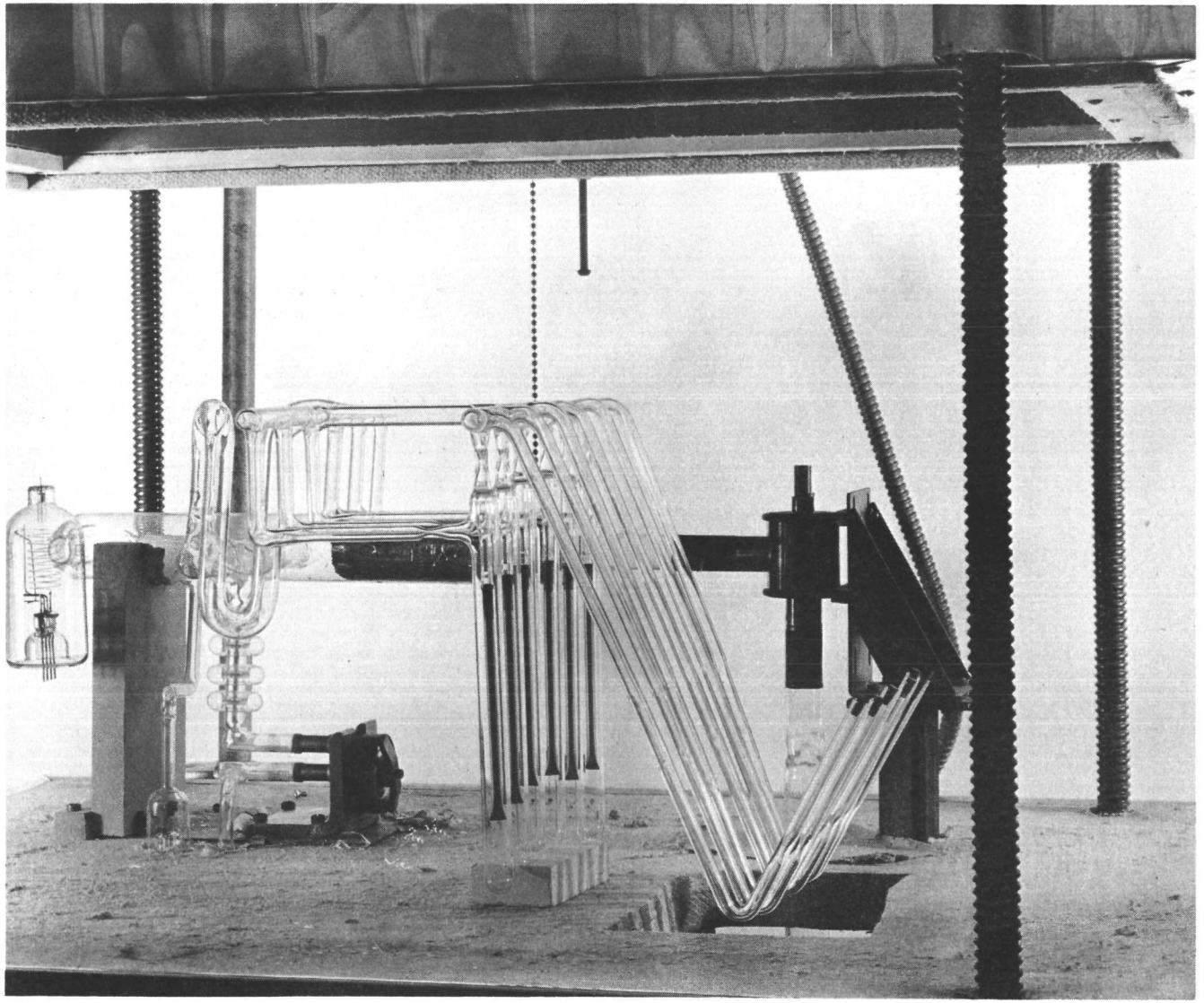

Fig. 16--Kovar capsule high-vacuum bakeout and cesium distillation system in bakeout oven

3.4 FUEL-EMITTER FABRICATION

During the program, work was carried out on fabrication of tungsten-clad UC fuel-emitters and on unclad UC-ZrC fuel-emitters for the out-of-pile and in-pile cells.

The tungsten-clad UC emitter of the current Mark VI cell is formed of machined tungsten and provides space for four emitter thermocouples. Two major difficulties have been encountered in the fabrication of this emitter. The first was the development of a reliable tungsten-to tungsten seal to prevent fuel and fission-product release to the cesium volume, and the second was the difficulty encountered in attempting to make thin-walled tungsten emitter sections leaktight. The UC fuels have now been successfully sealed using diffusion-bonding techniques to join tungsten to tungsten.

The problems associated with producing highly reliable thin-walled tungsten sections were attacked in two different ways. The cell design was modified so that it was not necessary to have a thin-walled tungsten emitter stem support structure. The tantalum-tungsten joint was then made by diffusion bonding. This modification removed one of the major causes for cell failure - the cracking of the thin-walled section in areas of high thermal gradients. In the simulation of typical cladding thicknesses by thin-walled machined tungsten, the major difficulty is primarily a material fabrication problem. Many of the tungsten samples received from suppliers have not only large grains but also incipient cracks.

The tungsten emitters for the Mark VI cell were fabricated from the following three types of tungsten during the development program:

1. Vacuum centrifugally-cast alloy of 98 percent tungsten and 2 percent molybdenum
2. Pressed, sintered and hot-swaged tungsten
3. Vacuum centrifugally-cast pure tungsten

In addition, the fabrication technique of thermal vapor deposition of tungsten-cladding over fuel forms was investigated.

Of all the materials investigated, the vapor-deposited tungsten had the finest grain structure; however, since this is primarily a development material, it was decided to use cast and hot-swaged 98 W-2 Mo alloy from the Oregon Metallurgical Corporation for the initial tests. This material has a grain size somewhat larger than the vapor-deposited tungsten but five times smaller than the cast-tungsten sample. Emitters fabricated from this W-Mo alloy have been successfully fabricated and thermal-cycled without apparent degradation.

With the exception of the vapor deposition method, the fabrication of the emitters from the three forms of tungsten is accomplished by carboloy tool machining, diamond grinding and cutting, and electrical discharge machines. The easiest type to fabricate is the W-Mo alloy.

The method that appears to offer potential economy is the vapor-deposition method. The feasibility of using vapor-deposited tungsten as a cladding for the fuel-emitter will be thoroughly investigated.

The principal problems with using either the cast or sintered tungsten were:

1. Difficult and costly machining
2. Brittle fracture of the bar during machining
3. Fracture of embrittled thin-walled sections (0.050 in. or less) after heating and thermal cycling

The 98 W-2 Mo alloy did not have the above disadvantages. However, in some of the fuel-emitters that were heated out-of-pile, the fuel apparently diffused through the emitter wall at temperatures in excess of 1800°C. A diffusion couple of this 98 W-2 Mo alloy showed that, at 1800°C, there was diffusion into the grain boundaries; however, this material is adequate for a tungsten emitter for periods of the order of 100 hours.

As a substitute for the W-Mo alloy, it is planned to develop an advanced fuel-emitter for the Mark VI test cell using the technique of thermochemical vapor deposition of tungsten. Experiments were conducted to assess the compatibility of chemical-vapor-deposited tungsten in contact with UC and UO_2. Also experiments to assess the thermal, mechanical, and dimensional stability of chemical-vapor-deposited tungsten cladding were conducted. UC pellets (1/4-in. diameter x 1/4-in. high) were coated with 0.030-in. thick tungsten and then thermally cycled to 1900°C five times. No change in the specimen dimension was noted, nor was any degradation of the coating observed during visual examination.

Studies of the orientation of vapor-deposited coatings on UC substrates were performed. While there is some disorientation, there is a heavily preferred orientation of the $\{100\}$ planes of the coating parallel to the specimen surface. Deposited coatings exhibit a rough appearance caused by tiny tetrahedra protruding perpendicular to the specimen surface. Measurements of the included angle at the apex of these tetrahedra, together with the crystallographic considerations, indicate that these are formed of familes of $\{111\}$ planes.

Techniques for fabricating 90 UC-10 ZrC emitters were investigated. One technique ivestigated was hot-pressing the carbide powder in a tungsten die at 1700°C and 650 psi. Densities up to 85 percent of theoretical were obtained. Also, a process for grading the emitter from high UC to 10 UC-90 ZrC or 100 percent ZrC during the hot-pressing was investigated. A satisfactory high-temperature brazed joint could then be made between the ZrC and a refractory metal with an equivalent thermal expansion coefficient.

During the second half of the program it was decided to use a lower fraction of UC in the UC-ZrC material because of information gained from out-of-pile cell tests which showed that the amount of UC in the compound did not alter the emission after the surface was activated. That is, the surface equilibrium concentration of uranium determines the emission rate, and this concentration is nearly independent of the bulk UC concentration. The nuclear calculations showed that a 5/8-in.-diameter UC-ZrC fuel-emitter with 20 mol-% or more of UC would result in sufficient fission power. Thus the 30UC-70ZrC was selected, since there was some fabrication experience with this compound. This eliminated the necessity of grading the emitter to a low-UC compound to join to a refractory metal lead. The emitter was made by cold-pressing enriched powder, followed by sintering and outgassing, after which it was finished to dimension by grinding. A thermocouple hole was drilled in the center. The top 1/4 in. of the emitter was normal uranium (to reduce the temperature at the joint to the tantalum stem).

This joining technique was practiced and metallurgical examination showed that excellent wetting was obtained when a Zr-Mo braze material was used. Thermal cycling of a practice piece indicated satisfactory braze performance. After three thermal cycles, the carbide practice piece cracked, but the joint remained integral. For the thermal-cycling test, the practice piece was directly heated by an electron bombardment filament. Since this method of cycling is much more severe than the uniform heating obtained in the reactor, it is felt that cracking of the carbide under these conditions did not reflect adversely on the experiment design.

An enriched unclad UC-ZrC fuel-emitter for the in-pile IC-2 test cell, was successfully fabricated and joined to a tantalum stem. The fuel-emitter assembly is shown in Fig. 17. During the brazing of the enriched fuel-emitter, a longitudinal crack developed in it. Thermal-cycling tests were performed and the crack did not propagate. The fuel-emitter was then used for the in-pile test in the Mark VI cell.

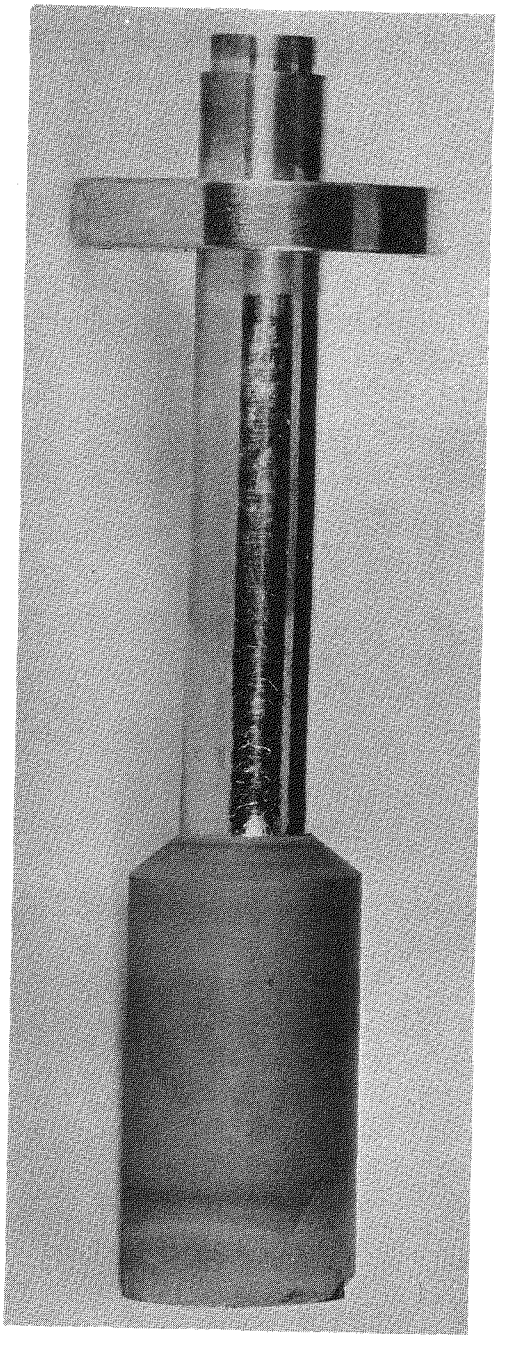

Fig. 17--Unclad UC-ZrC emitter for Mark VI single-cell in-pile testing

During the early development phase some development of UO_2 cermets was carried out before UC was selected for the Mark VI fuel-emitter. Pellets of W-UO_2 cermet were prepared by blending UO_2 and W powder (both minus 325 mesh) and hot-pressing in Mo-lined graphite dies. When the cermet with 95 wt-% UO_2 was hot-pressed at 1430°C and 1000 psi, the pellets were about 90 percent of theoretical density. Visual inspection showed that the W and UO_2 were somewhat segregated. It is believed that this resulted from packing of the UO_2 during the blending. The need for better mixing during blending is evident. Hot-pressing of W-UO_2 cermet containing 50 wt-% UO_2 at 1150°C and 800 psi yielded pellets of 82.5 percent theoretical density. A cermet containing 25 wt-% UO_2 could be bonded to W discs during hot-pressing but the densities of these pellets were not determined.

3.5 PROCESS AND COMPONENT EVALUATION

Before a process or component can be utilized in the fabrication of a thermionic cell, it must be established that it will satisfy the cell design objective. Work in this area during the reporting period has been confined to the evaluation of insulator-seals in a cesium environment and in the evaluation of bakeout procedures for the Mark VI thermionic test cell.

3.5.1 Insulator-Seal Environmental Tests

Insulator-seal environmental tests were designed to subject Al_2O_3-niobium insulator seals of the Mark VI design to the same environment, with the exception of radiation, that they will experience in test cells.

The ceramic-metal insulators previously used for the Mark VI cell were made of Al_2O_3, metalized and joined to niobium with copper braze. The types of high-density Al_2O_3 used were Coors AD-99 (99 percent pure) and Lucalox (99.99 percent pure). The insulators were tested at 800°C for compatibility with an internal cesium environment of 10 mm Hg of cesium vapor and an external environment of purified argon. The insulator made from Coors AD-99 leaked after 50 hr. The Lucalox insulator was leaktight after 140 hr, but leaked after nine thermal cycles between room temperature and 800°C. Metallographic examination showed that the leaks were in the Al_2O_3 of the Coors AD-99 insulator and in the braze joint of the Lucalox insulator. Two of the Lucalox insulators were then heated without cesium for more than 250 hr at 800°C and thermally cycled 15 times; they remained leaktight. The conclusion is that cesium (which is possibly part liquid during cycling) is responsible for the previous joint failures.

A Lucalox-to niobium insulator-seal was fabricated using the alloys Zr-Be and Zr-Be-Re and treated as follows:

1. It was thermally cycled six times between 300°C and 1200°C;
2. It was then run in a cesium atmosphere at a pressure of 10 mm Hg for 14 hr at 1015°C. The test was interrupted because of a cesium leak through a pinch-off seal.

Subsequent examination of the specimen showed it to be leaktight and unaffected by the cesium atmosphere. However, it must not be concluded from this test that the insulator-seal is at an advanced stage of development.

3.5.2 Cell Processing Evaluation

Throughout the assembly of the thermionic converter and particularly during the last step of the assembly before sealing, the cell requires careful bakeout and evacuation to assure that it is free from all adsorbed gases. Since it is not possible to instrument the cell directly to determine terminal pressures, gas evolution rates, and the effects of internal gettering, a test rig was constructed to evaluate them. This rig was a filament-heated Mark VI cell, as shown in Fig. 18. It was equipped with vacuum gauges on both ends of the cell and with a vac-ion pump at the internal pumpdown connection on the cesium reservior. There were no emitter themocouples; a sapphire window, however, allowed direct observation of the emitter temperature with the use of a pyrometer. The pressure-time curves observed on the two ion gauges for an ambient-temperature experiment are shown in Fig. 19. These data indicate that a pressure gradient of approximately one decade exists across the emitter during evacuation of a cell having an inter-electrode spacing of 0.010 in. This result is not unexpected, because the conductance of such a gap is of the order of 50 cm^3/sec.

Repeating the same experiment with heated electrodes indicated a slightly smaller pressure drop across the emitter. It is believed that the gettering characteristics of the niobium collector and the tantalum emitter stem assist in keeping the pressure gradient small. The examination of materials from the out-of-pile cells, OC-1 and OC-2, support this hypothesis.

The results of this experiment indicate a pressure equilibration time of approximately 1 hr across the emitter. On the basis of this result, final bakeout procedures for actual cells have been established to minimize deleterious effects due to outgassing. Assembly methods were modified so that cell components will be fully outgassed before assembly. This is discussed in Section 5.2.

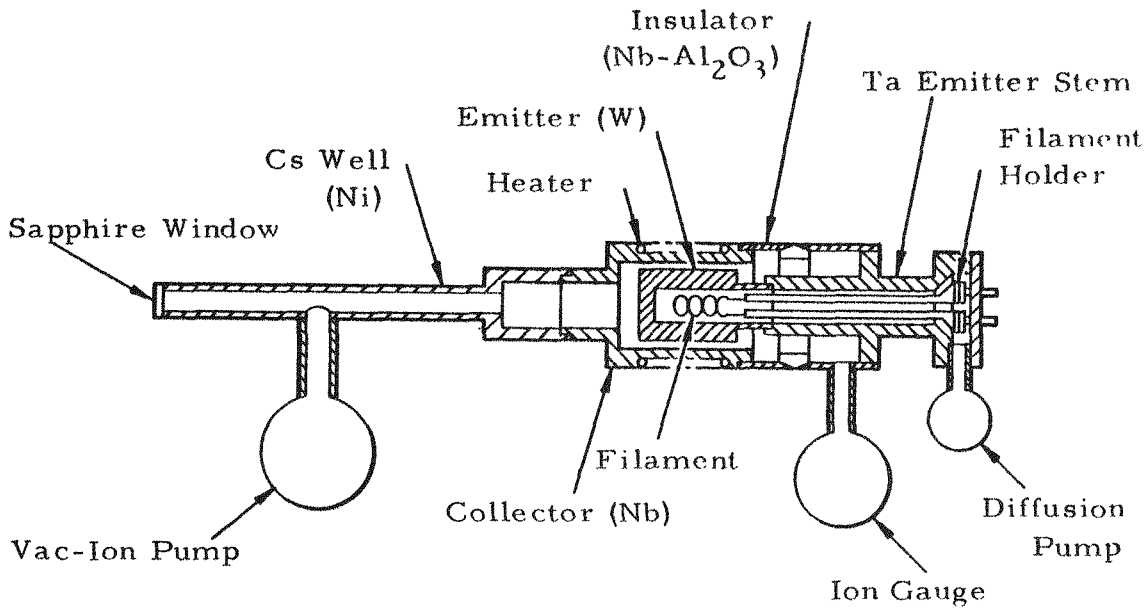

Fig. 18--Filament heated Mark VI test cell for pump-out test

3.6 SUMMARY OF FABRICATION

3.6.1 Materials Procurement

Type		
Niobium	Electron-Beam Melted	C, N, O < 50 ppm
Tantalum	Electron-Beam Melted	C, N, O < 50 ppm
Molybdenum	Electron-Beam Melted	C, N, O < 50 ppm
Tungsten	Arc Cast	
Tungsten	Sintered - Hot Swaged	
W-Mo Alloy	Arc Cast - Hot Swaged	
Copper		Oxygen-Free
Al_2O_3		High Purity, 99.9%
Al_2O_3-Nb Insulator	Metalized-Cu Braze	No Noble Metals or SiO_2

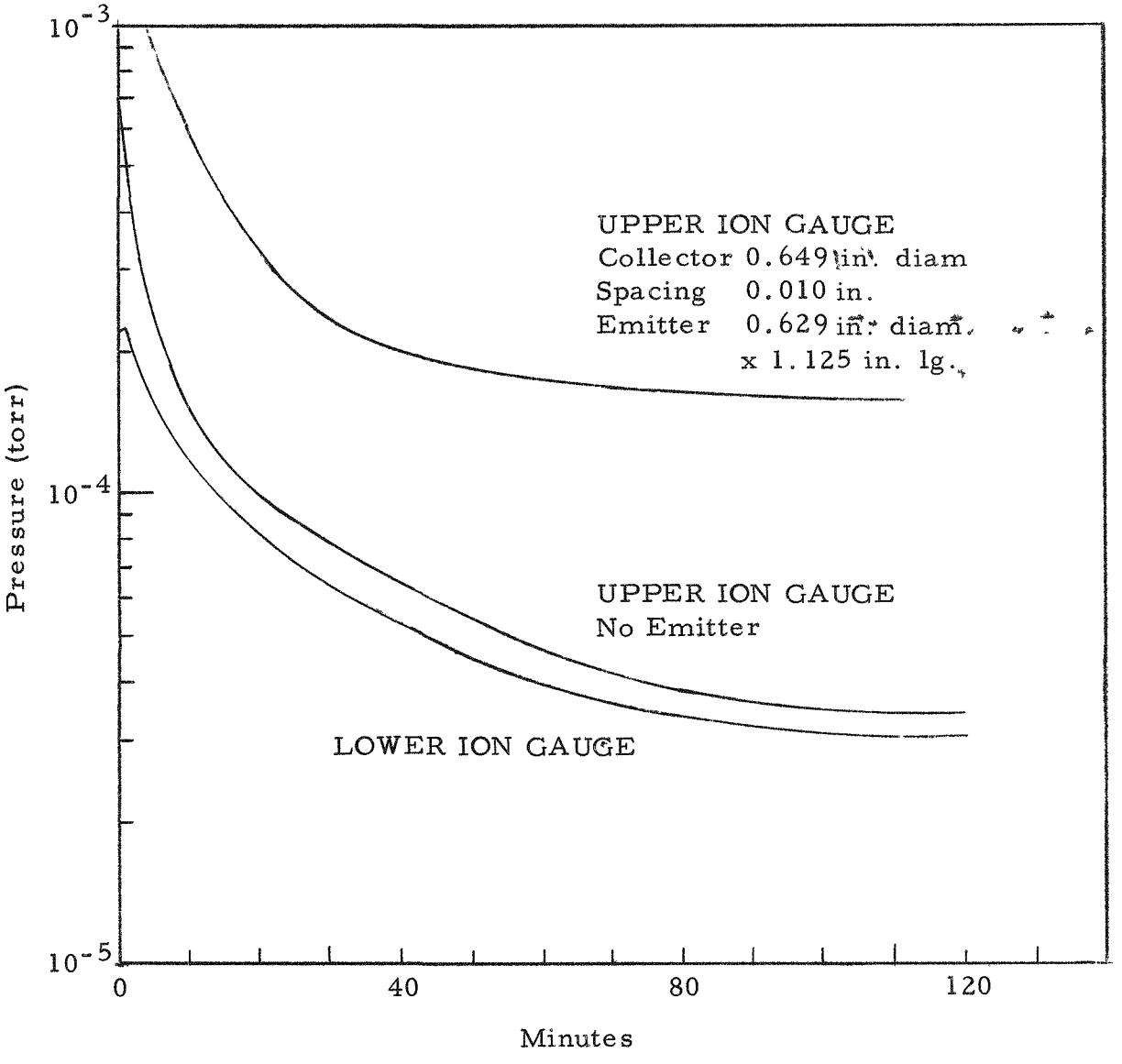

Fig.19--Results of ambient temperature experiment

3.6.2 General Process and Assembly Sequence

(1) Outgas materials.
(2) Braze or weld together emitter and collector subassemblies.
(3) Outgas subassemblies above operating temperature in high vacuum.
(4) Remotely assemble emitter and collector subassemblies.
(5) Final braze subassemblies together.
(6) Leak-check the cell.
(7) Pinch off copper pinch-off tube to seal cell.

3.6.3 Detailed Processing Subassembly and Final Assembly

(1) The emitter and collector parts are thoroughly outgassed in high vacuum at high temperature after machining.
(2) The fuel-emitter subassembly sequence is:
    (a) The fuel is sealed into the tungsten emitter by diffusion-bonding a tungsten cap to the emitter.
    (b) A tantalum bar is diffusion-bonded to the tungsten emitter and then machined to shape for an emitter stem.
    (c) The emitter stem is welded to the ceramic-metal insulator.
(3) The collector subassembly sequence is:
    (a) A tantalum-sheathed, insulated nichrome wire heater is brazed to the niobium collector with copper.
    (b) A niobium heat conductor is brazed to the niobium collector with copper.
    (c) A niobium cesium well is welded to the niobium collector by argon shielded arc weld.
    (d) A copper cesium well is welded to the niobium cesium well.
(4) The final assembly sequence is:
    (a) The insulator metal flange and collector cylinder are machined to fit within close tolerance.
    (b) The emitter and collector subassemblies are assembled in a vacuum induction-heating unit. The assemblies are outgassed at temperatures above their operating temperature.
    (c) The emitter and collector subassemblies are remotely assembled in the vacuum induction-heating unit. The assembly is brazed together with a copper braze ring which had been preplaced in the joint.
    (d) The cell assembly is leak-checked and the copper pinch-off tube is pinched off if leak tight.

BLANK

IV. IN-PILE TESTING OF THE MARK VI CELL

Three in-pile tests were conducted during the year utilizing the Mark VI test cell. In two of these tests, tungsten-clad uranium carbide fuel-emitters were employed and in the third, a UC-ZrC fuel-emitter was utilized. Testing procedure, prototype tests for the cell design, and the three Mark VI cell tests are described in detail in this section.

4.1 INSTRUMENTATION

The instrumentation shown schematically in Fig. 20 was used for both in-pile and bench testing of the Mark VI test cell. In addition, the bench test required a control circuit for the electron bombardment heating of the emitter. The emitter power input for the in-pile tests is regulated by adjusting the reactor power level. The main features of the instrumentation include: 1) Temperature measurement and control; 2) Power output measurement and regulation; and 3) Emitter power input supply, control, and measurement.

4.1.1 Temperature Measurement and Control

The fuel-emitter temperature was measured with four W(W-26Re) thermocouples imbedded in the emitter walls at different axial locations: two in the middle and one at each end. With that arrangement, the emitter temperature level and distribution can be measured during the operations. The absolute themocouple errors are in the order of 1 percent. Calibration of thermocouples of this type has shown their relative temperatures to be within $\pm 10^{\circ}C$ at $1900^{\circ}C$. The thermocouple emf was displayed on a 0-50 Mv Brown recorder. The recorder error is ±0.25 percent.

The temperatures of the collector, cesium reservoir, insulating seal, etc., were measured with floating shielded-type chromel-alumel thermocouples. Close regulation of the cesium reservoir was accomplished with a current-adjusting-type 3-action proportional controller-recorder. The measured reservoir temperature error is estimated to be $\pm 1^{\circ}C$. The collector temperature was automatically regulated with a current-adjusting-type single-action proportional controller within about $\pm 5^{\circ}C$. The other 16 converter temperatures were intermittently recorded on a 16-point Brown Recorder which is accurate within 0.25 percent.

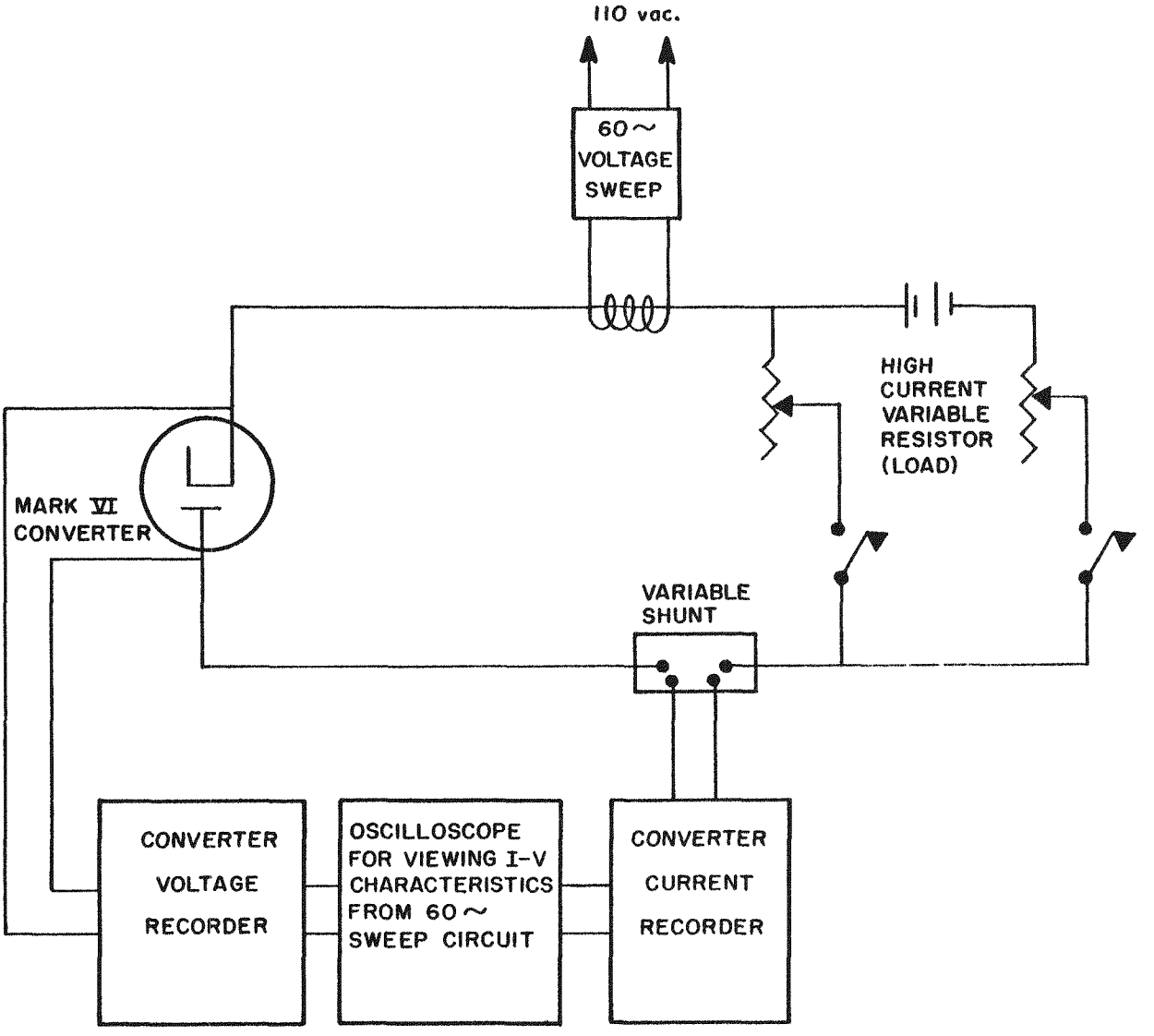

Fig. 20--Instrumentation for in-pile and bench testing of Mark VI test cell

4.1.2 Power Output Measurement and Regulation

The test cell voltage output was regulated by a high-current variable resistor (load) with a range of 0.001 milliohm to 1 ohm. For driving the test cell into the applied voltage region (+), the parallel battery circuit was used. The driving voltage was regulated with another high-current resistor.

Converter voltages were measured at the emitter and collector leads with copper probes. The currents were measured with precision shunts. Both the voltage and current were continuously recorded on a Brown two-point recorder. The voltage and current errors are estimated to be ±0.005 volts and ±0.2 amp. A 60 cps voltage sweeping circuit was also used to display voltage-current characteristics on an oscilloscope. Polaroid photographs were used to record the displays.

4.1.3 Emitter Power Input Supply and Control

For the bench tests, the emitters were heated artificially by electron bombardment accomplished with a double helical filament suspended in the emitter cavity and supported by 1/16-in. tantalum leads.

A schematic of the electron bombardment circuit is shown in Fig. 21. The ac current to the filament is supplied and regulated by a current-adjusting-type 3-action proportional controller. The controlled variable, the bombardment current, was sensed by a precision shunt. High voltage was supplied by a regulated dc power unit with 0-1000 volt and 0-5 amp range. The power to the emitter was accurately measured with calibrated precision ac and dc meters. The error in the power input measurements is estimated at 1 percent.

4.2 OUT-OF-PILE PROTOTYPE CELL TESTS

Two out-of-pile prototype cells, designated as OC-1 and OC-2, were operated out-of-pile for over 100 hours to study thermal performance and materials compatability. After operation, the cells were systematically disassembled and the cell components were examined.

The prototype OC-2 cell was placed in a fuel element containment tube and was operated in argon, helium, and vacuum environments to obtain heat transfer and collector calorimeter data. Containment tubes were operated within a tank of water to simulate reactor cooling conditions.

In addition to the two thermal tests (OC-1 and OC-2), a third out-of-pile prototype cell was operated as a cesium converter. Data from this

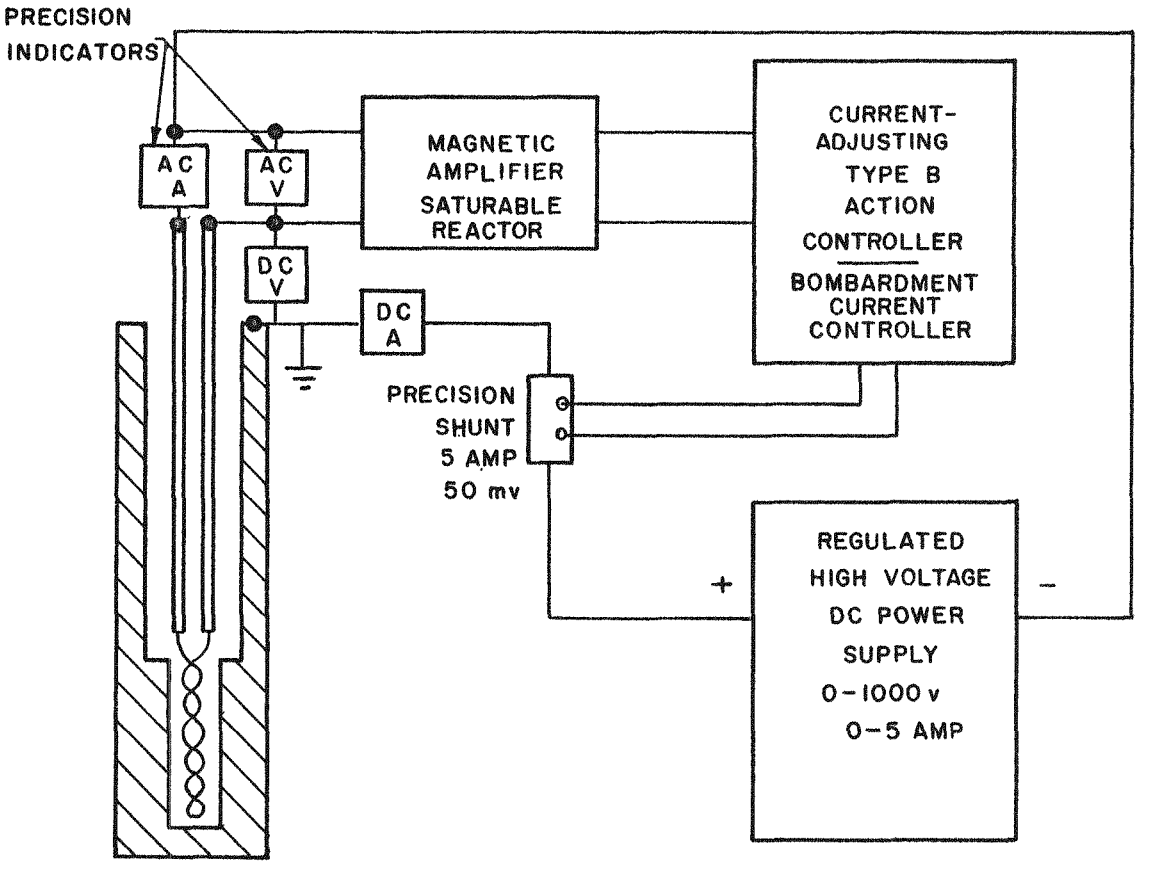

Fig. 21--Electron bombardment circuit

prototype cell provided reference points for the operation of the in-pile testing cell.

4.2.1 OC-1 Axial Temperature-Profile Data

The cell was instrumented with 24 thermocouples, 11 of which were used to obtain axial temperature-profile data in a vacuum and in an inert atmosphere. The collector radial temperature profiles intended for calorimetry of the collector waste heat were not usable because of distortions of the circumferential temperature distribution as a result of the method of mounting the cell.

The OC-1 temperature-profile data are shown in Fig. 22 for an emitter temperature of 1900°C. Table 3 lists the operating conditions depicted by curves A-D in Fig. 22. Of particular importance is the temperature distribution along the nickel tube of the cesium reservoir. Under test vehicle operating conditions, only the temperature of the end of the tube is measured. Hence, it is most important that this temperature be the lowest temperature in order to accurately register the cesium condensation temperature. Of course, when there is no heat applied to the reservoir-end, then the end (T/C No. 16) must be at the lower temperature since the heat sink is below the reservoir. This is observed in curves A and C of Fig. 22. In curves B and D, however, the reservoir is electrically heated to about 350°C (T/C No. 16) resulting in a lower temperature near the middle of the nickel tube (T/C No. 4 and No. 17) than at its end. The minimum temperature in that region is caused by radiation loss of heat from the nickel tube wall, as is evidenced by curve B. It is noted that the shape of the curves B and D are grossly the same in the region of the cesium reservoir except for their vertical displacement from each other. This indicates that the addition of argon convection cooling more or less equally cools the entire tube. In Fig. 22, the minimum temperature is near T/C No. 4. For the vacuum case, the temperature difference between T/C No. 16 and No. 4 is 64°C and for the argon case it is 13°C. It is seen, then, that the addition of argon cooling actually reduces the temperature difference. When the existence of a minimum temperature, other than that at the end of the reservoir tube was discovered, insulation and radiation shielding were applied to the reservoir tube walls to prevent heat losses.

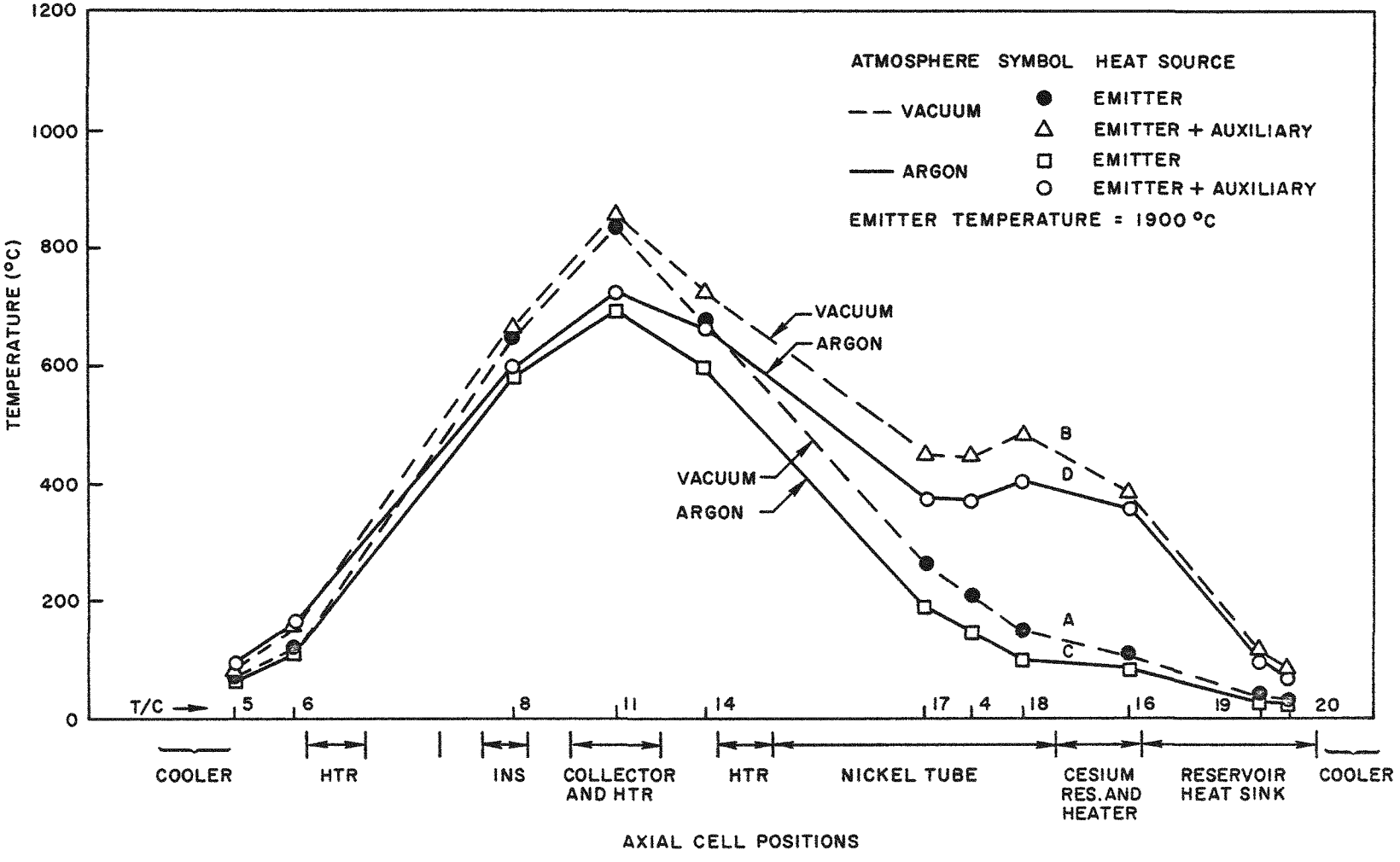

Fig. 22--OC-1 axial temperature-profile data at the emitter temperature of 1900°C

Table 3

OC-1 TEMPERATURE-PROFILE OPERATING CONDITIONS

Curve	Atmosphere	Emitter Temp (°C)	Heater Power Inputs (watts)			
			Emitter	Emitter Bus	Nickel Tube	Cesium Reservoir
A	Vacuum	1900	591	0	0	0
B	Vacuum	1900	592	58	84	97
C	Argon	1900	600	0	0	0
D	Argon	1900	601	58	81	97

4.2.2 OC-2 Heat-Transfer Data

The purpose of the heat transfer experiment with the OC-2 cell was to determine:

1. Emitter-heater powers for various emitter temperatures (negligible emitter electron cooling).
2. Effectiveness of regulating the collector temperature with argon and/or helium

The experimental configuration consisted of the Mark VI OC-2 out-of-pile prototype cell sealed into a Triga fuel-element tube immersed in a cooling tank filled with circulating water maintained at about 60°F. The converter was instrumented with 16 thermocouples distributed as follows:

Emitter - 4

Collector - 5

Insulator - 2

Reservoir - 2

Emitter Bus - 2

Nickel Tube Heater - 1

Four of the collector thermocouples were located for use in calibrating the heat flow through the collector in the radial direction.

The emitter power input required to heat the emitter to a given temperature is shown in Fig. 23 for two different days. At 1900°C, the power input range was between 580 and 635 watts. With the emitter area of 13.95 cm^2 (6.25 in. diam, 1.1 in. long), the power inputs corresponds to 41.5 and 45.5 watts/cm^2, respectively. Explanations for the observed differences are:

1. Changes in the ratio of filament power to the bombardment power alter the emitter temperature distribution.
2. The electrode emissivities change with time. (It was noted in the post-operational inspection of OC-2 that considerable blackening of the collector occurred.)

Using the data presented above, the effective emissivity of the OC-2 cell was calculated to be about 0.25. If the tungsten emissivity is 0.3, which is the maximum expected for the clean material, the computed value for the niobium collector is 0.6. This would indicate an increase in emissivity by a factor of 2 over the expected clean value.

Collector cooling is accomplished by radiation and by the addition of gases into the annular space between the collector outer surface and the fuel element containment tube. The effect of the gas pressure upon the collector temperature is shown in Fig. 24 for an emitter temperature at 1900°C. Figure 24 also shows the collector temperature at about 900°C in a vacuum. The addition of 1 atmosphere of argon or helium is shown to cool the collector to 840°C or 470°C, for argon or helium respectively.

In Fig. 24, very little effect on the collector temperature is observed for variations in gas pressure between 3 and 20 psia. Below 3 psia, the collector temperature increases rapidly to its vacuum value as the pressure is reduced. On the basis of this information, mixtures of argon and helium are used to give a coarse regulation of the collector temperature. The fine control is provided by the collector heater. Pressures greater than 1 atmosphere are maintained to reduce the leakage of air into the tube should the seal be defective.

When the converter is operated at high electrical currents, considerably greater power production will be required than for this zero-current test. If OC-2 had been run as a cesium converter, the power input to the emitter would be greater by approximately an additional

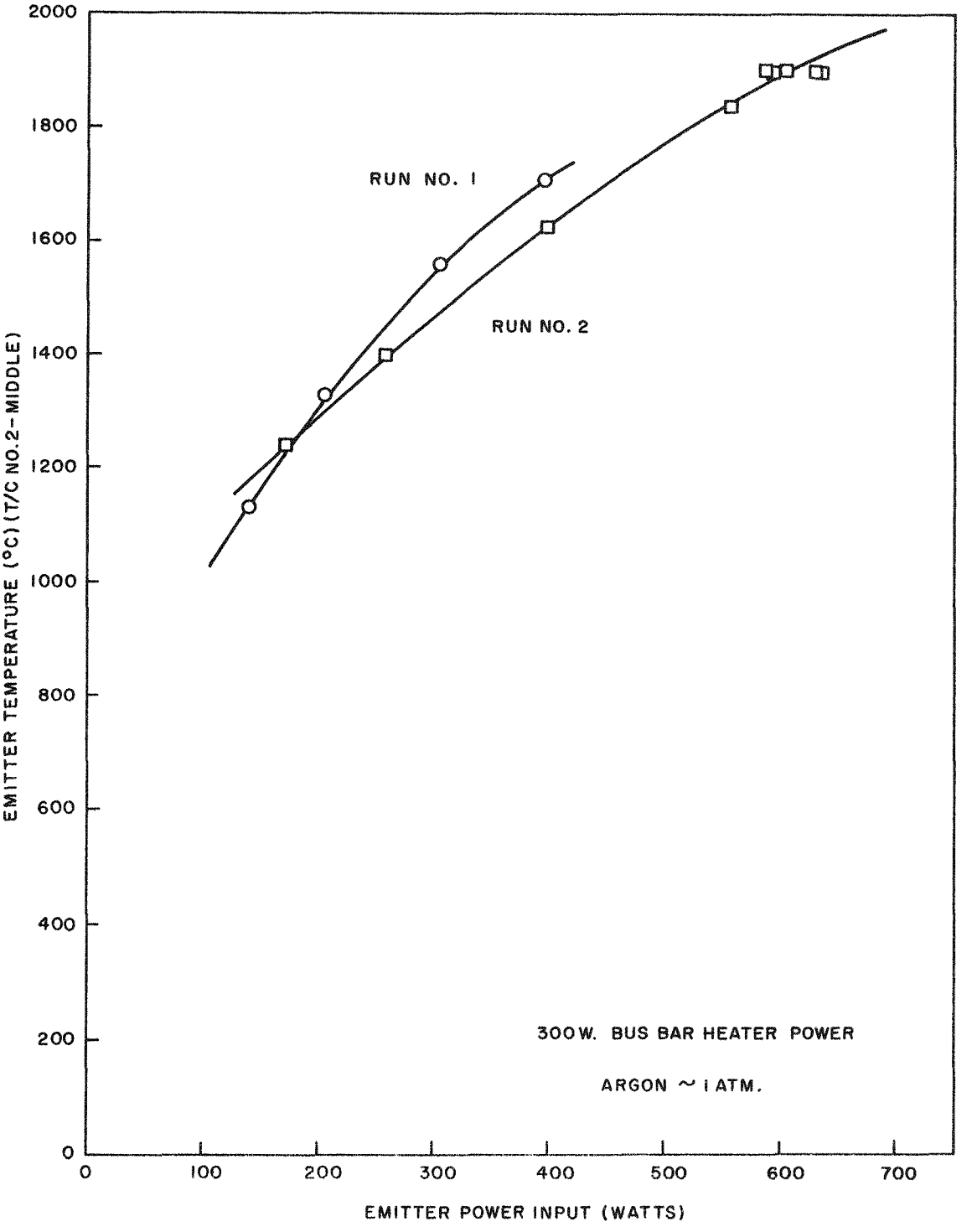

Fig. 23--Emitter temperature versus emitter power input

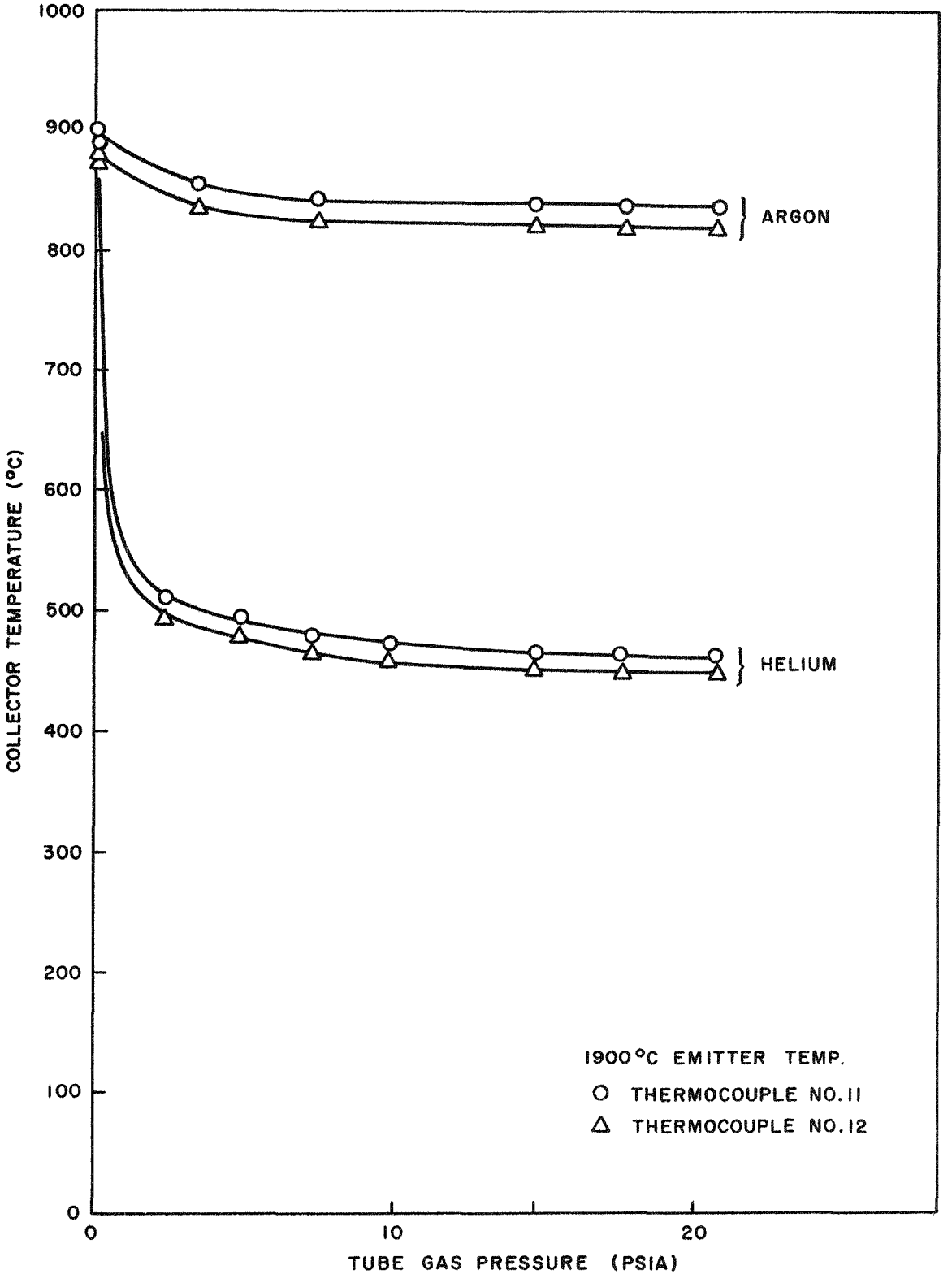

Fig. 24--Collector temperature versus argon and helium pressure

amount equal to $I(\Phi_E + 2kT_E)$, where

I = current

Φ_E = emitter work function

T_E = emitter temperature

k = Boltzmann's constant

At $T_E = 1900^{\circ}C$ and $I = 10$ amp/cm^2, the additional power removed from the emitter by electron cooling would have been about 500 watts, making the effective total power input to the emitter about 1100 watts or 80 watts/cm^2. During the test, 1100 watts were produced in the emitter and collector heater combined, while the tube pressure was maintained at about 1 atmosphere of helium. At this power input, collector temperatures at Thermocouples 11 and 12 were recorded as 675°C and 655°C, respectively. This test indicated that adequate collector cooling was provided for the Mark VI design for cesium-diode operation.

4.2.3 Test Data from OC-3

A third out-of-pile cell, OC-3, was operated as a cesium cell and data were obtained prior to the first in-pile test. The emitter of OC-3 was 98% W - 2% Mo alloy and contained UC fuel pins in the tungsten wall. The radial spacing between the emitter and collector was 0.010 in.

The first experiment performed with this cell was a series of emitter heating experiments at low cesium temperature and open-circuit conditions. The data obtained are shown in Fig. 25. These data, along with that of Fig. 23, were particularly useful for establishing a correlation between reactor power level and fission power generation in the fuel-emitter of the in-pile experiments.

The experiments were continued on OC-3 to determine its operating characteristics at emitter temperatures of 1500°C and 1600°C. Data obtained at 1500°C are shown in Figs. 26 through 28. These data indicate the existence of an ignited and unignited mode of operation at this emitter temperature. After optimizing cell operating parameters at this emitter temperature, a maximum power output of 18 w (1.3 w/cm^2) was obtained at a cesium temperature of 310°C and an electrical power input of 415 w. This yields an over-all cell efficiency of 4.5 percent.

Data obtained at an emitter temperature of 1700°C are shown in Figs. 29 and 30. Under these conditions, a maximum power output of 26 w was attained with a cesium temperature of 330°C and a power input of 598 w. The over-all operating efficiency was 4.4 percent. In Fig. 31, the emitter temperature is shown as a function of the power input from the Mark VI tests, OC-2 and OC-3. At temperatures below 1200°C, the power

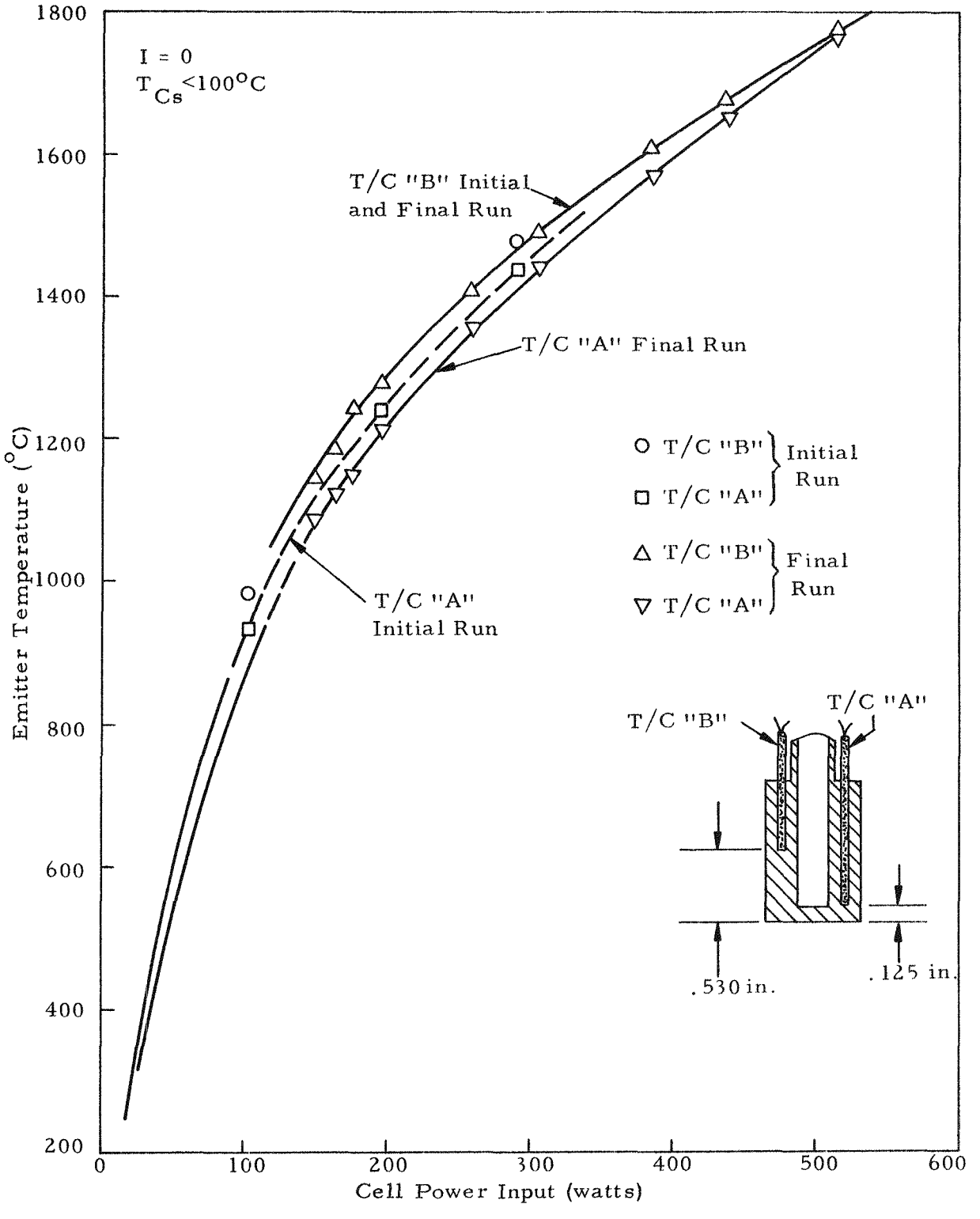

Fig. 25--Emitter temperature versus power input data from first series of emitter heating experiments on Mark VI cell OC-3

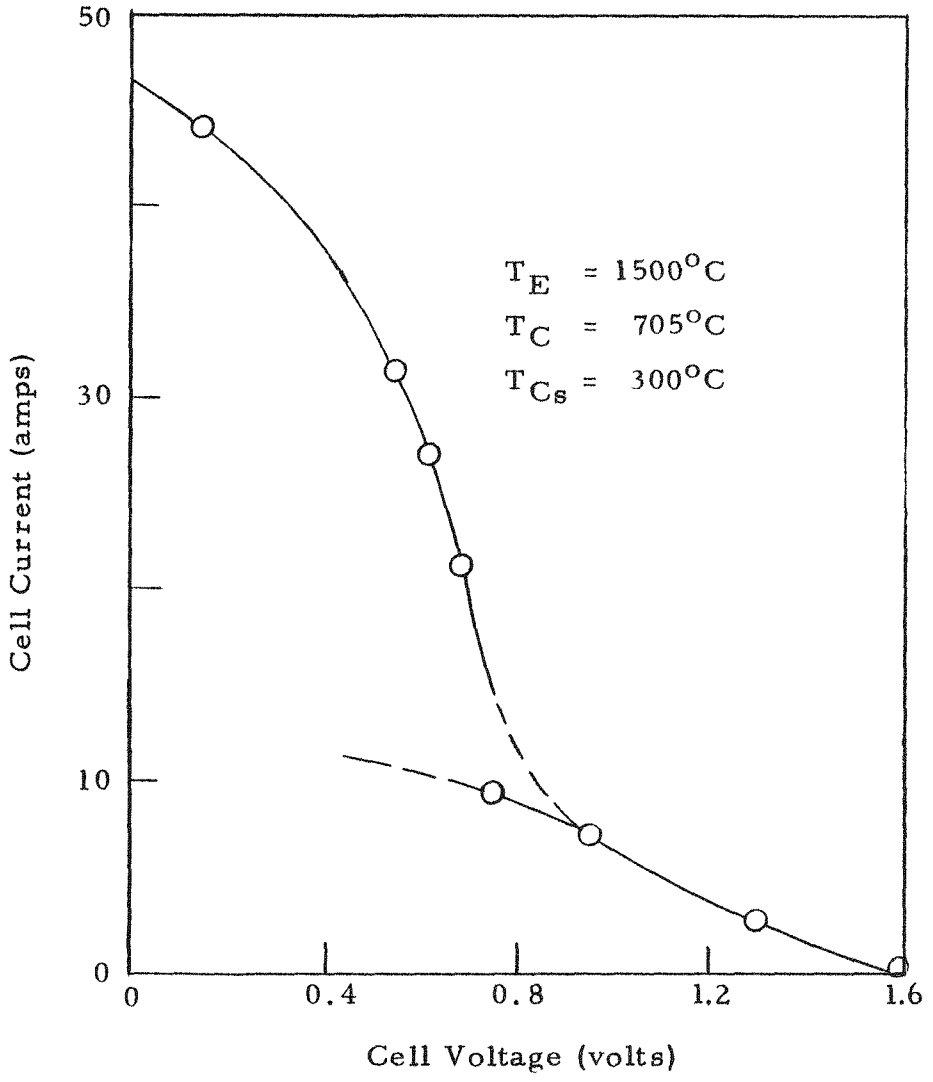

Fig. 26--Current versus voltage data obtained from Mark VI cell OC-3 with emitter temperature at 1500°C

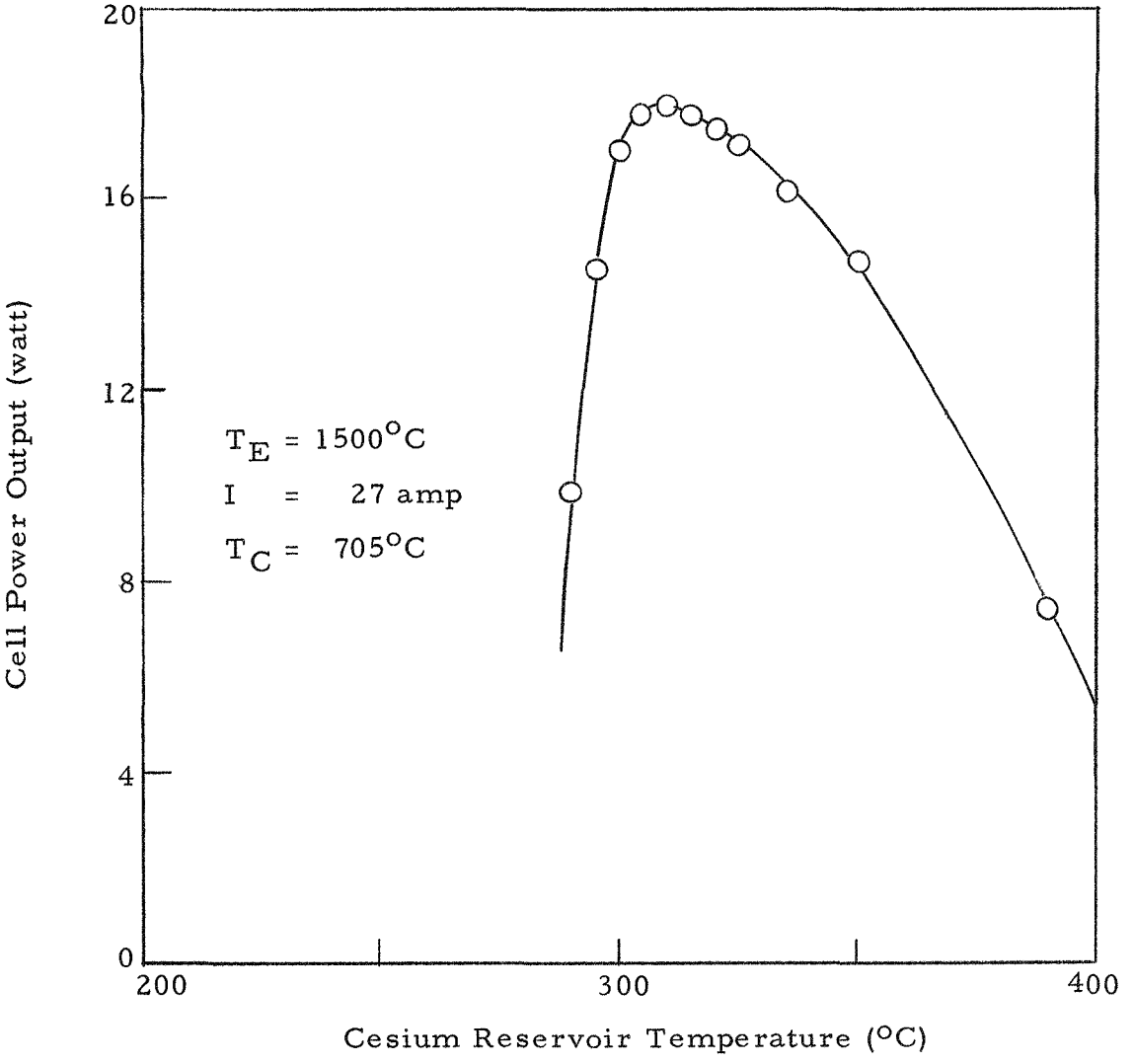

Fig. 27 --Power output versus cesium temperature data obtained from Mark VI cell OC-3 with emitter temperature at 1500°C

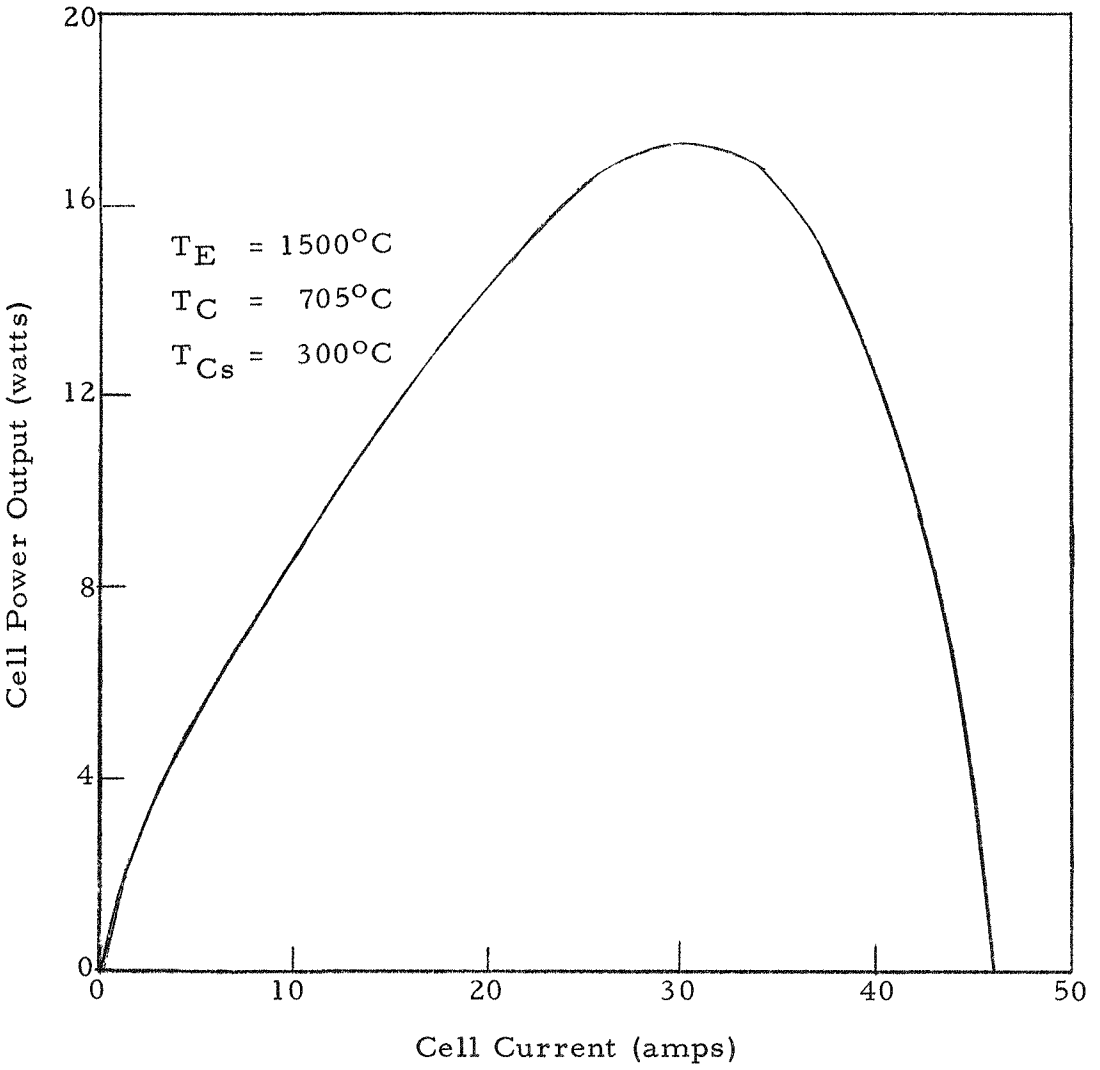

Fig. 28--Power output versus current data obtained from Mark VI cell OC-3 with emitter temperature at 1500°C

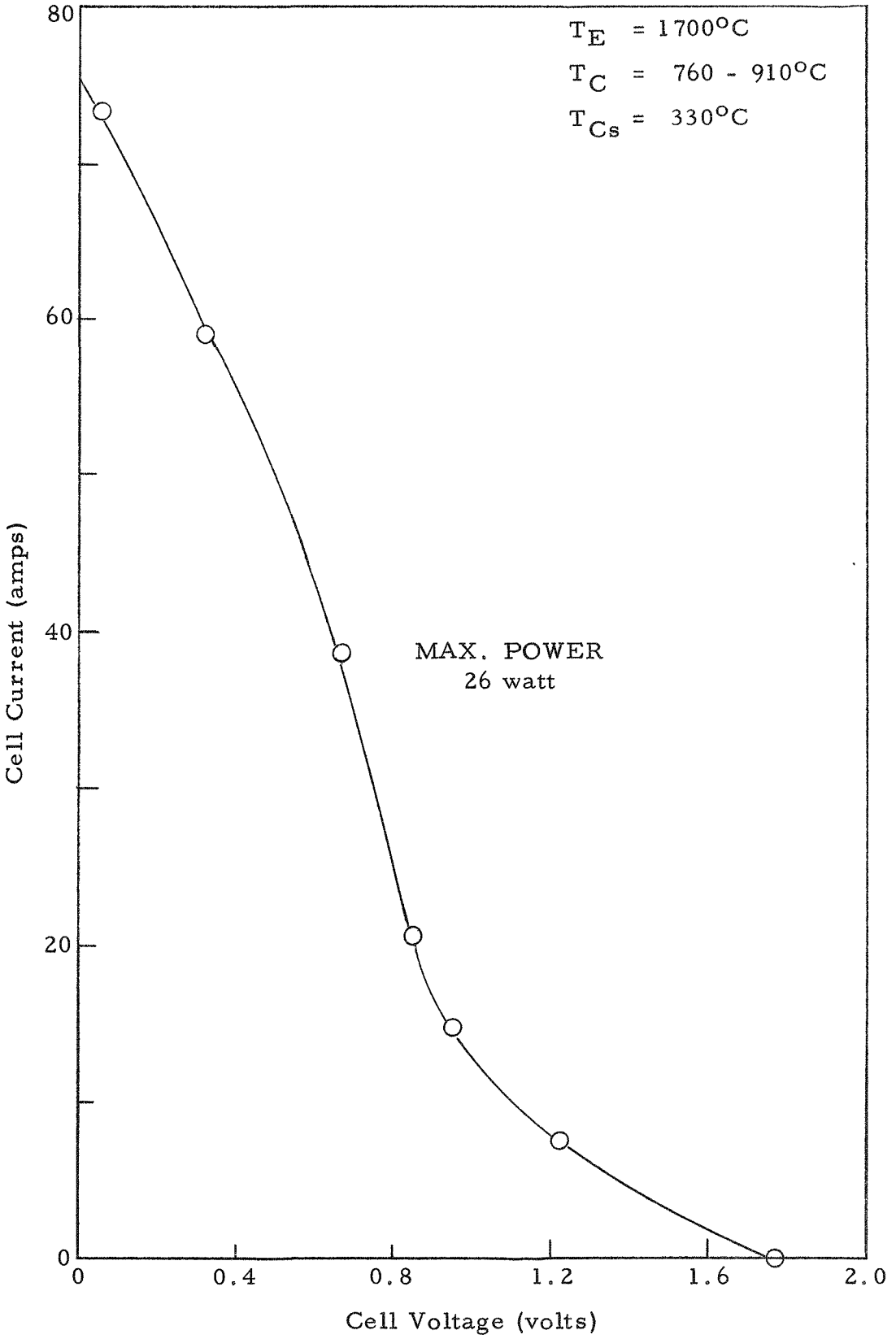

Fig. 29--Current versus voltage data obtained from Mark VI cell OC-3 with emitter temperature at 1700°C

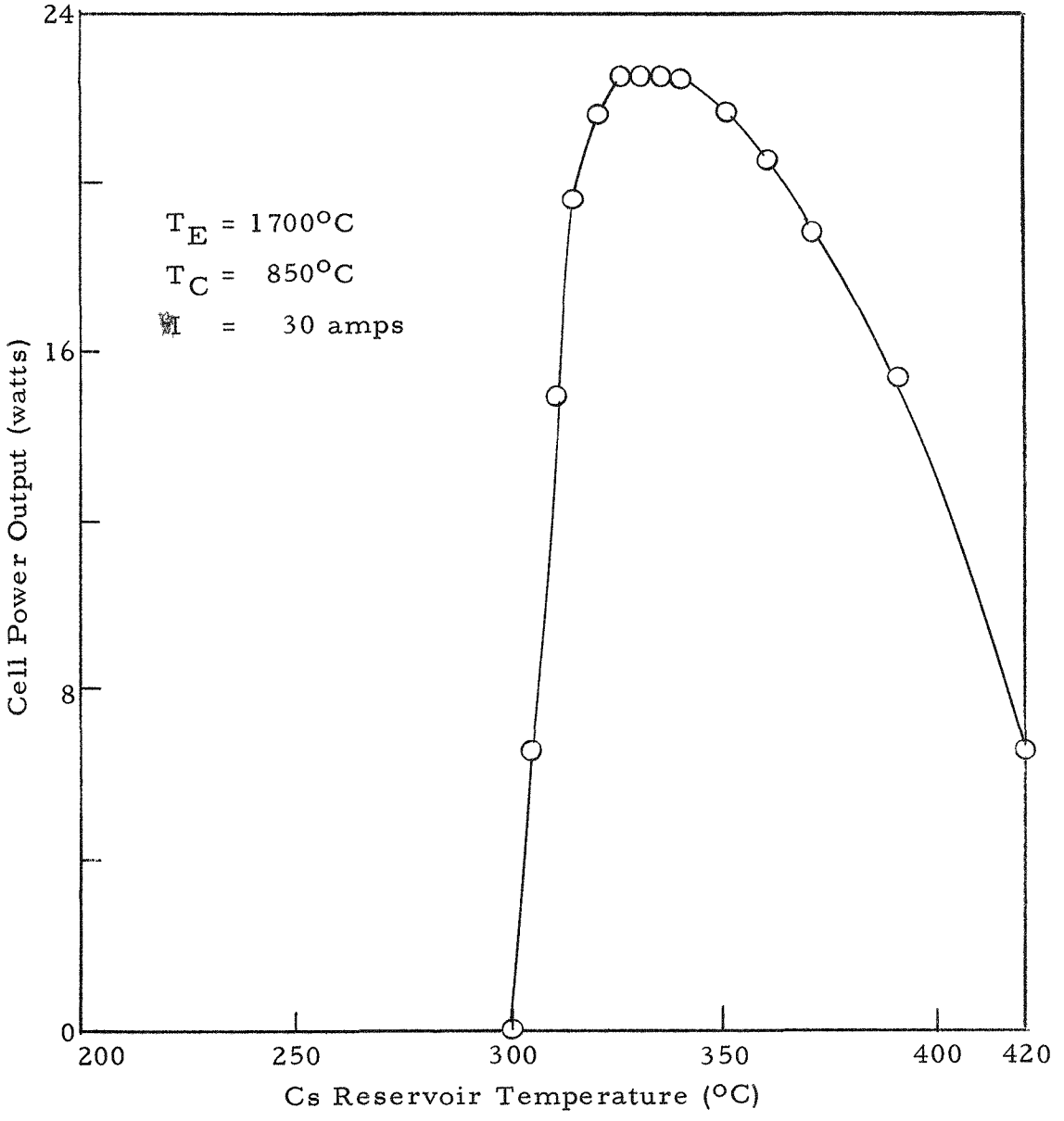

Fig. 30--Power output versus cesium temperature data obtained from Mark VI cell OC-3 with emitter temperature at 1700°C

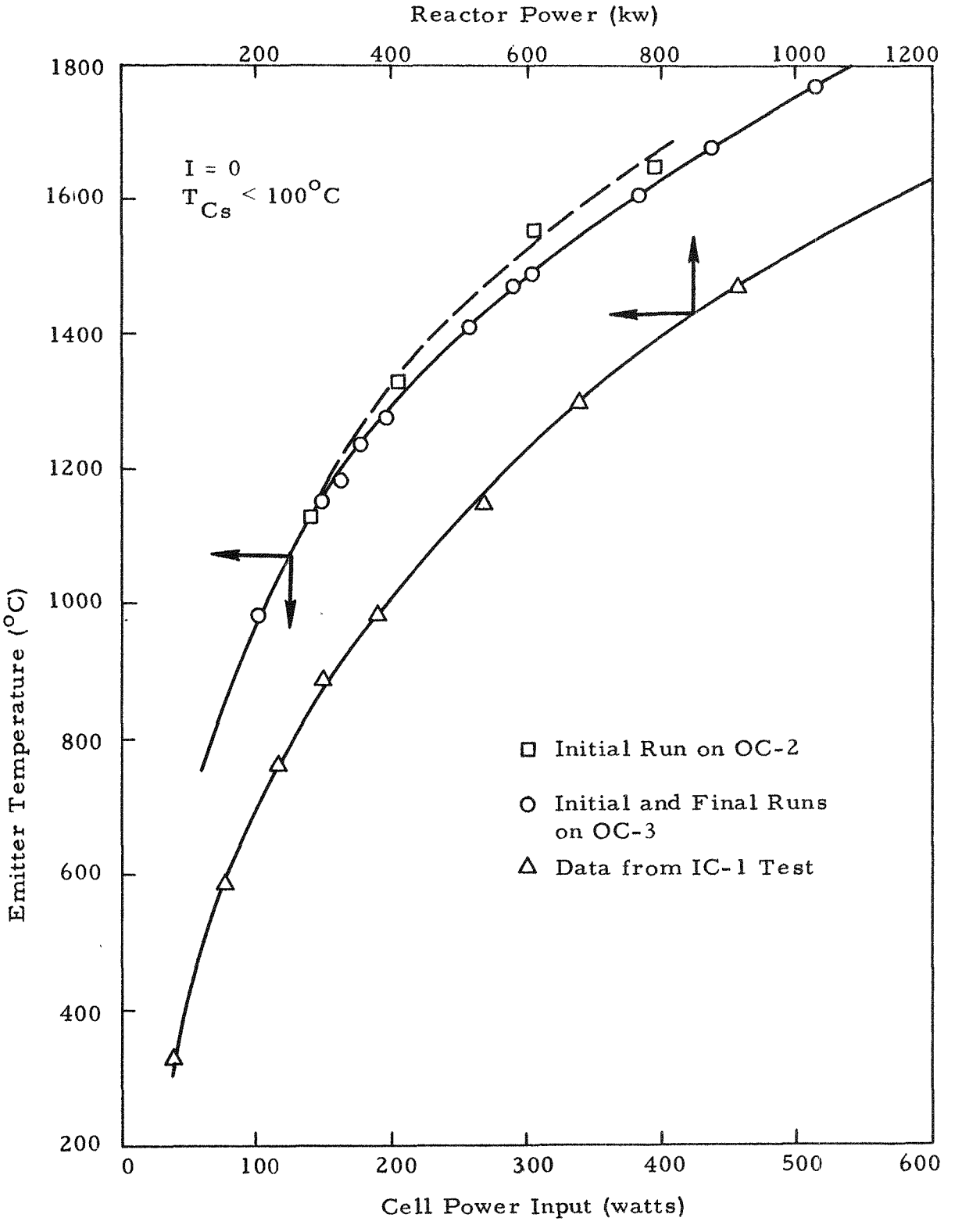

Fig. 31--Emitter temperature versus power input data obtained from Mark VI cells IC-1, OC-2, and OC-3

input to these cells was nearly equal, but at higher temperatures, OC-3 required greater power input for a given emitter temperature.

During the preliminary experiments on OC-3, the cell performance degraded rapidly, and both emitter thermocouples eventually failed. Further experiments were attempted, but the results are inconclusive without emitter temperatures.

The cell was disassembled for examination in an inert atmosphere. About 1/2 gram of cesium remained in the cesium well. The emitter appeared bright and shiny; however, the collector had a dark deposit. This deposit was darker and thicker at the ends of the collector. The emitter and collector were checked by alpha counting to determine if the uranium had diffused through the tungsten. The results were negative. The cell was then assembled in a vacuum bell jar station and vacuum emission data were taken. The emitter work function was calculated to be about 4.3 ev, which compares to the value for tungsten.

X-ray diffraction analyses of the inner surfaces at the ends of the collector showed that the deposits contained niobium oxide and niobium dioxide. Emission mass spectrometry analyses showed that the loose black deposits on the collector flange surfaces contained 4 percent cesium.

The over-all conclusion from OC-3 post-operational disassesmbly and operation is that a source of gas was leaking into its interior during the initial phases of operation. This could have been a virtual source from a break in the thermocouple sheath.

4.3 IN-PILE TEST DATA

Three in-pile tests were performed. The test cells with fuel-emitters of UC canned in tungsten were designated IC-1 and IC-1'. The third cell employing an unclad UC-ZrC fuel-emitter was designated as IC-2.

4.3.1 Test Data from IC-1

Operation of the IC-1 cell in the Triga Mark F reactor commenced on March 18, 1963 and continued through March 20. A total of 21 operational hours were accumulated on this cell. The maximum observed power output near the end of the operating time was approximately 5 w/cm^2 with an emitter temperature of 1750°C, collector temperature of 900°C, and cesium temperature of 330°C. This power density was obtained at 0.8 v and 86 amp. The efficiency is estimated to be between 11 and 12 percent

at the maximum power output.

The operations were complicated by variable shunting resistance between adjacent instrumentation leads about 6 in. above the cell. During the operations, methods were developed for measuring this shunting resistance and calculating the current through it. After 21 hours, the value of the shunting resistance became so low that it was no longer possible to make reliable measurements.

On March 20, the converter was moved from the reactor core and attempts were made to fix the instrumentation difficulties. The converter was again inserted in the reactor on March 21 and the reactor was operated for approximately 4 hours. However, this additional operation showed that the attempts at repair had been unsuccessful.

The test assembly was then moved to the Hot Cell where it was examined. After removal of the secondary containment can, the cell and its associated instrumentation were examined. The area of the short appeared to be just above the cell in the region of the emitter stem heater. The exterior surfaces of the refractory metals of the cell itself had oxidized considerably due to outgassing of the cell assembly materials during operation. The containment was periodically purged during the operating period, but this is not sufficient for tantalum and niobium. In subsequent tests, the containment was continuously purged with purified helium and/or neon. Neon was used instead of argon for the low conductivity inert gas. The radioactivity of the argon leaving the reactor is too high to permit exhausting to the atmosphere even at very low flow rates.

The problem of shorting in the instrumentation leads was alleviated by providing more rigid spacing insulation between leads.

The emitter of IC-1 appeared to be in good condition. There was no apparent reaction between the fuel and the 98% tungsten - 2% molybdenum alloy which was the emitter material. The joint between the emitter cap and the emitter was still integral and it is believed that it was leak tight. The mechanical bond between the tantalum stem and the emitter was also integral. The insulator and collector inside surfaces were in very good condition as compared to similar surfaces of the OC-3 out-of-pile cell.

The data obtained from the in-pile test are given in Figs. 32 and 33. The short testing time did not permit investigation of optimum operating conditions. However, the data compared favorably with data from other out-of-pile cells. The conclusion from the comparison in Fig. 33 is that the thermionic performance of the in-pile cell was superior to that of the OC-3 out-of-pile cell. This strengthens the conclusion that OC-3 suffered a decrease in power output due to degradation in surface characteristics.

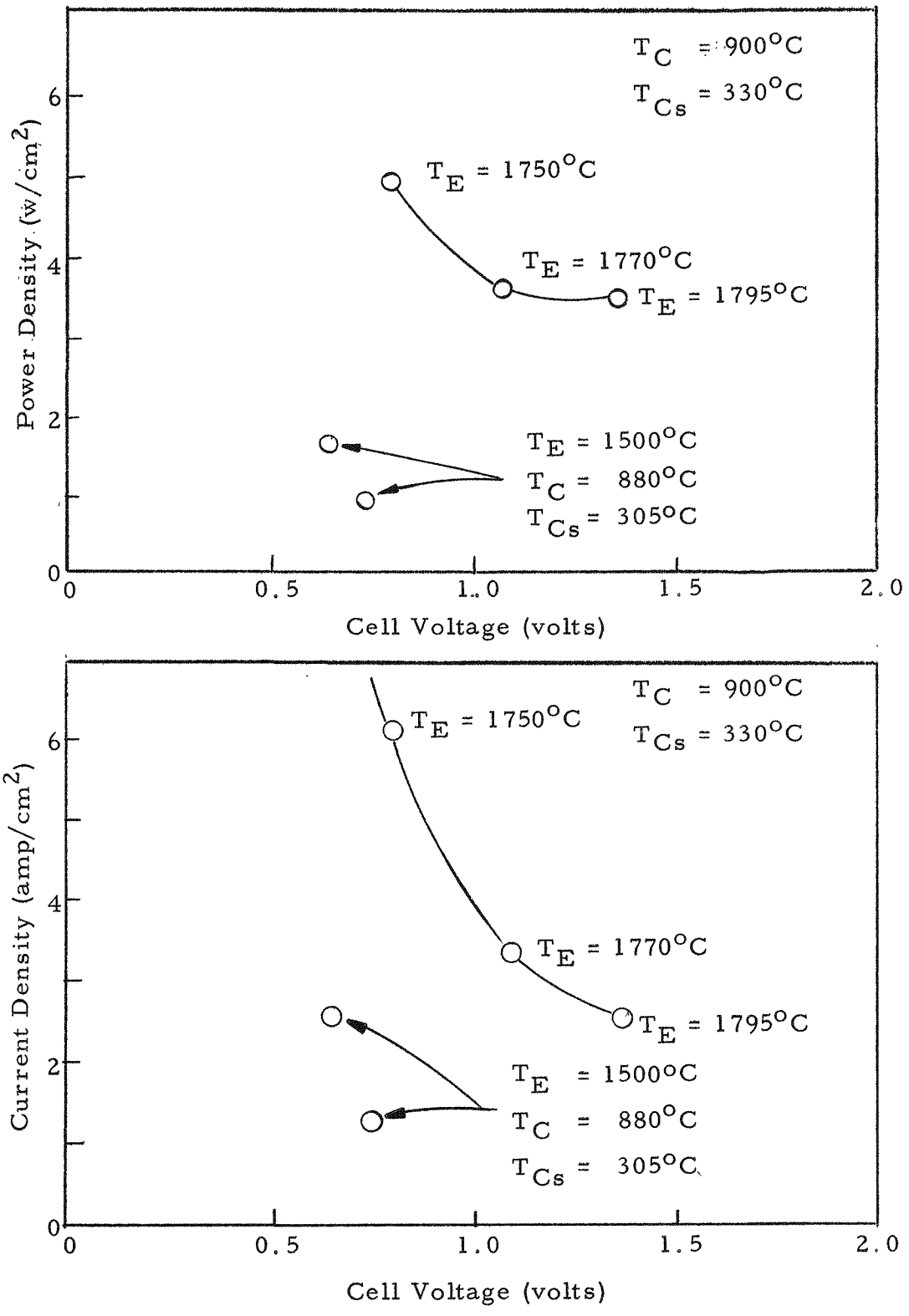

Fig. 32--Data obtained on current density and power density versus voltage during in-pile test of Mark VI cell IC-1

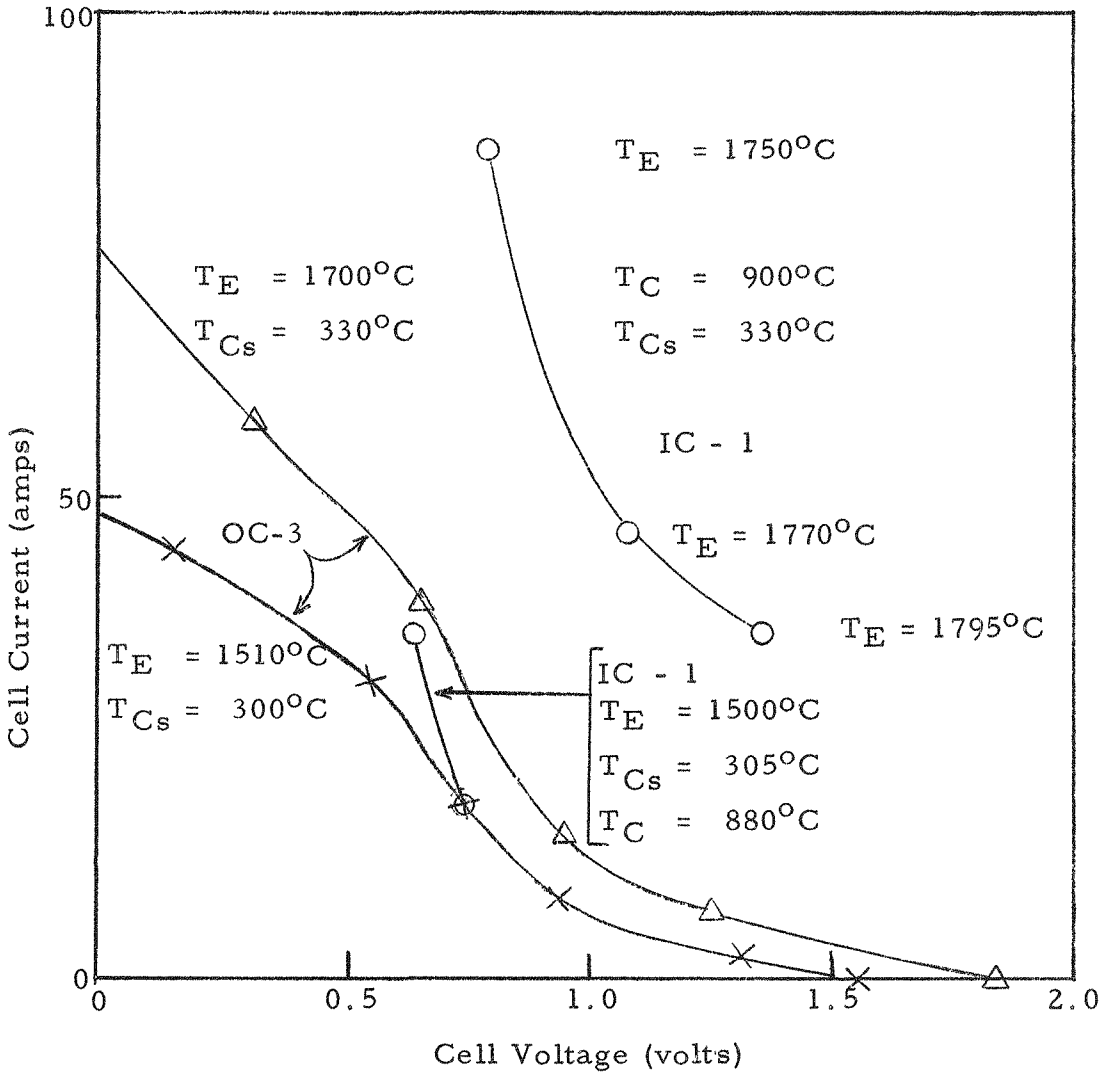

Fig. 33 --Current versus voltage data obtained during in-pile test of Mark VI cell IC-1 and out-of-pile test of cell OC-3

The inside surfaces of IC-1 were in excellent condition as compared to the surfaces of OC-3.

4.3.2 Test Data from IC-2

On April 15, 1963, the second in-pile test on Cell IC-2 was initiated. This cell had the unclad 30 UC-70 ZrC fuel emitter shown in Fig. 17; the cell assembly is shown in Fig. 34. The cell was operated for about 12 hours. The output was very low, indicating the possibility of a poisoned surface. The central fuel-emitter temperature was 1750°C. When the cesium temperature was raised from 180°C to 300°C, the output power continuously decreased.

The next approach was an attempt to activate the emitter surface. The temperature was raised to 1860°C with the cesium temperature at 200°C. This was maintained for 1 hour to evaporate the oxide from the emitter surface. The emitter temperature was then decreased to 1600°C and the cesium temperature was raised to 260°C. For a short time, the current increased, but after a few minutes it decreased to the previous values.

The IC-2 cell was operated for about 14 hours in further attempts to diagnose the difficulty and then the test was terminated. This cell will be examined in the Hot Cell. It is possible that the above anomalous behavior was due to an inert gas pressure. A gas puncture device may be used to determine the presence of gas inside the collector.

4.3.3 Test Data from IC-1'

On April 16, 1963, the next cell with a tungsten-clad UC-fueled emitter was installed and testing was begun on April 17. This cell was the back-up to IC-1 and designated IC-1'. The emitter was fabricated from the alloy 98W-2Mo. The modifications from the IC-1 configuration were:

1. The tantalum emitter stem was welded above the insulator to prevent the secondary containment gas from entering the hollow stem.
2. The cesium reservoir was niobium, replacing the nickel reservoir used previously.
3. The insulator was welded to the tantalum stem, replacing the copper-titanium.
4. The thermocouples were sealed into the tantalum stem with copper replacing the zirconium-beryllium braze used previously.

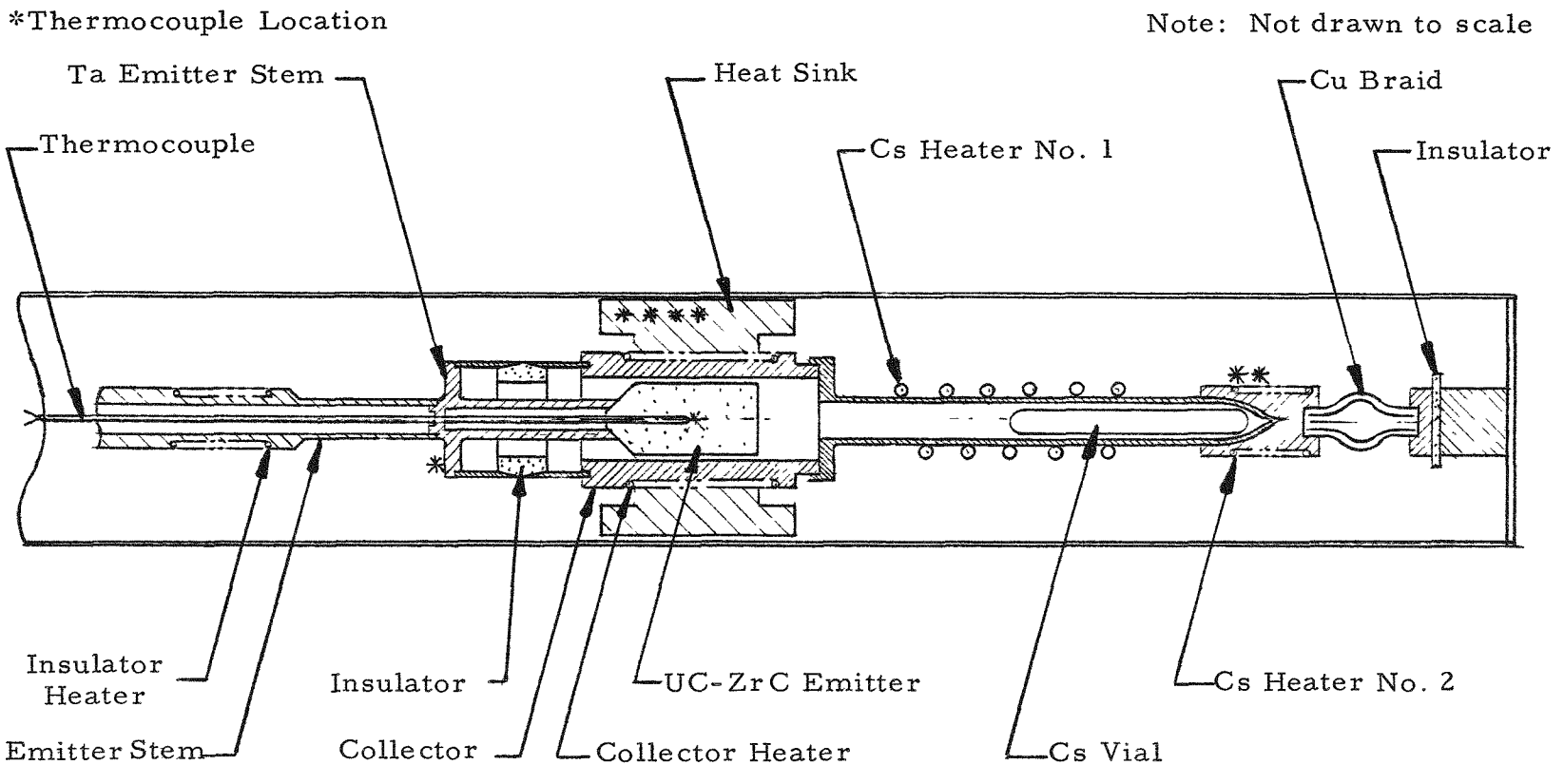

Fig. 34--Mark VI in-pile test cell (IC-2)

The first data obtained were the open-circuit emitter temperatures as a function of reactor power, as shown in Fig. 35. The next data obtained were the performance at a constant reactor power of 800 kw with varying electrical load. At each load condition, the cesium reservoir temperature was optimized. The results are shown in Fig. 36. The maximum power measured was 26.8 w ($\sim$2w/cm^2) at an emitter temperature of 1455°C and a cesium temperature of 330°C.

The next test procedure was to measure the power output at a constant emitter temperature of 1800°C. The initial performance at a mean emitter surface temperature of 1710°C is shown by the upper curve in Fig. 37. The maximum power output on this curve was 64 or 4.8 w/cm^2 at 83 amp. It is noted that the high-temperature operation began 5 hours after the test was initiated. When it was attempted to reproduce the curve, the power had degraded about 10 percent. This degradation continued for about 15 hours, as shown by Fig. 38.

After 20 hours of total operation, the power output had degraded about 50 percent, or about 2.4 w/cm^2. The data of Fig. 35 were used to estimate the fission power input to the cell. A correlation of cell power versus reactor power has been made between this data and the data from the operation of laboratory cells OC-2 and OC-3 which are given in Fig. 39. This correlation is given in Fig. 40 and was used to calculate the thermal efficiency. The maximum cell efficiency at the low emitter temperature of 1455°C was 8.2 percent. The maximum cell efficiency at the emitter temperature of 1710°C was about 12 percent. The degradation of efficiency is shown in Fig. 38. The final calculated efficiency was about 5.6 percent. The degradation of thermionic power and efficiency decreased for about 20 hours of operation and then remained constant. After a total of 80 hours operation, the test was terminated.

The observed degradation of performance was similar to the out-of-pile cell OC-3. Post-operative examination of OC-3 showed that the collector surface was heavily oxidized. It is believed that the source for oxidation was the thermocouple insulation, after its sheath developed a crack. This cell is now awaiting Hot Cell examination.

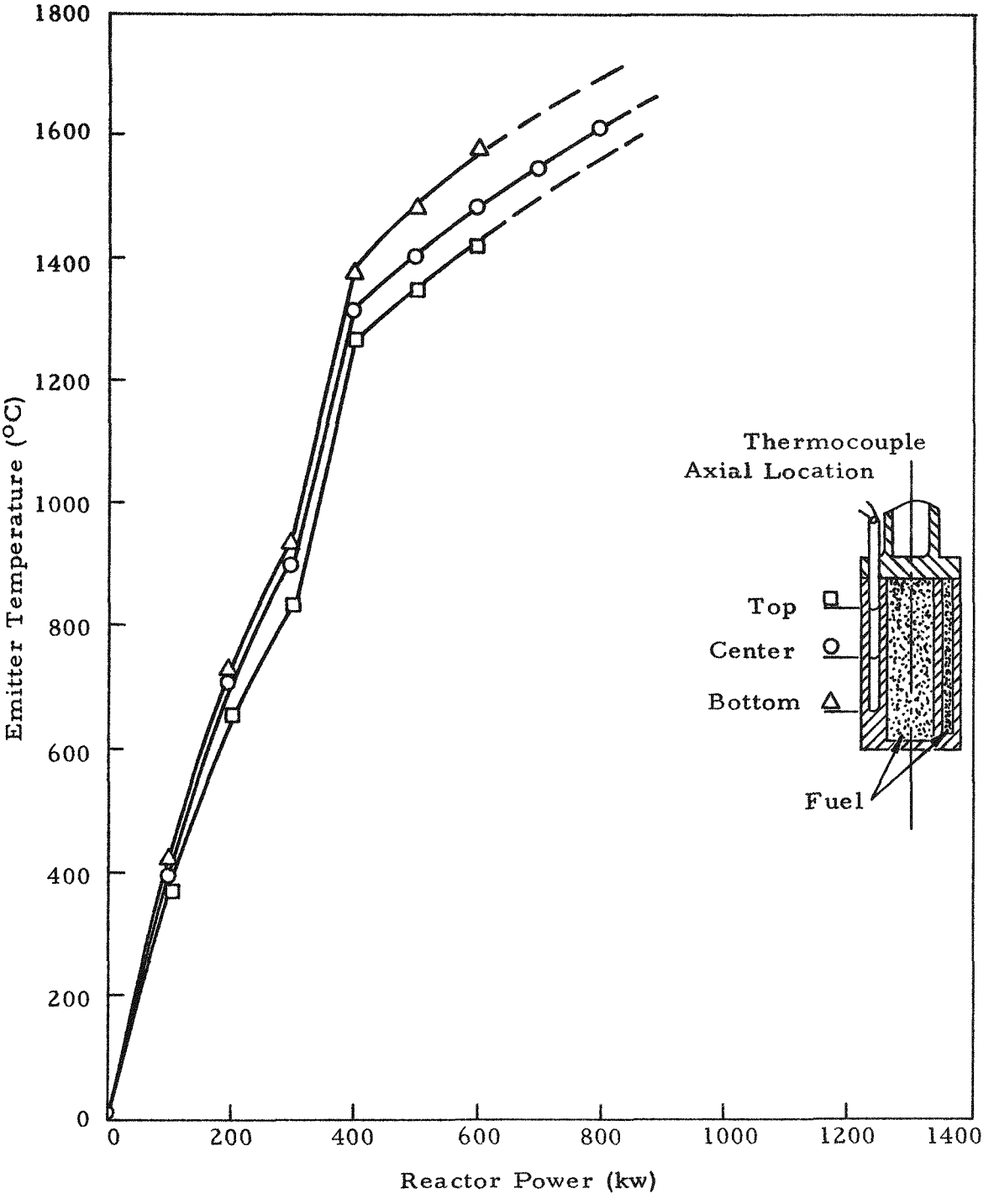

Fig. 35--Open-circuit emitter temperature versus reactor power for in-pile testing of IC-1' test cell

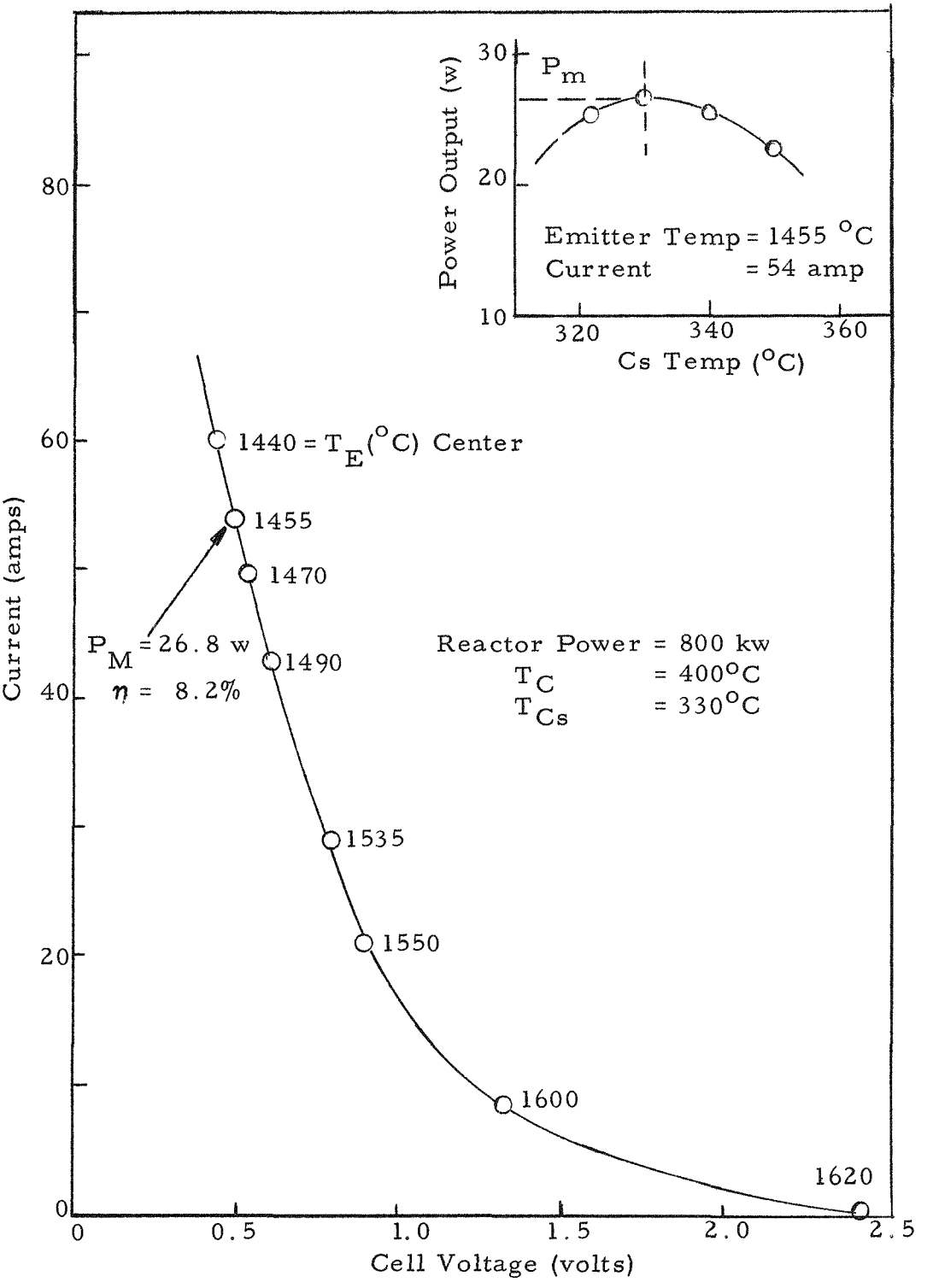

Fig. 36--IC-1' current-voltage characteristic at 800 kw reactor power

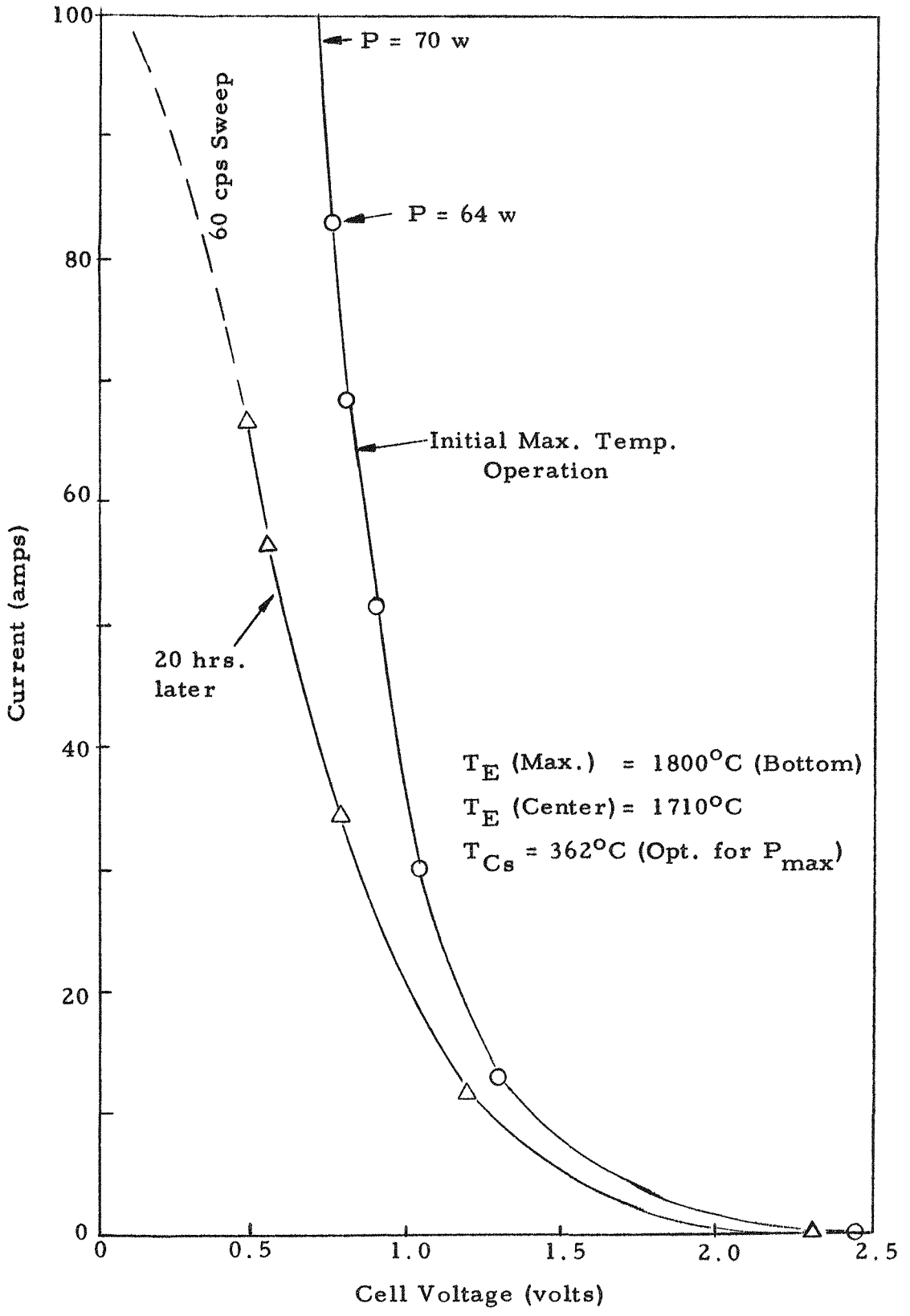

Fig. 37--IC-1' current-voltage characteristics

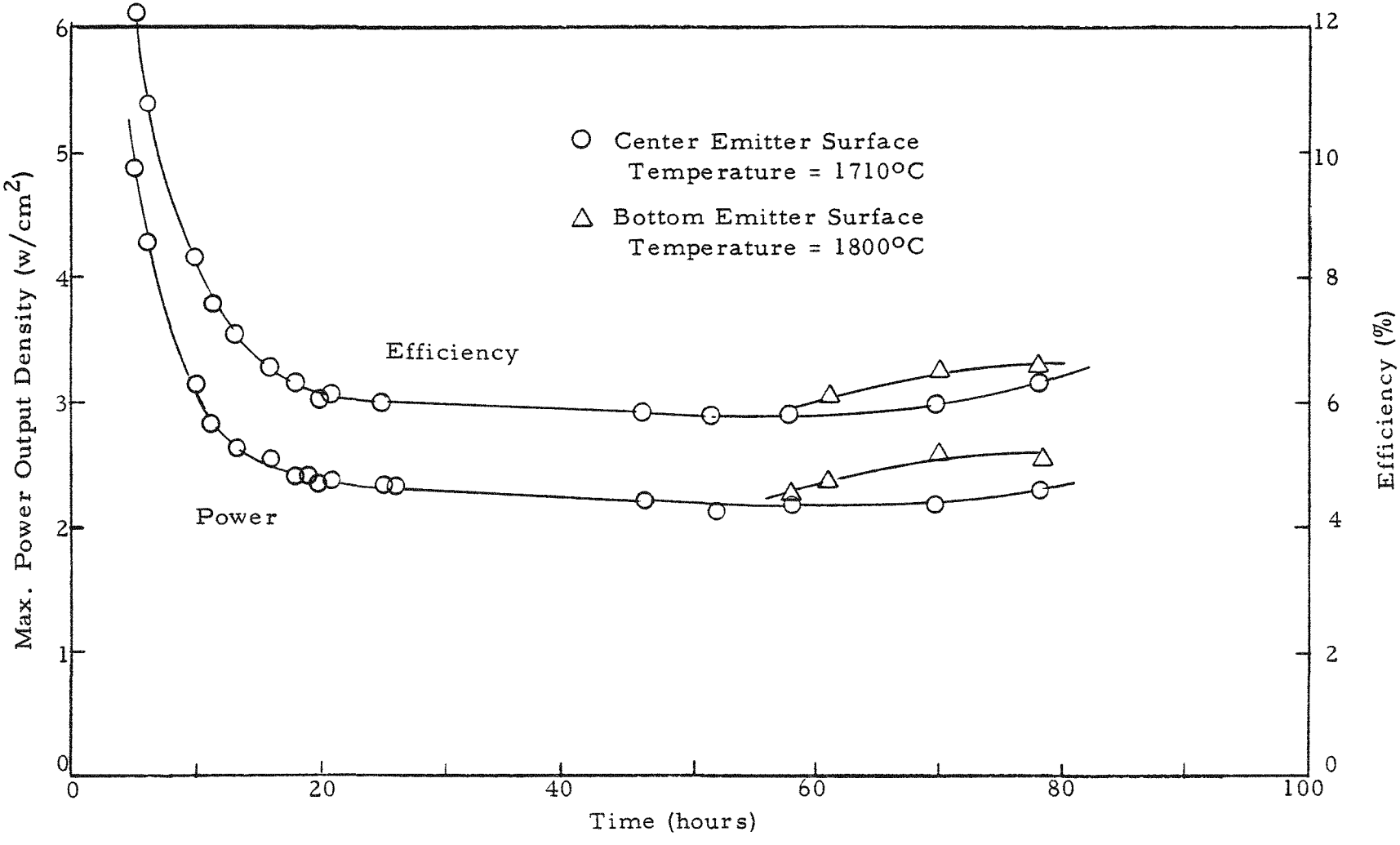

Fig. 38--IC-1' performance versus time

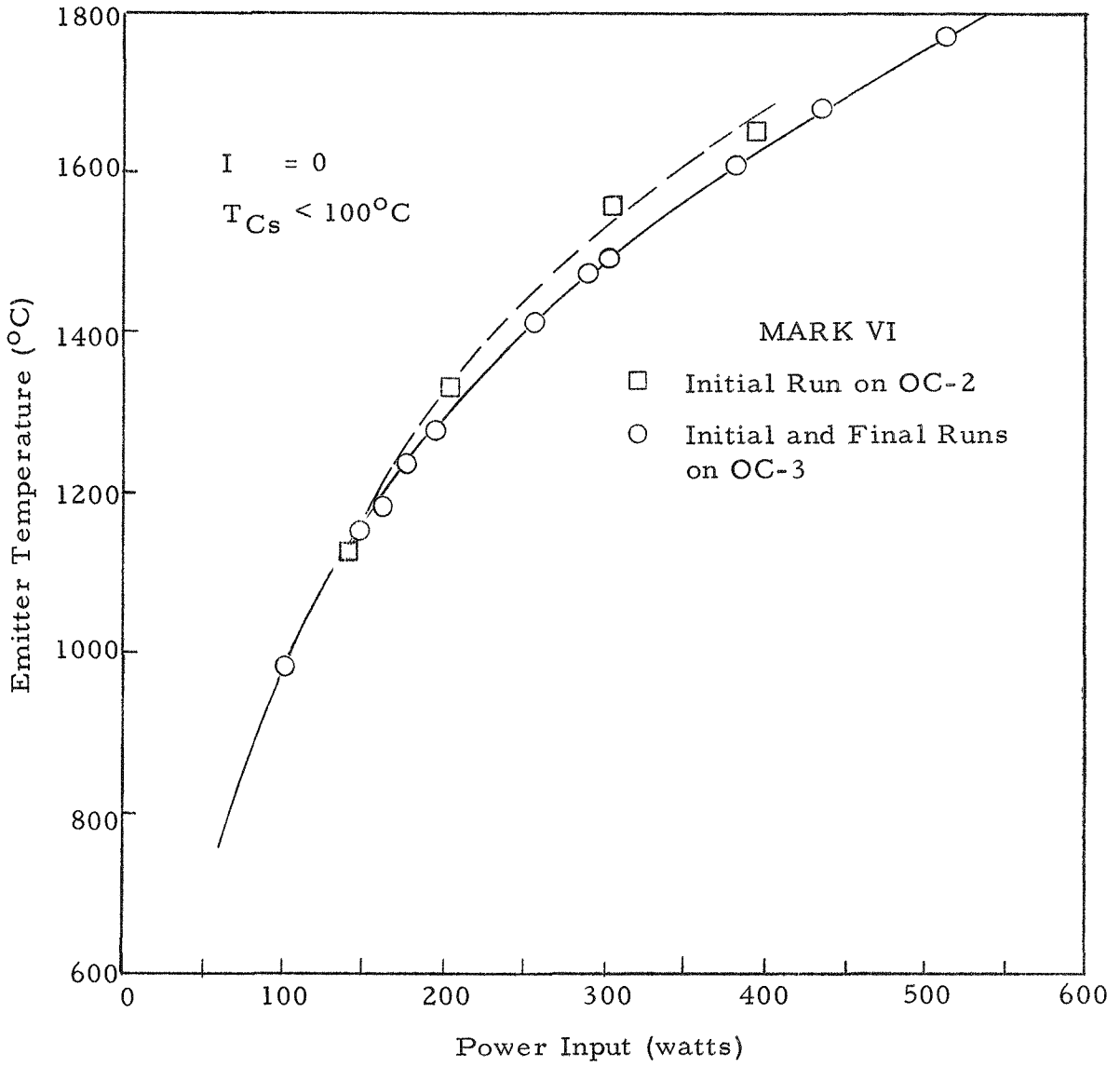

Fig. 39--Emitter temperature versus power input data obtained from Mark VI cells OC-2 and OC-3

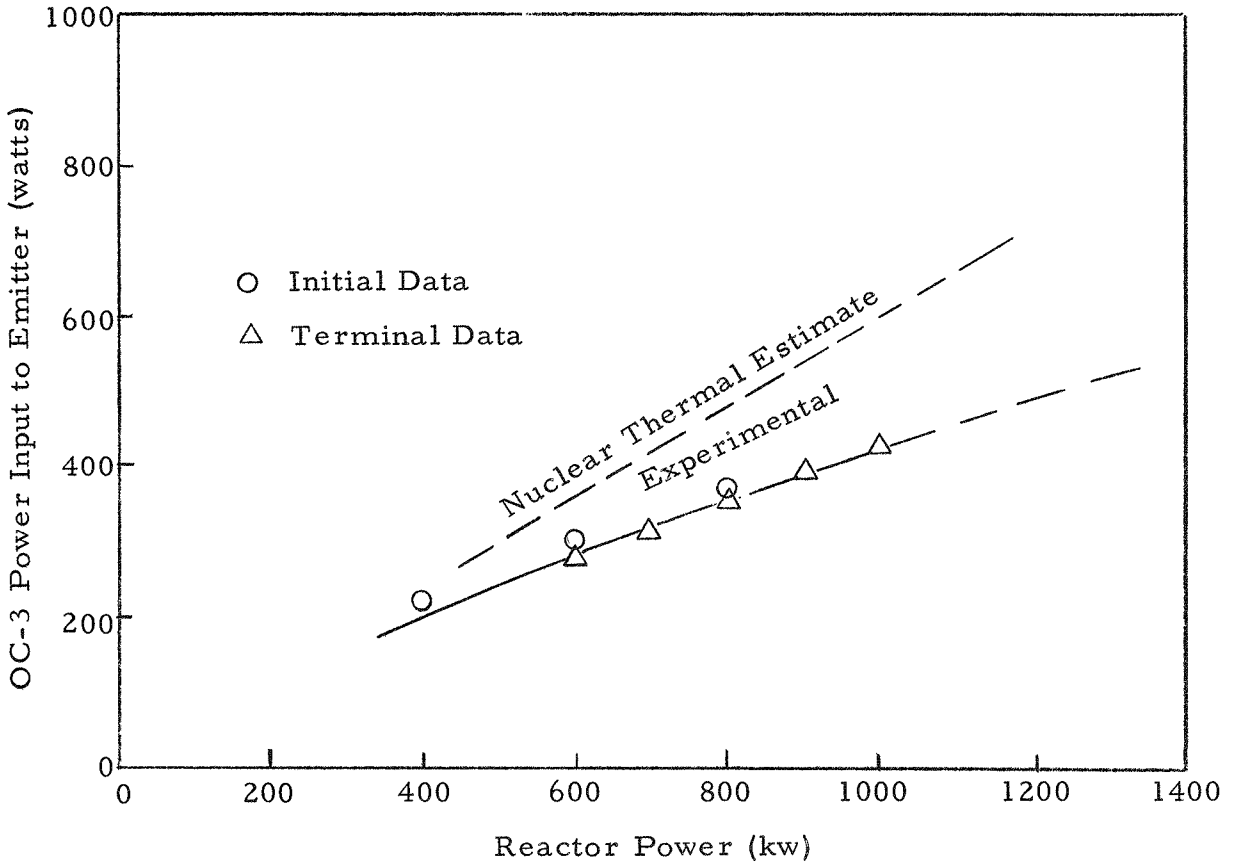

Fig. 40--IC-1' correlation of reactor power to emitter power input of OC-3

BLANK

V. FAST REACTOR SYSTEMS

Parametric studies have been performed on in-pile space thermionic reactor systems. In the reactor design, the nuclear thermionic and heat-transfer performance of reactors at each power level were considered. For comparison two liquid metal coolants were assumed, Li and NaK. In addition to the reactor, other components considered in these studies were the coolant pump and radiator. The problems of shielding, dc-to-ac conversion, and detailed structural design have not been investigated in detail. The most critical of these is the dc-to-ac conversion equipment which has inadequate data for analysis.

5.1 GENERAL FEATURES

Each reactor was a reflector-moderated-and-controlled fast reactor utilizing in-pile thermionics. The reactor was cooled by liquid metal which was circulated by electromagnetic pumps to a single-phase radiator system.

5.1.1 Basic Assumptions

The basic assumptions used in these design studies were:

(1) Utilizing the basic fuel element design (W-clad UC-ZrC emitter, Mark VI cell) three fuel compositions were assumed, i.e., UC/ZrC ratios of 90/10, 50/50 and 30/70 utilizing fully enriched U-235.

(2) For each fuel composition, a minimum-size reactor was determined under the assumption of suitable excess reactivity for a 10,000-hour life.

(3) Assuming a maximum allowable fuel centerline temperature of 1900°C, thermal and thermionic analyses were performed on the systems to determine the specific thermal power operation and the electrical power output for each system.

(4) In considering the liquid-metal cooling of these systems, it was assumed that the NaK and Li systems were limited to design temperatures of 1300°F and 2000°F, respectively. In all cases, temperatures and flow data were estimated using the average flow-channel concept. A uniform heat input along the channel was assumed. No hot-channel factors were applied and no attempt was made to optimize flow rates on an over-all weight basis.

(5) Finned-tube radiator configurations were assumed for system performance estimates. The criteria that the radiator coolant pressure drop was equal to the reactor core pressure drop was used to estimate the tube length, radiator aspect ratio, and manifold tube diameter.
(6) The coolant pump performance estimates were based upon the conceptual design of high-temperature electromagnetic pumps.

5.1.2 System Size

Over-all system configurations were not considered in detail. However, for all systems the size of the reactor and radiator were estimated. These estimates are shown in Tables 4 and 5.

Table 4

SIZES OF REACTOR COMPONENTS

Power Level (ekw)	Core Diameter (inches)	Core Length (inches)	Reflector Thickness (inches)
80	9.3	9.6	2.0
230	12.0	12.6	2.0
2000	23.3	21.6	2.0

Table 5

RADIATING AREA FOR TUBE AND FIN RADIATORS

Power Level (ekw)	NaK System (area in ft^2)	Li System (area in ft^2)
80	454	107
230	1430	324
2000	10,000	2,480

5.1.3 Operating Parameters

The estimated operating parameters for each reactor for a nominal 10,000-hour life are summarized in Tables 6, 7 and 8.

Table 6

OPERATING PARAMETERS OF THE 80 KW(E) REACTOR

General Characteristics	
Reactor thermal power	1,100 kw
Electrical output	80 kw(e)
Reactor Characteristics	
Configuration	Right cylinder
U-235 Loading	55 kg
Fuel composition	90% UC - 10% ZrC
Median fission energy	0.48 Mev
Electrical Characteristics	
Average current density/diode	11.7 amps/cm^2
Average power density/diode	6.35 w(e)/cm^2
Number of diodes/module	110
Power output/module	376 amps at 54 volts
Cesium reservoir temperature	623°K

Table 7

OPERATING CHARACTERISTICS OF THE 230 KW(E) REACTOR

General Characteristics	
Reactor thermal power	3,330 kw
Electrical output	80 kw(e)
Reactor Characteristics	
Configuration	Right cylinder
U-235 loading	80 kg
Fuel composition	50% UC - 50% ZrC
Median fission energy	0.32 Mev
Electrical Characteristics	
Average current density/diode	16.5 amps/cm^2
Average power density/diode	7.18 W(e)/cm^2
Number of diode/module	96
Power output/module	300 amps at 41.5 volts
Cesium reservoir temperature	623°K

Table 8

OPERATING CHARACTERISTICS OF THE 2000 KW(E) REACTOR

General Characteristics	
Reactor thermal power	27,000 kw
Electrical output	2,000 kw(e)
Reactor Characteristics	
Configuration	Right cylinder
U-235 loading	187 kg
Fuel composition	30% UC - 70% ZrC
Median fission energy	0.18 Mev
Electrical Characteristics	
Average current density/diode	15.2 amps/cm^2
Average power density/diode	7.25 w(e)/cm^2
Number of diode/module	96
Power output/module	184 amps at 51.6 volts
Cesium reservoir temperature	623°K

5.1.4 System Weights

Estimated weights of the components of each system are given in Tables 9, 10, and 11.

Table 9

ESTIMATED WEIGHTS OF 80 KW(E) SYSTEM

	NaK Cooled		Li Cooled	
Component	Weight (lb)	Specific Weight (lb/kw(e))	Weight (lb)	Specific Weight (lb/kw(e))
Core	234	2.93	234	2.93
Reflector	133	1.67	133	1.67
Radiator	297	3.71	121	1.51
Pumps	54	0.68	40	0.50
Total	718	8.99	528	6.60

Table 10

ESTIMATED WEIGHTS OF 230 KW(E) SYSTEM

Component	NaK Cooled		Li Cooled	
	Weight (lb)	Specific Weight (lb/kw(e))	Weight (lb)	Specific Weight (lb/kw(e))
Core	446	1.94	446	1.94
Reflector	208	0.91	208	0.91
Radiator	1106	4.81	454	1.97
Pumps	101	0.44	74	0.32
Total	1861	8.10	1,181	5.13

Table 11

ESTIMATED WEIGHTS OF 2000 KW(E) SYSTEM

Component	NaK Cooled		Li Cooled	
	Weight (lb)	Specific Weight (lb/kw(e))	Weight (lb)	Specific Weight (lb/kw(e))
Core	2622	1.31	2622	1.31
Reflector	658	0.33	658	0.33
Radiator	13,040	6.52	4,892	2.45
Pumps	690	0.35	500	0.25
Total	17,010	8.51	8,666	4.34

5.2 POWER FLATTENING

The effect of a non-uniform fission power distribution upon the thermionic performance as a function of load voltage is shown for each system in Figs. 41, 42, and 43 for two cesium temperatures. For comparison, the performance of each fuel element is shown under flat power generation conditions. From the results, it is obvious that power flattening techniques must be utilized on any reactor which employs thermionic generator in-pile. Fuel zoning provides the most direct method for power flattening in fast reactor systems. However, there are serious disadvantages to this approach in thermionic reactors because of the complications involved in varying the fuel content of various diodes appropriately to achieve the desired power flattening capability. A more reasonable approach appears to be that of adjusting the reflector thickness in order to maintain a flat power generation rate over a large fraction of the core. Figure 44 shows the effect on the power generation rate that can be obtained with this type

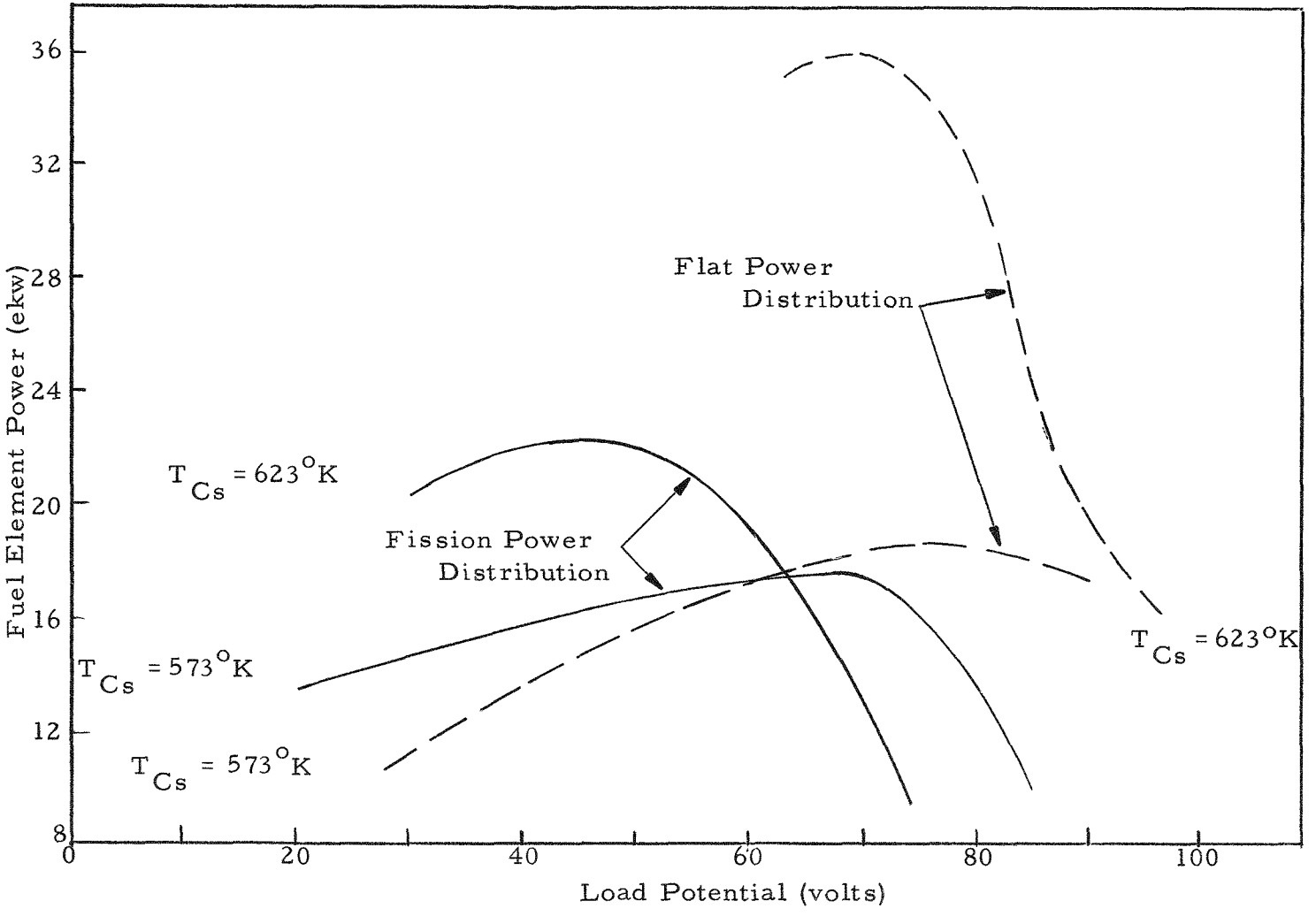

Fig. 41--Effect of nonuniform fission power distribution on thermionic performance as a function of load voltage (80 ekw reactor system)

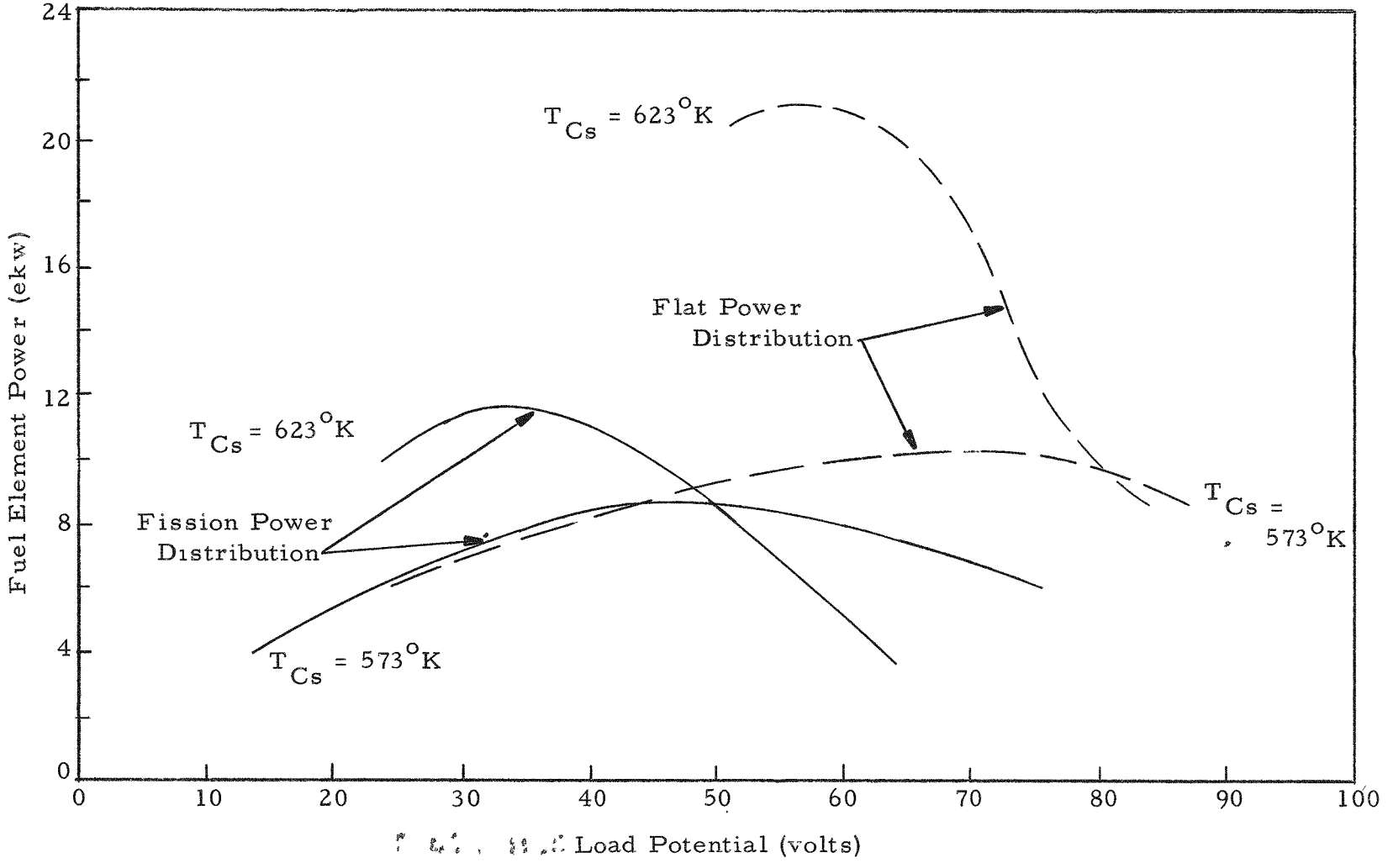

Fig. 42--Effect of nonuniform fission power distribution on thermionic performance as a function of load voltage (230 ekw reactor system)

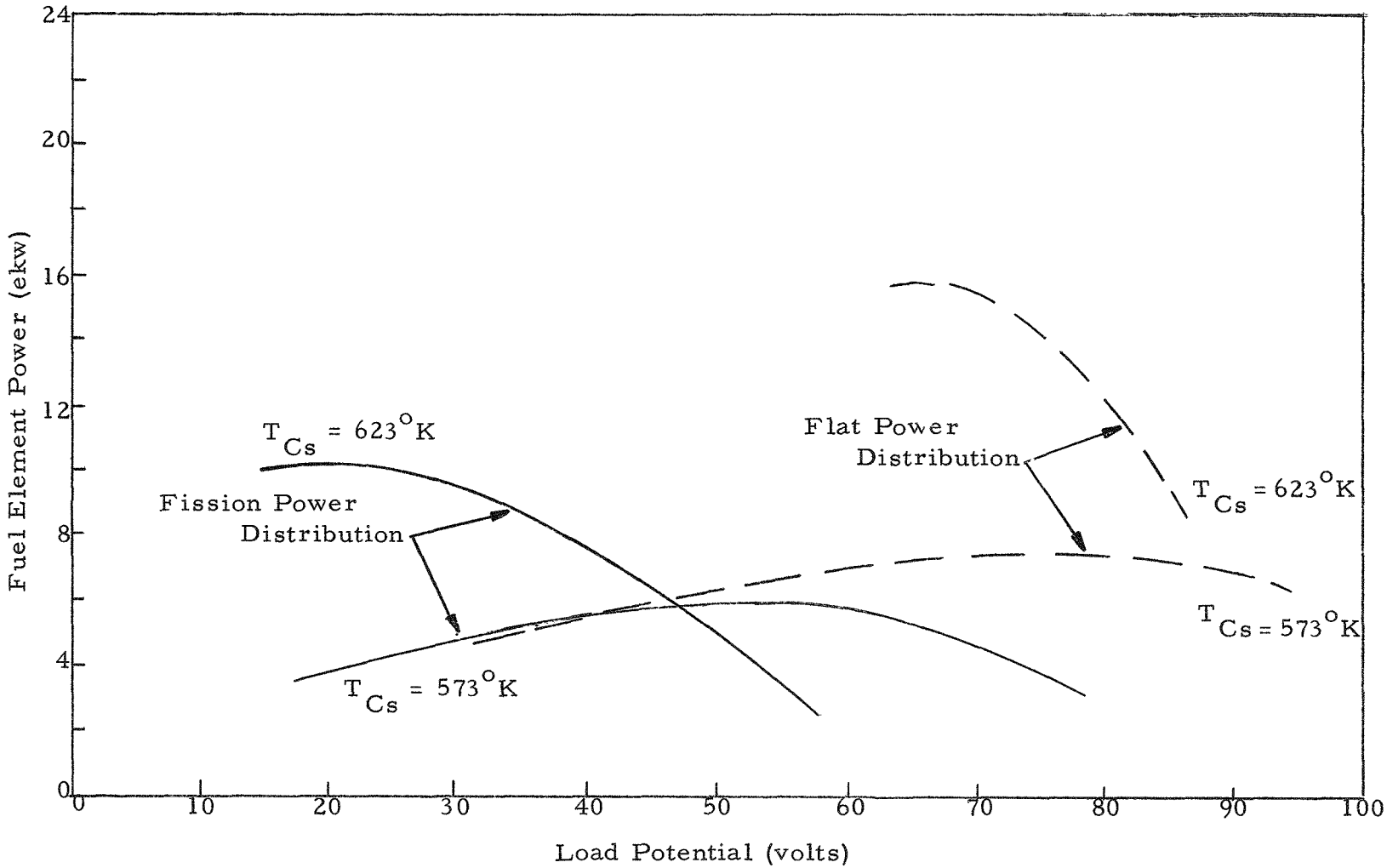

Fig. 43--Effect of nonuniform fission power distribution on thermionic performance as a function of load voltage (2000 ekw reactor system)

of approach. The power generation rate in the case of a 6-inch reflector (as shown in this figure) is quite flat over a large fraction of the core volume. Additional steps would have to be taken, however, to accommodate the power peak near the core reflector interface.

5.3 CONTROL METHODS

Preliminary estimates on the feasibility of reflector control for the thermionic reactor have been made. For the systems studied, it appears that adequate shutdown control can be provided by removable side reflectors which would be locked in place during operation. Shim control to maintain constant reactor power could conceivably be obtained by relatively small displacements of the end reflectors since only a very small reactivity change is introduced by fuel burnup and fission product build-up throughout the reactor lifetime.

The coupling between the reactor control system and the conversion system has been examined with respect to the change in the distribution of fission power production during the expected lifetime and the effect of this change on the thermionic performance. Below 1 Mw(e) this change in power distribution would not be sufficient to effect thermionic performance. As the power level is increased (for compact systems) to much above 1 Mw(e) the effect would become more severe and would have to be investigated in detail.

The kinetics of fast thermionic reactor systems present unique problems, primarily because the thermal-to-electrical power conversion takes place directly within the fuel element and because the mechanisms for energy transfer from the fuel to the coolant are considerably different from those encountered in a conventional reactor. One peculiarity of thermionic systems is the parallel arrangement of the heat dump and electrical system. Any demand for electrical power will lead to an increase in the current production of the diodes with an accompaning electron cooling effect. However, this effect involves only a small part of the power since most of the power is dumped. In addition, the temperature of the thermionic emitter varies relatively slowly with the input fission power to the emitter because of the mode of energy transfer (electron and radiative cooling). Hence, the relationship between reactor thermal power and the electrical power output is quite complicated. However, the general problem of thermionic reactor kinetics should be considered in some detail in order to identify the features of the over-all system.

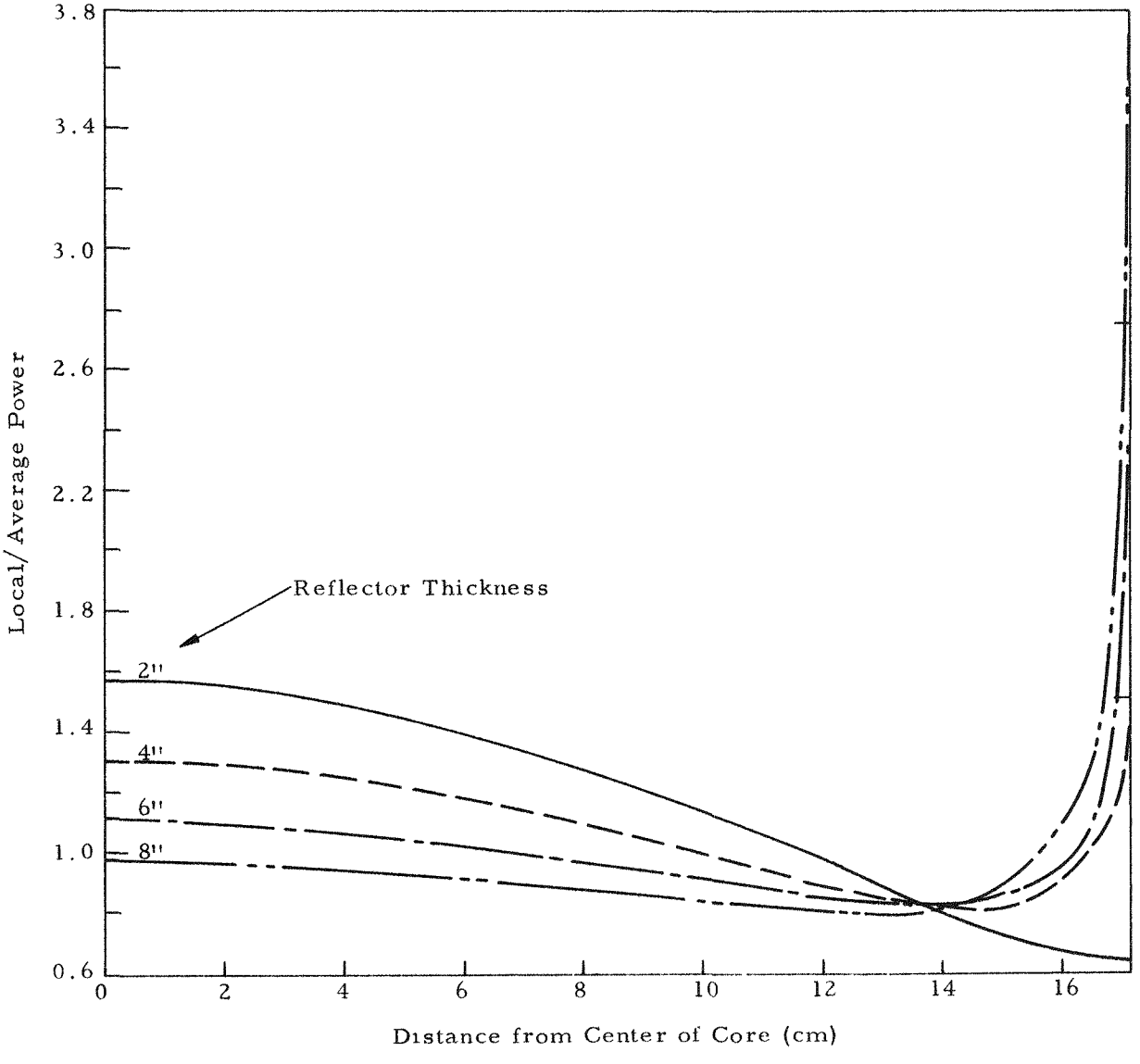

Fig. 44--Effect of reflector thickness on flatness of power generation rate

5.4 HEAT-REJECTION SYSTEM

For the three reactor power levels, temperatures and flow data have been estimated for both NaK and Li coolants. Approximately the same pressure drops for both coolants at each power level were used. Coolant flow rates and temperatures are given in Tables 12, 13 and 14.

Table 12

80 KW(E) SYSTEM COOLANT SUMMARY

Coolant	NaK	Lithium
Number of coolant sub-arrays	4	4
Fuel elements per sub-array	18	18
Coolant mass flow rate per sub-array	5 lb/sec	3.7 lb/sec
Coolant inlet temperature	1100°F	1942°F
Coolant outlet temperature	1300°F	2000°F
Coolant system pressure	15 psia	6 psia
Pressure drop, total	2.0 psi	1.8 psi
Maximum fuel temperature*	3430°F	3430°F
Average film temperature drop	64°F	34°F

*No hot channel factor applied.

Table 13

230 KW(E) SYSTEM COOLANT SUMMARY

Coolant	NaK	Lithium
Number of coolant sub-arrays	18	18
Fuel elements per sub-array	12	12
Coolant mass flow rate per sub-array	2.5 lb/sec	1.8 lb/sec
Coolant inlet temperature	1033°F	1922°F
Coolant outlet temperature	1300°F	2000°F
Coolant system pressure	15 psia	6 psia
Pressure drop, total	2.5 psi	2.0 psi
Maximum fuel temperature*	3420°F	3420°F
Average film temperature drop	64°F	53°F

*No hot channel factor applied.

Table 14

2000 KW(E) SYSTEM COOLANT SUMMARY

Coolant	NaK	Lithium
Number of coolant sub-arrays	70	70
Fuel elements per sub-array	18	18
Coolant mass flow rate per sub-array	12 lb/sec	8.8 lb/sec
Coolant inlet temperature	1249°F	1960°F
Coolant outlet temperature	1300°F	2000°F
Coolant system pressure	15 psia	6 psia
Pressure drop, total	2.2 psi	2.2 psi
Maximum fuel temperature*	3330°F	3330°F
Average film temperature drop	55°F	30°F

*No hot channel factor applied.

Estimations of radiator performance were based upon finned-tube configurations using niobium-1%, zirconium tubes. Summaries of the characteristics of the estimated radiator designs are given in Tables 15, 16, and 17.

Table 15

80 KW(E) SYSTEM RADIATOR SUMMARY

Coolant	NaK	Lithium
Number of tubes	53	46
Tube length	5.5 ft	3.3 ft
Tube inside diameter	0.5 in.	0.5 in.
Tube thickness	0.020 in.	0.020 in.
Tube pitch	0.763 ft	0.343 ft
Fin thickness	0.020 in.	0.025 in.
Aspect ratio	3.7	2.4
Manifold length, half	40.5 ft	15.8 ft
Manifold inside diameter	1.50 in.	1.39 in.
Manifold tube thickness	0.060 in.	0.056 in.
Manifold armor thickness	0.103 in.	0.071 in.

Table 16

230 KW(E) SYSTEM RADIATOR SUMMARY

Coolant	NaK	Lithium
Number of tubes	116	99
Tube length	8.0 ft	4.3 ft
Tube inside diameter	0.5 in.	0.5 in.
Tube thickness	0.020 in.	0.020 in.
Tube armor thickness	0.140 in	0.109 in
Tube pitch	0.768 ft	0.381 ft
Fin thickness	0.020 in.	0.030 in
Aspect ratio	5.6	4 4
Manifold length, half	89.3 ft	37.6 ft
Manifold inside diameter	2.00 in.	1 85 in.
Manifold tube thickness	0.080 in.	0 074 in.
Manifold armor thickness	0.134 in.	0 094 in

Table 17

2000 KW(E) SYSTEM RADIATOR SUMMARY

Coolant	NaK	Lithium
Number of tubes	266	157
Tube length	17.4 ft	15.5 ft
Tube inside diameter	0.5 in.	0.75 in.
Tube thickness	0.030 in.	0.030 in.
Tube armor thickness	0.270 in.	0.206 in.
Tube pitch	1.11 ft	0.506 ft
Fin thickness	0.045 in.	0.050 in.
Aspect ratio	4.2	2.6
Manifold length, half	295	79.7 ft
Manifold inside diameter	4.58 in.	3.80 in.
Manifold tube thickness	0.100 in.	0.100 in.
Manifold armor thickness	0.251 in.	0.147 in.

Meteoroid protection was assumed to be provided by beryllium and beryllia armor for both systems. Although beryllium has an armor figure of merit which is approximately a factor of 2 superior to beryllia at 1300°F, the high vapor pressure, lower strength, and lower figure of merit of beryllium at 2000°F indicate that BeO is a more promising armor candidate material for high-temperature application. In addition, thermal expansion properties of beryllia are close to those of niobium and considerable irradiation data exists for this material.

BLANK

Appendix

STATUS OF THERMIONIC FISSION HEAT CONVERSION TECHNOLOGY

This Appendix is intended as a brief summary of thermionic technology covering cell tests, in-pile and out-of-pile life tests, fuel element design studies and the status of materials research.

A. CESIUM CELL TESTING RESULTS

1. Nature of Cells Tested

The nature of cesium cells tested can be illustrated as follows:

a. Unclad fuel-emitter

(mixture of fuel and emitter material	(a) In-pile fission heated (b) Out-pile electrically heated

b. Clad fuel-emitter

(nuclear fuel clad with emitter material)	(a) In-pile fission heated (b) Out-of-pile electrically heated in absence of fuel

There have been no reported out-of-pile life-test results on cells containing clad fuel-emitters, although such tests are currently being performed at General Atomic and in a number of other laboratories. Numerous out-of-pile studies of clad cells containing no fuels have been made. The results, as illustrated in Fig. A-1,[3] however,, should not be considered as life tests because of the absence of one of the most important ingredients of a fission heated conversion cell.

2. Test Results

The results so far obtained are summarized in Table A-1.

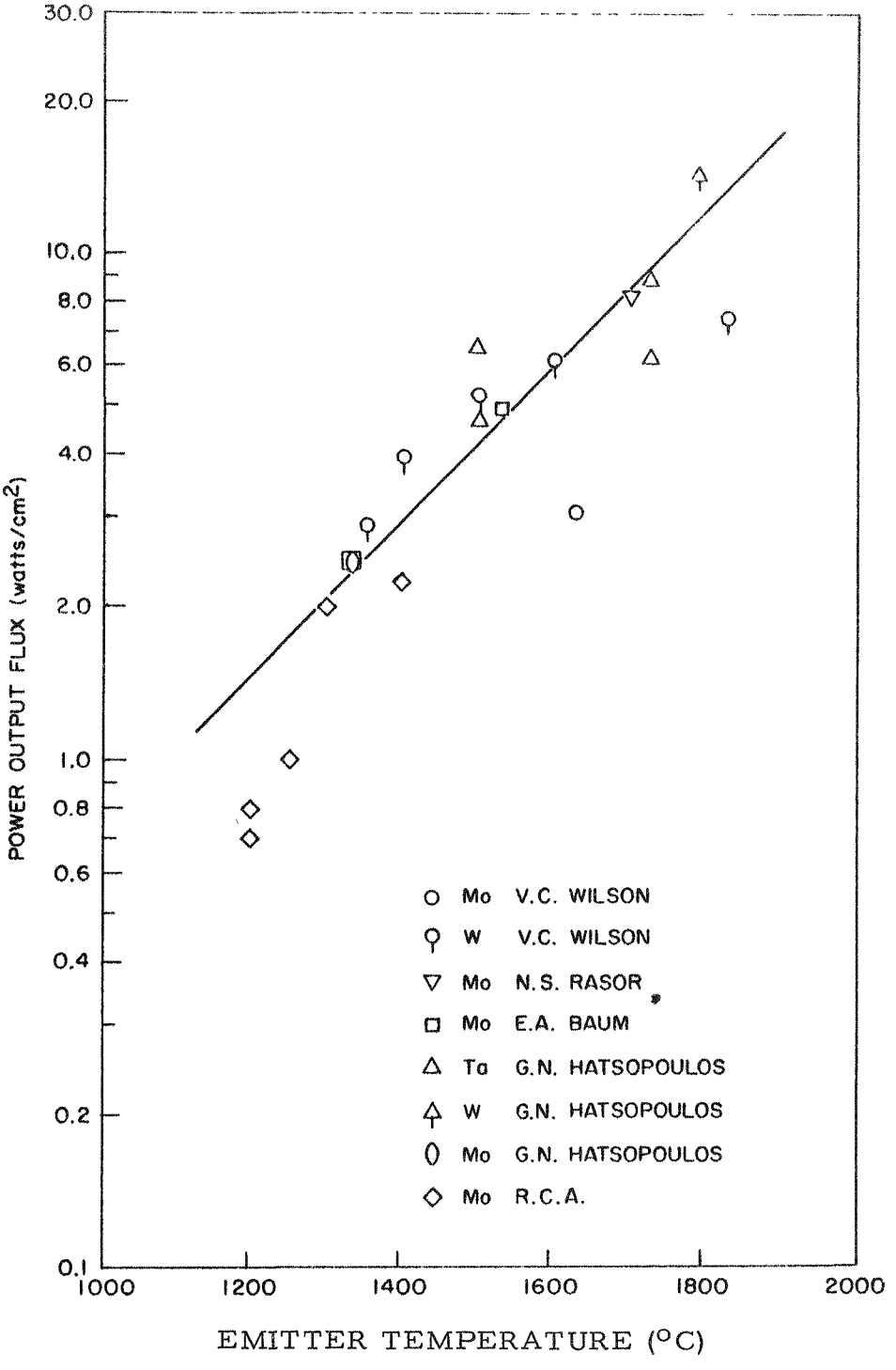

Fig.A-1--Power output experience for cesiated refractory metal thermionic converters (adapted from Ref. 1).

Table A-1

TEST RESULTS

Year	Cathode Material (at-%)	Cathode Temperature (°C)	Electrode Spacing (mils)	Power Output (watt/cm^2)	Time of Operation (hrs)	Efficiency (%)	Mode of Failure	Testing Party
			A. On In-Pile Unclad Cells					
1960	90 UC - 10 ZrC	~2000	20	12	20	10	Electrical shortage due to vaporization and condensation of cathode material	General Atomic
1961	30 UC - 70 ZrC	~2000	40	12	230	8	Cathode broken	Los Alamos
1961	30 UC - 70 ZrC	~2000	40	16	284	7	Ceramic seal broken	Los Alamos
1962	30 UC - 70 ZrC	~2000	40	10	48	-	Leakage in cell envelope	Los Alamos
1962	30 UC - 70 ZrC	~2000	40	17	112	9	Shortage due to cathode disalignment	Los Alamos
			B. On Out-Of-Pile Unclad Cells					
1960	10 UC - 90 ZrC	1730	10	1.5	1750	-	Leakage in cell envelope in all cases	General Atomic
to		1730	10	1.5	1500	-		
1963	10 UC - 90 ZrC	1900	10	4	150	-		
		1730	10	1.5	1000	-		
		1730	10	1.5	480	-		
			C. On In-Pile Clad Cells					
1961	Mo-clad UO_2	1700	30	3.5	63	-	Shortage inside cell	General Electric
1963	Mo-clad UO_2	1350	7	2	283	11	Power output declined after temperature raised to 1500°C; reason unknown	RCA
1963	W clad UC	1710	10	2.5 - 5	80	-	Turned off deliberately	General Atomic

3. Discussion

Although the results in Table A-1 are self-explanatory, several points are worthy of further discussions.

a. The data in Fig. A-1 indicates that empirically the power output of a cesium cell increases with the emitter temperature. This is also borne out qualitatively by the test results shown in Table A-1.

b. The operating temperature of the out-of-pile unclad cell is limited not by the properties of the 10 UC-90 ZrC emitter itself, but by the interaction between the carbide and the Ta support separating the cesium cell from the electron gun chamber. Since this problem does not exist in the in-pile cell configuration, the results in Table A-1 should not be used to set the limits of the life and performance of in-pile carbide cells.

c. Since most of the fueled cells were fabricated and tested before the fabrication techniques were refined and the materials properties were thoroughly studied, these tests should be considered as demonstrations and should not be used to judge the feasibility of thermionic fission-heated conversion systems. Failure by faulty fabrication procedures can be overcome by improving the fabrication techniques, while failure by material limitations can be avoided by understanding the critical material problems involved. Refinement of cell fabrication techniques is being actively pursued by workers in this field and the increasing understanding of the critical materials problem has made it possible to select the materials and the operating conditions more intelligently. Both should contribute greatly to the realization of more successful cell testing.

B. STATUS OF FUEL ELEMENT DESIGN

Initial parametric studied and preliminary design studies of thermionic reactors have been based upon the multi-cell series thermionic fuel element concept. In this concept it is assumed that the thermionic cells are arranged within a cylindrical fuel element with the cells connected in series, so that the final array resembles a multibattery flashlight. Parametric surveys have been made on conceptual reactors composed of this type of element to examine the nuclear design and heat removal problems so that preliminary guidelines can be established for the fuel element design based upon fuel loading, power flattening and coolant system requirements. Considerations such as these relate directly to the materials development program. In addition to the parametric surveys, calculational tools have been developed at General Atomic with which detailed neutronic, thermionic and thermal analysis can be performed.

1. Parametric Studies

(a) Fuel Loading - For a particular fuel element design and assumed thermionic cell performance, a minimum size (minimum mass) reactor can be specified that will produce a given electrical power output. The fuel fraction of the reactor is restricted by the fuel element design. However, the enrichment of the uranium concentration in the fuel must be sufficient to maintain the reactor power throughout the life of the system. Hence, metallurgical investigations of fuel-emitters can be related qualitatively to particular reactor systems. This type of analysis has been performed in conjunction with the present series of capsule irradiations. Figure A-2 shows the qualitative relation between the atom percent UC in UC-ZrC and the nominal electrical power output of a minimum mass reactor employing UC-ZrC emitters.

(b) Power Flattening - A number of calculations have been made on the effect of nonuniform power generation on the performance of a multicell fuel element. The results of these calculations indicate that, if power flattening techniques are not employed in the reactor, the thermionic performance of the fuel element is seriously degraded (factors of 2 or greater) compared with that of single cells of the same design operating under comparable conditions. This type of result must be taken into account in the program of materials development since, for example, it affects the choice of fuel employed. In particular a nominal operating power of 300 ekw implies a UC concentration of 50 to 60 atom% according to Fig. A-2. If the degradation due to non-flat power is taken into account, the nominal power level drops to 150 ekw and the applicable concentration range of UC increases to 80 atom%. In addition, if fuel zoning is employed to flatten the power, higher concentrations of UC would, in all probability, be used in some parts of the reactor.

(c) Coolant System Requirements - Considerations for the removal of waste heat from the thermionic fuel element are strongly dependent on the specific fuel element design. Sandwich insulators between the collector and the fuel element cladding have generally been assumed in preliminary analytical studies and estimates have been made of the thermal stresses and heat removal by the coolant. However, the configuration, the thermal stress, and heat removal problems have not as yet been analyzed in detail for a particular design. Information derived from such analysis is necessary to provide guidance for materials research and fabrication development.

2. Methods Development

(a) Nuclear Design Methods - Presently conceived thermionic reactors have very fast neutron spectra with mean fission energies lying

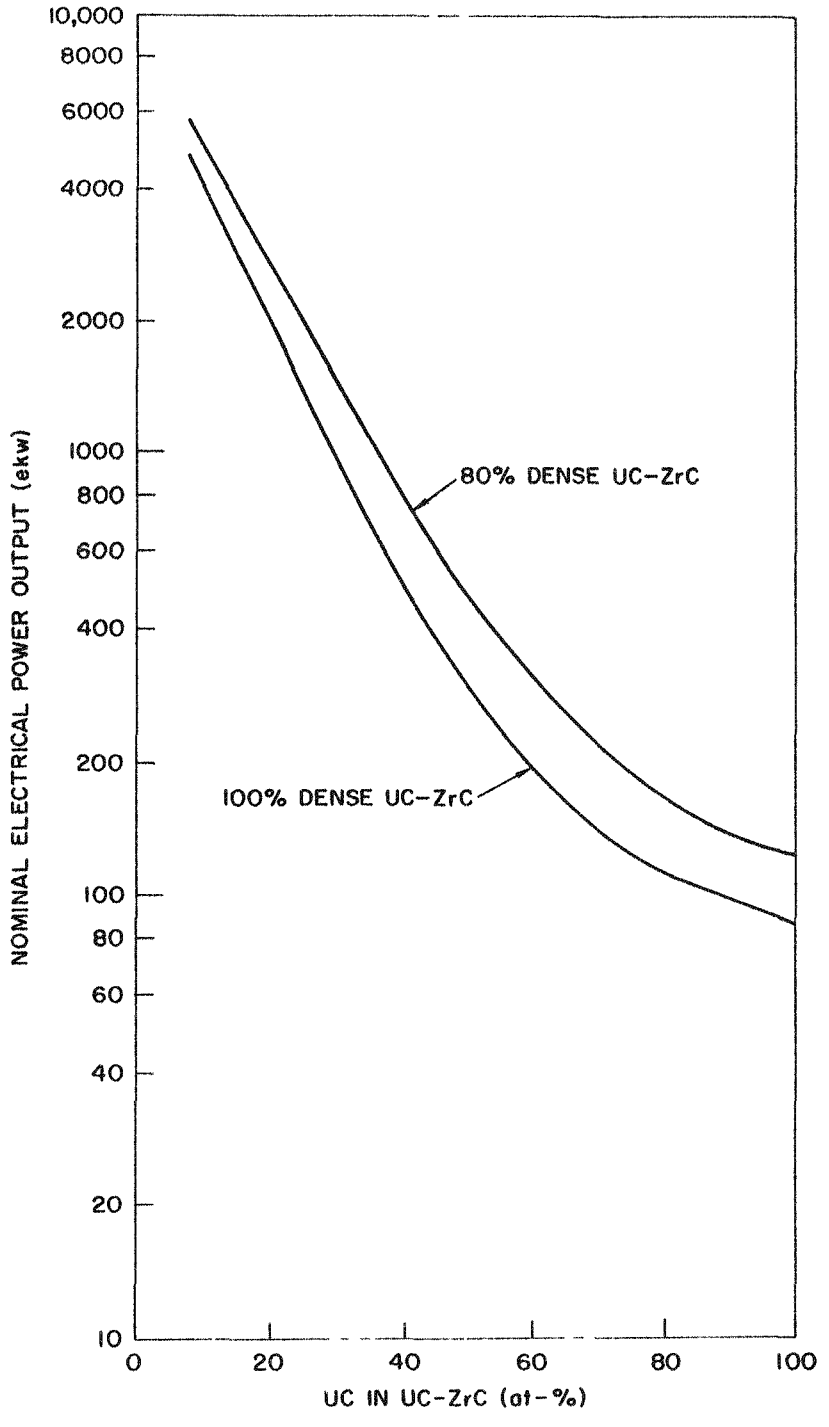

Fig. A-2 --Fuel compositions for conceptual thermionic reactors of various power levels

in the 100 to 500 kv region. In the analysis of reactors of this type, it is essential that highly-accurate neutron cross-section data be employed and that transport theory calculations of the core reactivity and power generation rate be utilized. Of interest in fast reactor systems is the availability of cross sections that include a high order of anisotropy scattering. This allows a more accurate treatment of anisotropic scattering and its effect on the competition between absorption, fission, slowing down and leakage. A digital computer code, GAM-II, has been developed by General Atomic for the computation of neutron spectra and group-averaged cross sections for fast reactor systems. During the last two years a large library of nuclear data has been prepared for approximately 150 nuclides. Using this data, GAM-II generates neutron spectra for specified compositions on a mesh of 99 energy groups using the B_n approximation. Group cross sections and transfer coefficients are averaged over the particular spectrum of interest. In addition to GAM-II, an extension of the Los Alamos DSN code has recently been developed at General Atomic. This code, GAPLSN, is a one-dimensional multigroup transport theory that contains an arbitrary energy transfer matrix and in which any degree of anisotropic scattering can be included. With these two computational tools, the nuclear design of fast reactor systems can now be carried out with a reasonable degree of accuracy.

(b) Thermionic Analysis - During the past year a digital computer code which describes the performance of networks of thermionic cells within a reactor has been developed. Detailed data derived from physics research on operating thermionic cells are incorporated in the library of this code. With the data now available, semi-quantitative estimates can be made of thermionic performance of single cells and of networks of these cells in a reactor environment. With the type of analysis that the code employes it is possible to examine the performance of any specified thermionic fuel element design under either optimum or off-optimum conditions. Hence, a calculational tool is now available by which the effects of design changes can be evaluated.

(c) Thermal Analysis - During the last two years digital computer codes have been developed at General Atomic which calculate one and two-dimensional temperature distributions as a function of space and time-dependent internal heat generation rates. Provisions for temperature-dependent properties, thermal conductivity, coefficient of thermal expansion, heat and total emissivity are included. Flow boundary conditions, radiator heat transfer, thermal contact resistances between the materials, dimensional changes due to both isotropic and anisotropic thermal expansion can be handled by these codes. Recently a method has been developed by which thermionic boundary conditions at the emitter surface (i.e. electron cooling) can be included in the problem description. With these

codes, 3-dimensional temperature profiles can be determined for the fuel element design.

In summary, it can be stated that parametric studies performed to date have defined problem areas which have served to establish general guidelines for the development of a thermionic fuel element. With the methods now available, specific fuel element design problems can be examined in detail so that specific materials problems can be formulated.

C. CURRENT STATUS MATERIALS RESEARCH

1. Fuel Swelling and Change of Dimension of Emitter upon Irradiation at High Temperatures

The pressure of fission gases built up inside nuclear fuels upon irradiation at high temperatures tends to deform the fuel bodies and lead to electrical shorting with the collector for either the unclad or the clad system. Work carried out at Los Alamos[4] has shown that high density (~97 percent theoretical density) 30 UC-70 ZrC samples, irradiated at 1800°C - 2200°C to burnups of 1 - 3 percent of the total uranium atoms in the samples, suffered from dimensional swelling or even fragmentation and disintegration due to the internal buildup of high pressure fission gas bubbles inside these samples. The remedy prescribed to overcome this difficulty is the use of low density fuel-emitters containing a large amount of open pores through which fission gases could escape. This has been substantiated by some post-irradiation annealing studies at Los Alamos[4] and at General Atomic[5]; both low-density 30 UC-70 ZrC bodies (~80 - 85 percent theoretical density) and fine 30 UC-70ZrC powder (<325 mesh) lost most of the fission gas built up inside the material upon annealing at 1800 - 1900°C for 10 - 20 hours. Currently, both Los Alamos and General Atomic are studying the dimensional stability of thermionic fuel bodies upon irradiation at high temperatures in capsules. At Los Alamos,[4] a 30 UC - 70 ZrC fuel pin of about 85 percent theoretical density prepared by General Atomic is being irradiated at 1900 - 2000°C in an argon atmosphere and the dimension of the pin is being checked intermittently by X-ray radiography. No detectable change in dimension has been observed in 370 hours and the test is being continued.

At General Atomic, capsule irradiation of UC-ZrC of various compositions (90, 50, and 20 mol-% UC) and densities (95, 90, and 85% theoretical densities) at 1700 - 1800°C is being carried out under NASA sponsorship.[5] High temperature thermocouples have been incorporated in the center of these fuel bodies to monitor their temperatures as a function of irradiation time. A burnup equivalent to that for 1000 hours of operation of a 1-megawatt thermionic reactor has been achieved, with no

indication that the low density and the medium density fuel bodies have suffered significant dimensional change. The temperature of the high density fuel bodies, however, decreased steadily with time of irradiation, indicating an increasing loss of heat, probably due to fuel swelling. Although a definite conclusion cannot be reached until the samples are examined in the Hot Cell, the indications are that the fuel-swelling problem is not unsolvable. Irradiations of a clad capsule will be started during the first week of June, 1963, and will be continued until a burnup equivalent to that for 1000 hours operation of a 1-megawatt thermionic reactor is achieved. By the fall of 1963, it is expected that some definite conclusions can be reached on the approaches for solving the fuel swelling problem, and on the direction in which future long-term irradiation studies should proceed.

2. Loss of Fuel Materials by Vaporization

It is generally recognized that the loss of fuel materials by vaporization is a critical material problem for the unclad cells. However, it had not been fully realized until recently that the loss of fuel materials by vaporization is also a critical material problem for the clad cells. This is because, as described in the preceding section, fission gases have to be released from the fuel bodies to prevent fuel swelling, and in view of the low strength of emitter cladding at high temperatures, the released fission gases would have to be vented from the emitter to avoid its deformation. In venting the fission gases, however, the fuel materials are also lost or redistributed. Information on the rates of vaporization of fuel bodies of various densities (therefore various pore structures) is therefore needed for the judicious selection of fuel materials for both the unclad and the clad cells. Figure A-3 shows the rates of vaporation of UO_2,[6] UC,[7] and UC-ZrC[1][2] at various temperatures, and various compositions and pore structures measured in vacuum. Although the information is by no means complete, the following conclusions can be drawn:

(a) UO_2, which is excluded for use as an unclad emitter material because of its poor electrical conductivity, is also unsuitable as a fuel for vented clad fuel-emitters for high temperature thermionic cells because of its very high rate of vaporization (about 10^4 higher than that of a 20 UC - 80 ZrC). This difficulty is amplified by its poor thermal conductivity so that, for the heat flux and configuration needed for a thermionic emitter, the center of the UO_2 fuel may be molten, thus further contributing to the enhancement of the vaporization loss.

(b) If carbide fuels of low densities (85 - 90 percent dense) containing large portions of open pores (such as B_1 - 9 and B_1 - 2 as shown in Fig. A-3) are needed to prevent fuel swelling and a limit of 10^{-9} gm/cm^2/sec of vaporization loss is set, then the vacuum rates of vaporization of the

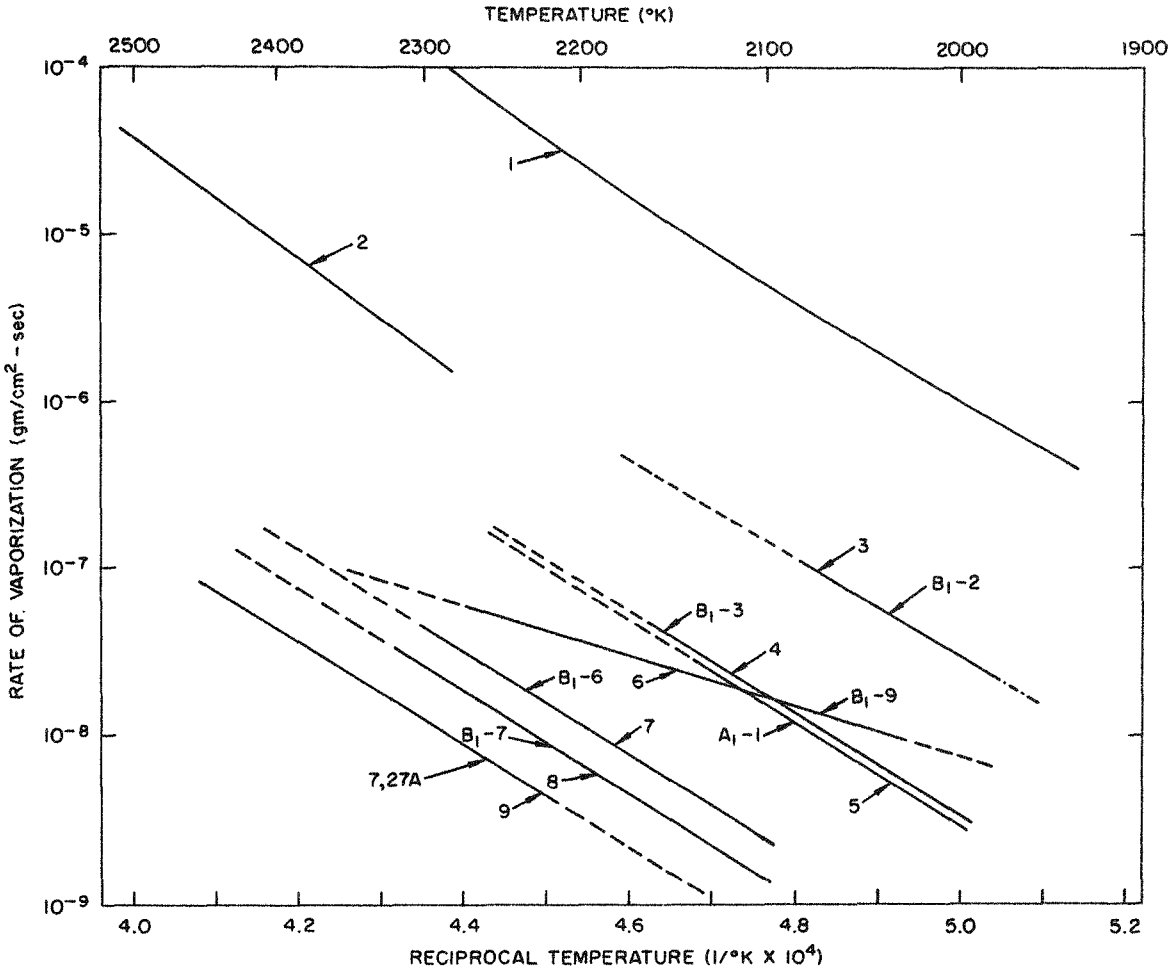

Note: A_1, B_1, 27A refer to sample numbers

1. UO_2 (Knudsen cell measurements)
2. UC 95% dense, cold pressed and sintered
3. 88UC-12ZrC, 88.5% dense, 89% open porosity cold pressed and sintered
4. 90 UC - 10ZrC nominal, 95.5% dense, cast and decarburized
5. 89UC - 11ZrC, 97.6% dense, cast and decarburized
6. 28.3 UC - 71.7 ZrC, 86.7% dense, 89% open porosity, cold pressed and sintered
7. 27.5 UC - 72.5 ZrC, 88.4% dense, 40% open porosity, hot pressed
8. 27.4 UC - 72.6 ZrC, 90% dense, 33.5% open porosity, hot pressed
9. 19 UC - 81 ZrC, 93.1% and 93.8% dense, hot pressed

Fig. A-3--Rates of vaporization of UO_2, UC, and UC-ZrC of various compositions and pore structures

30 UC-70 ZrC and the 90 UC-10 ZrC are too high by factors of 10 and 100 respectively for an unclad emitter temperature of 1800°C. In the presence of cesium vapor and a high temperature collector surface at close vicinity, the vaporization loss of the carbide emitter may be reduced. Whether the goal 10^{-9} gm/cm^2/sec could be reached under such conditions is currently being investigated under NASA sponsorship.[5]

(c) Although the vacuum rates of vaporization of low density 30 UC-70 ZrC and 90 UC-10 ZrC are higher than the goal 10^{-9} gm/cm^2/sec when used as unclad emitters (so that the total surface is exposed) at 1800°C, it is possible for these materials to be qualified as fuels for clad emitters. at 1800°C even if this stringent requirement (10^{-9} gm/cm^2/sec) is kept, since the total surface of the fuel does not have to be exposed to vacuum to vent the fission gas released.

Assuming an opening of 10^{-2} cm^2 per cm^2 fuel surface area is kept in the emitter cladding to vent the fission gases* by using baffles, the losses of fuel materials at 1800°C from the emitter cladding would be 10^{-10} gm/cm^2 fuel area/sec and 10^{-9} gm/cm^2 fuel area/sec for B_1-9 (30 UC-70 ZrC) and B_1-2 (90 UC-10 ZrC) respectively instead of 10^{-8} gm/cm^2 fuel area/sec and 10^{-7} gm/cm^2 fuel area/sec as shown in Fig. A-3, if the total surface areas of these fuels are exposed to vacuum as in the case of unclad emitters. Thus from the point of view of loss of fuel materials by vaporization, UC-ZrC is already qualified as fuel for the clad emitters, although its feasibility as unclad emitters would depend upon how its rate of vaporization is reduced by the presence of cesium vapor and a high temperature collector surface.

3. Release of Fission Products through Fuels and Cladding, and the Effect of Fission Product Contamination on the Performance of Cesium Cells

There is practically no information available on this important aspect of thermionic fission heat conversion. In the longest in-pile test (~300 hr) using 30 UC-70 ZrC emitters at Los Alamos, no such effect was observed, probably due to insufficient release or buildup of fission products in the cells. For unclad cells designed for one year or more of life expectancy and aiming for fission gas release to prevent fuel swelling, the fission product contamination effect cannot be ignored. The gaseous fission products released into the interelectrode space would have to be bled to avoid excessive scattering of the electrons from the emitters. The

*It can be shown this opening is ample for the venting of fission gases at the rate of production of fission gas atoms for the fission heat generation rate in thermionic fuels.

fission products forming stable carbides may stay in the emitter or on its surface to change its emission properties. In addition, volatile non-gaseous fission products may condense on the collector surface to cause changes in its cesium wetting properties. For the clad emitters, the fission products may diffuse through the clad at its operating temperatures to cause similar changes in cell performance. Although the ultimate answers can only be found in long-term in-pile tests, measurements of the rate of release of various fission products from fuels and through the cladding are needed to define the problem. In addition, on the basis of the release results, studies using simulated fission products should be made in the laboratory to determine the seriousness of these effects in order to guide the more expensive long-term in-pile tests, since these effects are not expected to depend on the isotopic forms of the elements concerned.

4. Interaction between Emitter and Fuel in the Clad Emitters

Considerable information has been accumulated during the last two years[1, 2] on the compatibility between refractory metal and alloy emitter materials and uranium-containing nuclear fuels. Most of these studies were carried out by the standard diffusion techniques at 1800 - 2000°C for periods of 10 - 50 hr*. The results are summarized in Table A-2. Of the various cases studied, W-clad UC and UC-ZrC, and W-clad UO_2 are found to be the most promising high temperature clad emitter system. The W-clad UO_2 system, however, suffers from the high rate of vaporization of UO_2. Although W-UO_2 cermets may be used to overcome this difficulty, the dimensional stability of such cermet fuel upon irradiation at high temperatures remains to be proved. This is currently being studied at General Atomic.[5]

In addition to gross diffusion studies, a more sensitive method has been devised[2] to study the effects of diffusion of traces of fuel components into emitter on its emission properties. Currently, the systems W-clad UC** and 30 UC-70 ZrC are being studied for periods greater than 1000 hr. The feasibility of using such clad emitter systems in thermionic fission heat conversion from the point of view of emitter-fuel interaction should be firmly established by the fall of 1963.

---

*The cases W versus UC and 90 UC-10 ZrC have been studied for periods of 1000 hr at 1750°C.

**W formed by the thermochemical decomposition of $WF_6 + H_2$.

Table A-2

SUMMARY OF COMPATABILITY DATA

Fuel	Temperature (°K)	Refractory Metal								
		Tungsten	Molybdenum	Niobium	Tantalum	Iridium	Rhenium	W - 26 Re	W - 5 Mo	W - 2 Mo
UC	2073	Suitable	Unsuitable[a]	Unsuitable[a]	Unsuitable[a]	Unsuitable[a]	Unsuitable[e]	Questionable[e]	Unsuitable[a]	Unsuitable[a]
UC_2	2073	Unsuitable[b]	Unsuitable[b]	Unsuitable[b]	Unsuitable[b]	-	-	-	-	-
10 mol - % UC 90 mol - % ZrC	2073	Suitable	Suitable	Unsuitable[c]	Unsuitable[c]	-	-	-	-	-
30 mol - % UC, 70 mol - % ZrC	2073	Suitable	-	-	-	-	-	-	-	Questionable[d]
90 mol - % UC, 10 mol - % ZrC	2073	Suitable	Unsuitable[a]	Unsuitable[a]	Unsuitable[a]	-	-	-	-	Unsuitable[a]
UO_2	2073	Suitable	Unsuitable[d]	Unsuitable[d]	Unsuitable[d]	-	-	-	-	
	2273	Suitable	Unsuitable[d]	Unsuitable[d]	Unsuitable[d]	-	-	-	-	-

(a) Liquid-phase formation.

(b) Excessive carbide-layer formation and grain-boundary penetration.

(c) Uranium and zirconium diffusion through metal at too rapid a rate.

(d) Fuel component diffusing through grain boundaries.

(e) Reaction layers or products detected at interfaces

5. Fabrication of Fuel-Emitter Materials of Reproducible Structures, Compositions, and Properties

(a) Unclad Fuel-Emitters - Considerable progress has been made during recent years on the fabrication of UC-ZrC of single-phase structures and controlled compositions. By using cold-pressing and sintering techniques, samples containing large amounts of open pores may be prepared over the whole UC-ZrC composition range to facilitate fission gas release and thus avoid fuel swelling. Metal-rich fuel bodies have been successfully treated thermally in vacuum to attain stoichiometry. However, much remains to be studied on the relationship among the cold-pressing, sintering and thermal treatment conditions, the size distribution of the carbide powder, the pore structures, and the total true surface area of the fuel bodies obtained. It is only through these quantitative correlations that the quality control of the unclad UC-ZrC fuel-emitters can be realized.

(b) Clad Fuel-Emitters - The present status of UC-ZrC carbide fuels has been described above. Cermet fuel fabrication has been studied in two ways. Mo-UO_2 cermet has been prepared by hot pressing Mo-coated UO_2 particles, and W-UO_2 and W-UC cermets have been fabricated by hot pressing a blended mixture of W and fuel powders. The cermets possess good electrical and thermal conductivity and may have better resistance to radiation effects than the single phase fuels. Cermet bodies prepared from metal-coated particles in general show a more uniformly dispersed structure than those made of a blended mixture of W and fuel powders and therefore are more desirable.

From the point of view of fuel-emitter compatibility, tungsten is by far one of the most promising emitter materials. Cladding with machined tungsten, however, is difficult because of its poor machinability. Recently carbide and cermet fuels have been clad with tungsten formed by the thermochemical decomposition of a mixture of $WF_6 + H_2$. The technique not only produces clad emitters which are dimensionally and structurally stable upon thermal cycling but also may promise an emitter which is more uniform and reproducible in structure and properties than the machined ones.

6. Problems Associated with Ceramic Electrical Insulators and Seals

Although various ceramic materials have been studied, the currently used seals are made of high purity Al_2O_3 bonded to Fe-Ni alloy or refractory metal (e.g., Nb and Ta) flanges either by using braze alloys through a metallizing layer, or by using active metal brazes directly (e.g., V, Zr, and Ti alloy brazes). Various studies have been made to check the corrosion resistance of these seals toward cesium[8] and work carried out

at Los Alamos[9] has shown that metal-to-ceramic seals made of Fe-Ni alloys bonded to Al_2O_3 by the metallizing method remained leak free after being irradiated to an integrated total neutron flux of 7×10^{20} nvt at room temperature. No irradiation studies, however, were performed in the presence of cesium vapor.

In addition to ceramic seals, ceramic materials may also be needed in a thermionic fuel element as thin layers of electric (but not thermal) insulation. The changes in physical properties under irradiation are important to such an application. Most of the available irradiation results were obtained at temperatures lower than 400°C. Generally speaking, Al_2O_3 has been shown[10] to be dimensionally stable, or very nearly so, after exposure to an integrated fast neutron flux of up to 10^{21} nvt; the thermal conductivity may decrease as much as 50 percent, but this decrease appears to saturate at about 10^{20}-10^{21} nvt. The electrical resistivity of Al_2O_3 tends to decrease promptly on exposure to neutron radiation. The effect, however, saturates and the resistivity tends to increase with time in the presence of radiation, high temperature, or an applied voltage. Since Al_2O_3 has a high electrical resistivity (about 10^{14} ohm at room temperature), the change is of no serious consequence. Studies have also been made on the dielectric strength of Al_2O_3-base ceramics in the presence of gamma-radiation. A dose of 10^9 rads decreases the strength to about 300-400 volt/mil[11]. Since conventional Al_2O_3 seals are much thicker than 1 mil, it is generally concluded that the effectiveness of these seals as insulating materials will not be seriously impaired by irradiation.

7. Material and Fabrication Problems in Integrating Single Thermionic Cells into a Reactor Fuel Element

The ultimate goal of the thermionic materials research and development program is to develop a thermionic fuel element consisting of a number of single cells arranged in a way compatible with materials limitations and reactor design requirements. The fabrication problems involved may be entirely different from those of a single cesium cell. To date, there have been no concerted efforts in this direction, although there are enough material information and design data available.

BLANK

REFERENCES

1. "Investigations of Carbides as Cathodes for Thermionic Space Reactors," Final Report on Contract NAS 5-1253 for period May 15, 1961 through August 31, 1962, General Atomic report GA-3523.

2. "Investigations of Carbides as Cathodes for Thermionic Space Reactors," Second Quarterly Progress Report on Contract NAS 3-2532, General Atomic report GA-4173, May 15, 1963.

3. Voorhees, B. G., "Progress Toward Nuclear Thermionic Space Power." Presented at American Rocket Society Space Systems Power Conference, Santa Monica, California, September 25-26, 1962.

4. Private communication from G. Grover of Los Alamos Scientific Laboratory, Los Alamos, New Mexico.

5. "Investigations of Carbides as Cathodes for Thermionic Space Reactors." Work in progress at General Atomic under Contract NAS 3-2532 with National Aeronautics and Space Administration.

6. Ackerman, R. J., P. W. Gilles, and R. J. Thorn, "High Temperature Thermodynamic Properties of UO_2," J. Chem. Phys. 25, 1089 (1956).

7. Vozzella, P. A., A. D. Miller, and M. A. De Crecente, "The Thermal Decomposition of Uranium Monocarbide, Pratt and Whitney report PWAC-378, January 15, 1962.

8. "Semiannual Technical Summary Report on Vapor Filled Thermionic Converter Materials and Joining Problems, Plasma Research Pertinent to Thermionic Converter Operation," on Contract No. NObs-86220 with Power Tube Department, General Electric Co., Schenectady, N. Y., General Electric report No. R-572 SA-1, 1962.

9. "Quarterly Status Report of LASL Plasma Thermocouple Development Program," Los Alamos Scientific Laboratory report LAMS-2447, June, 1960.

REFERENCES (Cont.)

10. "Radiation Effects State of the Art, 1960-1961," Battelle Memorial Institute Radiation Effects Information Center, report REIC-22, June 30, 1961.

11. Lawrence, W. L. and S. Mayburg, "A Guide to the Effect of Gamma-Irradiation on the Properties of Non-Metals," Westinghouse Electric Corp., Atomic Power Division, Pittsburgh, report WAPD-P-95, 1951.